AD_____

Award Number: DAMD17-99-1-9552

TITLE: Opening of the Mitochondrial Permeability Transition Pore by Reactive Oxygen Species is a Basic Event Neurodegeneration

PRINCIPAL INVESTIGATOR: John Savory, Ph.D.

CONTRACTING ORGANIZATION: University of Virginia
Charlottesville, Virginia 22906

REPORT DATE: July 2001

TYPE OF REPORT: Annual

PREPARED FOR: U.S. Army Medical Research and Materiel Command
Fort Detrick, Maryland 21702-5012

REPORT DOCUMENTATION PAGE

Form Approved
OMB No. 074-0188

1. AGENCY USE ONLY (Leave blank)	2. REPORT DATE	3. REPORT TYPE AND DATES COVERED
	July 2001	Annual (01 Jul 00 - 30 Jun 01)

4. TITLE AND SUBTITLE
Opening of the Mitochondrial Permeability Transition Pore by Reactive Oxygen Species is a Basic Event Neurodegeneration

5. FUNDING NUMBERS
DAMD17-99-1-9552

6. AUTHOR(S)
John Savory, Ph.D.

7. PERFORMING ORGANIZATION NAME(S) AND ADDRESS(ES)
University of Virginia
Charlottesville, Virginia 22906

E-Mail: js2r@virginia.edu

8. PERFORMING ORGANIZATION REPORT NUMBER

9. SPONSORING / MONITORING AGENCY NAME(S) AND ADDRESS(ES)
U.S. Army Medical Research and Materiel Command
Fort Detrick, Maryland 21702-5012

10. SPONSORING / MONITORING AGENCY REPORT NUMBER

11. SUPPLEMENTARY NOTES
Report contains color

12a. DISTRIBUTION / AVAILABILITY STATEMENT
Approved for Public Release; Distribution Unlimited

12b. DISTRIBUTION CODE

13. Abstract ***(Maximum 200 Words)*** *(abstract should contain no proprietary or confidential information)*

This investigation focuses on mitochondrial injury in the brain and subsequent apoptosis, as a major factor in neurodegeneration. The animal model system involves the direct injection of Al maltolate directly into the brains of New Zealand white rabbits via the intracisternal route. Our hypothesis was that Al maltolate induced oxidative stress resulting in opening of the mitochondrial permeability transition pore (PTP) and release of cytochrome *c*. This event was predicted to induce apoptosis. Our original proposal was to emphasize the use of immunohistochemical techniques for this study with confirmation by Western blot analysis. We have now developed cell fractionation techniques to that we can obtain mitochondrial, cytoplasmic, endoplasmic reticulum and nuclear fractions, with appropriate markers, with confirmation by immunohistochemistry. We have shown, as originally proposed, that aged rabbits do indeed demonstrate opening of the PTP and cytochrome *c* release, whereas young adult rabbits are not affected. However, this event does not necessarily lead to caspase-3 activation and apoptosis. We have now demonstrated that the endoplasmic reticulum and caspase-12 is important in the overall process of neurodegeneration and have been able to demonstrate neuroprotection with GDNF. We have performed studies on 70 rabbits during the time period covered by this present report.

14. Subject Terms (keywords previously assigned to proposal abstract or terms which apply to this award)
Neurotoxin

15. NUMBER OF PAGES
160

16. PRICE CODE

17. SECURITY CLASSIFICATION OF REPORT	18. SECURITY CLASSIFICATION OF THIS PAGE	19. SECURITY CLASSIFICATION OF ABSTRACT	20. LIMITATION OF ABSTRACT
Unclassified	Unclassified	Unclassified	Unlimited

Table of Contents

INTRODUCTION:

The overall objective of the research supported by the Department of Defense is to study mechanisms of neuronal injury and death, particularly resulting from neurotoxins. The focus of the present work is to determine if mitochondrial injury resulting from direct injection of the electroneutral aluminum compound, aluminum maltolate, is the main event causing apoptosis, and if aging increases the susceptibility to this toxic injury. There have been many advances over the past two years in understanding cell death via apoptosis. Although mitochondrial injury represents one important pathway, it is becoming apparent that the endoplasmic reticulum (ER) is also important. Cross-talk occurs between these two organelles and it is important to study these events in order to understand the process of neurodegeneration, particularly as induced by neurotoxic agents. An understanding of these processes is important in designing neuroprotection strategies. Thus, we have extended our studies to both mitochondria and ER, and in fact find that a comprehensive assessment of changes induced by the neurotoxin, aluminum maltolate, also requires monitoring the cytosolic and nuclear fractions. We initially proposed using immunohistochemical methods for our studies, with confirmation by Western blot analysis. In fact, we have had to change this approach, and we now obtain most information from subcellular fractionation and Western blotting.

Summarized here are our studies over the past 12 months, although we also present some data from the previous year as part of a paper in press.

BODY:

Animal studies: We have refined our techniques for processing tissue, and these are summarized in each of the papers that we attach describing our findings over the past year.

Mitochondrial injury in Al-induced neurotoxicity in rabbits: Our earlier research primarily involved immunohistochemistry for demonstrating the toxic effects of the intracisternal administration of Al maltolate. We have extended this work by using subcellular fractionation of brain tissue from treated rabbits, and we now routinely separate the cytosolic, mitochondrial, ER and nuclear fractions. We have demonstrated that Al maltolate induces cytochrome *c* translocation from mitochondria into the cytosol as early as 3 hours in the hippocampus of aged rabbits, but not of young rabbits. Pretreatment with cyclosporin A, an inhibitor of the mitochondria permeability transition pore (MTP), blocks the release of cytochrome *c*. Therefore, it appears that Al-induced cytochrome *c* release results from opening of the MTP. This effect implicates aging as a prerequisite factor, since the MTP does not open in young animals. Mitochondrial injury thus may represent a primary initiator of neurodegeneration, although in this initial work we have been unable to demonstrate caspase-3 activation. A report of this work is in press (1) and this paper is attached as **Appendix I**. This work has actually confirmed our initial hypothesis, that in fact the MTP is involved in the increased susceptibility of aged animals to neurotoxic injury. However, since we were unable to demonstrate caspase-3 activation, we were not convinced that this opening of the MTP, and the release of

cytochrome *c*, was in fact a true indicator that apoptosis had been initiated.

Our first studies evaluating the role of the opening of the MTP and cytochrome *c* release, were carried out using a dose of Al maltolate of 2.5 µmole (100 µL of 25 mM Al maltolate). In order to initiate caspase activation, we performed a series of experiments where we doubled the Al maltolate dose to 5 µmole. This was injected intracisternally into 6 young adult and 7 aged New Zealand white rabbits, and young adults were similarly injected with saline to act as controls. After 2 days, all of the young adult rabbits treated with Al maltolate developed severe neurological symptoms and had to be sacrificed. Surprisingly, the aged rabbit did not develop symptoms at this time; however, we sacrificed 5 of them at 2 days. The remaining 2 adults eventually developed symptoms at 8 days and were sacrificed at this time. At approximately the time we started these experiments, a report appeared in Nature describing the role of the ER in a new apoptosis pathway involving the activation of a newly described caspase, caspase-12 (2). Using this information we began to add an additional step using ultracentrifugation in our subcellular fractionation technique, in order to separate the cytosolic and ER fractions. Subsequently, we also isolated the nuclear fraction. A typical gel obtained from these studies is shown in Figure 1.

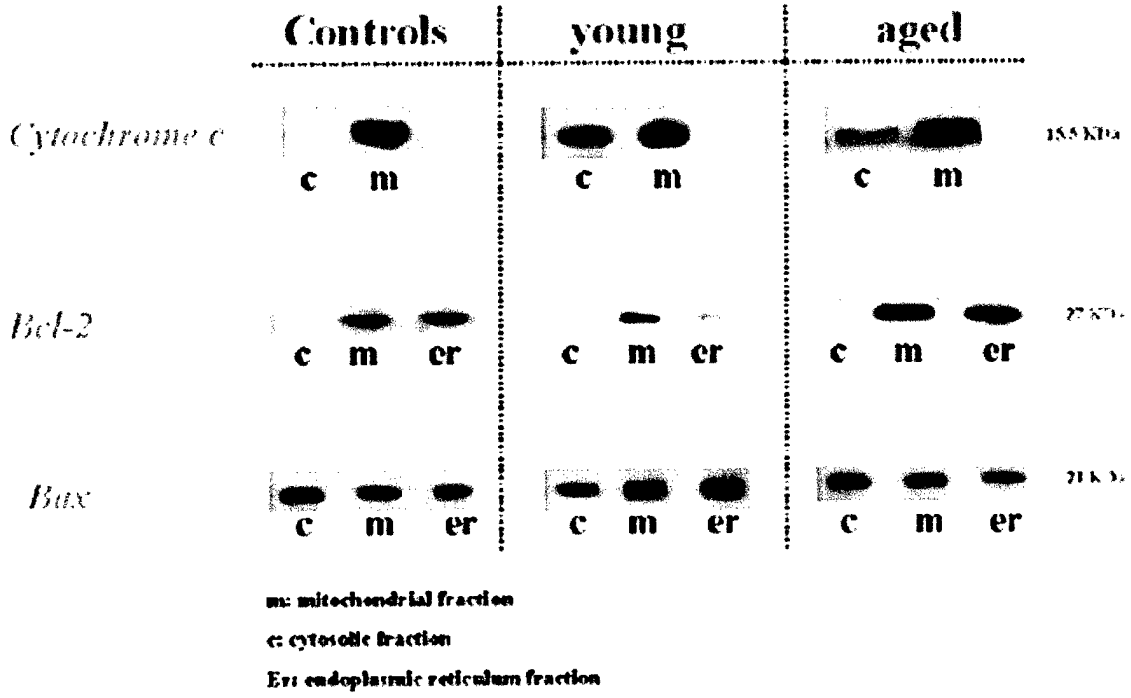

***Figure 1**: New Zealand white rabbits treated intracisternally with saline (control) or Al maltolate in the case of a young adult and aged animal. Rabbits were sacrificed at 2 days, and tissue from the hippocampus was fractionated by ultracentrifugation into cytosol (c), mitochondria (m) and endoplasmic reticulum (er). Western blots show translocation of cytochrome c from the mitochondria to the cytoplasm in the young animal, with a much diminished translocation in the aged rabbit. In the control the cytochrome c is exclusively found in the mitochondria. Bcl-2 is much diminished in the*

ER and to some extent in mitochondria in the young rabbit, but is at control values in the aged animal. Bax is increased in both the mitochondria and to a greater extent in the ER in the young Al-treated rabbit, whereas the aged animal has values similar to the control group.

As could be predicted from the Western blots in Figure 1, there is caspase-3 activation in tissue from the young Al-treated animals, but not in aged rabbits also treated with Al. This caspase activity was measured by its enzymatic activity using a fluorescent substrate. This method is described in detail in our paper which has just appeared in Brain Research (3), a reprint of which is attached **(Appendix II)**. Caspase-3 activities measured in this experiment, with young and aged rabbits treated with 5 µmole Al maltolate, are illustrated in Figure 2.

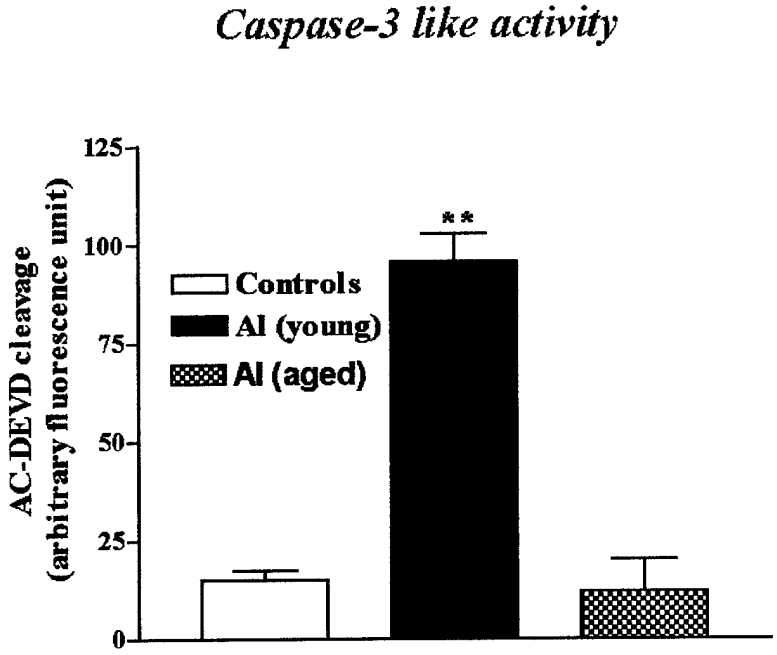

Figure 2: *Caspase-3 activity is shown in hippocampal lysates of controls (white bars) and Al treated animals (black bars). In controls, low caspase-3 activity is detected. Aluminum treatment induces a 5.5-fold increase in the caspase-3 activity. Data are presented as mean ± SEM.*

Caspase-3 immunoreactivity was also detected in brain tissue from the young Al-treated rabbits as shown in Figure 3 (also in **Appendix II**).

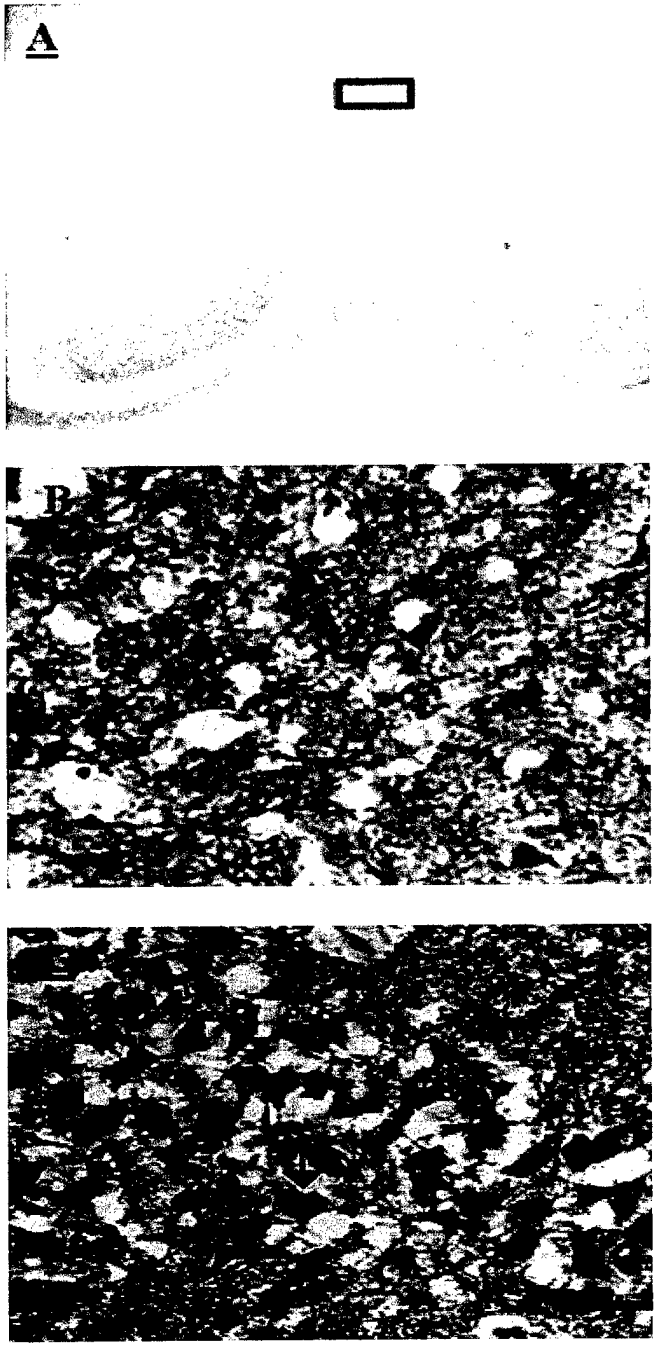

Figure 3: *Immunohistochemical localization of caspase-3 was examined in the pyramidal cell layer of the hippocampus* ***(A,*** *rectangular box).* ***B:*** *Pyramidal cell layer of controls showed no immunoreactivity for caspase-3 (x 400).* ***C:*** *Positive immunoreactivity for caspase-3 (arrows) was found in the pyramidal cell layer in Al treated animals (x 400). Bar in C = 25 μm.*

Further evidence for apoptosis in the young rabbits treated with Al is given in Figure 4

where TUNEL staining is positive in these animals, as compared to a lack of fluorescence in the controls.

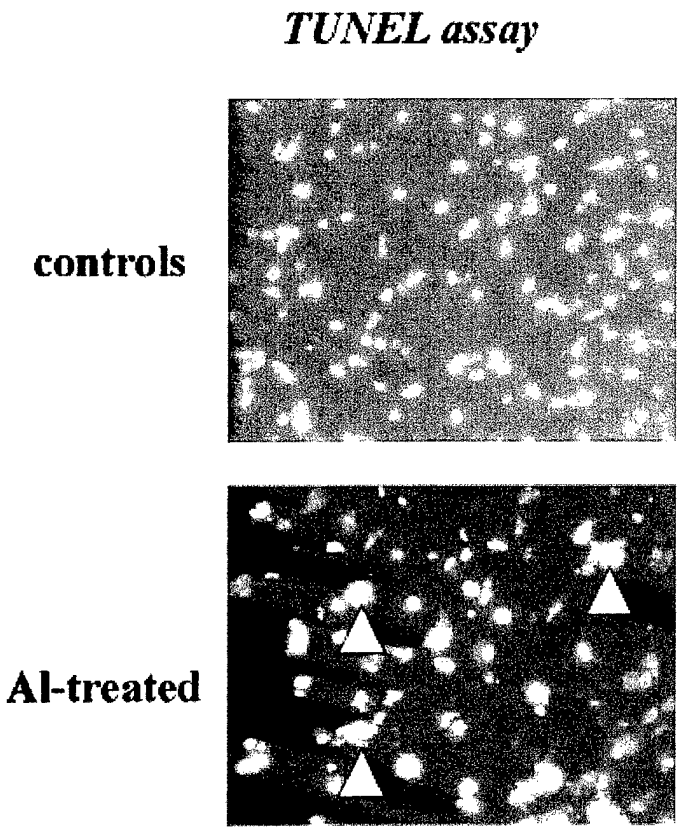

Figure 4: *TUNEL staining of Al-treated young rabbit in the pyramidal cell layer of the hippocampus (same location as Figure 3). Negative TUNEL staining is seen in a control.*

We have published part of this work as described above, in Brain Research (3) and, as mentioned above, a reprint is attached in **Appendix II**. The work published is the first description of ER changes following Bcl-2 and Bax, but only covers young adult rabbits treated with Al maltolate. We are surprised by the results following the 5 μmole dose of Al in aged rabbits, since there is obviously some rapid neuroprotective response to this highly toxic dose which is not occurring in the younger animals. These results offer us the opportunity to identify this neuroprotective response, but we have not yet performed these experiments. Our plan for such experiments will be to supplement our present techniques with quantitative real time RT-PCR, and we have made a preliminary start on such studies.

GDNF protects against Al-induced apoptosis in rabbits by upregulating Bcl-2 and Bcl-X_L, and by inhibiting mitochondrial Bax translocation:

The results of the experiments described above, in which a 5 μmole dose of Al maltolate

was injected into young and aged rabbits, strongly suggest that increased Bcl-2 in the ER is neuroprotective, as is the case with mitochondria. In addition, diminished levels of Bax in the ER appear to be proapoptotic, more so than similar changes in mitochondria. In order to further validate these results, we initiated a study where we have administered glial cell-derived nerve growth factor (GDNF) via the intracisternal route, since this agent has been shown to be neuroprotective and to upregulate Bcl-2. However, there have been no reports as to where Bcl-2 is increased in the cell. We speculate that the ER might be an important site for this action, and that cross-talk between ER and mitochondria could be significant in determining if a cell survives neurotoxic injury, or whether apoptosis is initiated. These studies with GDNF are described in detail in **Appendix III**, which is a paper in press in Neurobiology of Disease.

The results are summarized as follows: Using the rabbit system with co-administration (intracisternally) of Al maltolate and GDNF, we have obtained the following results: Al-treated rabbits again exhibit cytochrome *c* translocation into the cytoplasm, and there is a decrease in Bcl-2 and an increase in Bax in both the mitochondria and the ER. Changes in the levels of these proteins are accompanied by the activation of caspase-3 and DNA fragmentation. Co-treatment with GDNF does not inhibit cytochrome *c* release; rather it reverses the increase in levels of the proapoptotic protein Bax, enhances the levels of the antiapoptotic proteins Bcl-2, abolishes the caspase-3 activity, and dramatically reduces apoptosis. Also, these GDNF-treated rabbits do not demonstrate neurological symptoms for at least 9 days in 50% of the animals, while the remaining 50% have survived for up to 2 months before we terminated the experiment. In contrast, all the rabbits that did not receive GDNF developed severe symptoms after 2-3 days and require sacrifice. These results confirm the antiapoptotic properties of GDNF and identify the ER as a probable target for its neuroprotective properties, perhaps by raising the ER levels of Bcl-2 and thereby controlling calcium stores in the ER as previously reported (4). It appears from this work that the antiapoptotic effect of GDNF is independent of the blockade of cytochrome *c* release, and that Bcl-X_L is increased, thereby binding Apaf-1 and rendering cytoplasmic cytochrome *c* harmless. These studies are now in press (5). Representative Western blots and TUNEL staining for apoptosis are shown below in Figure 5:

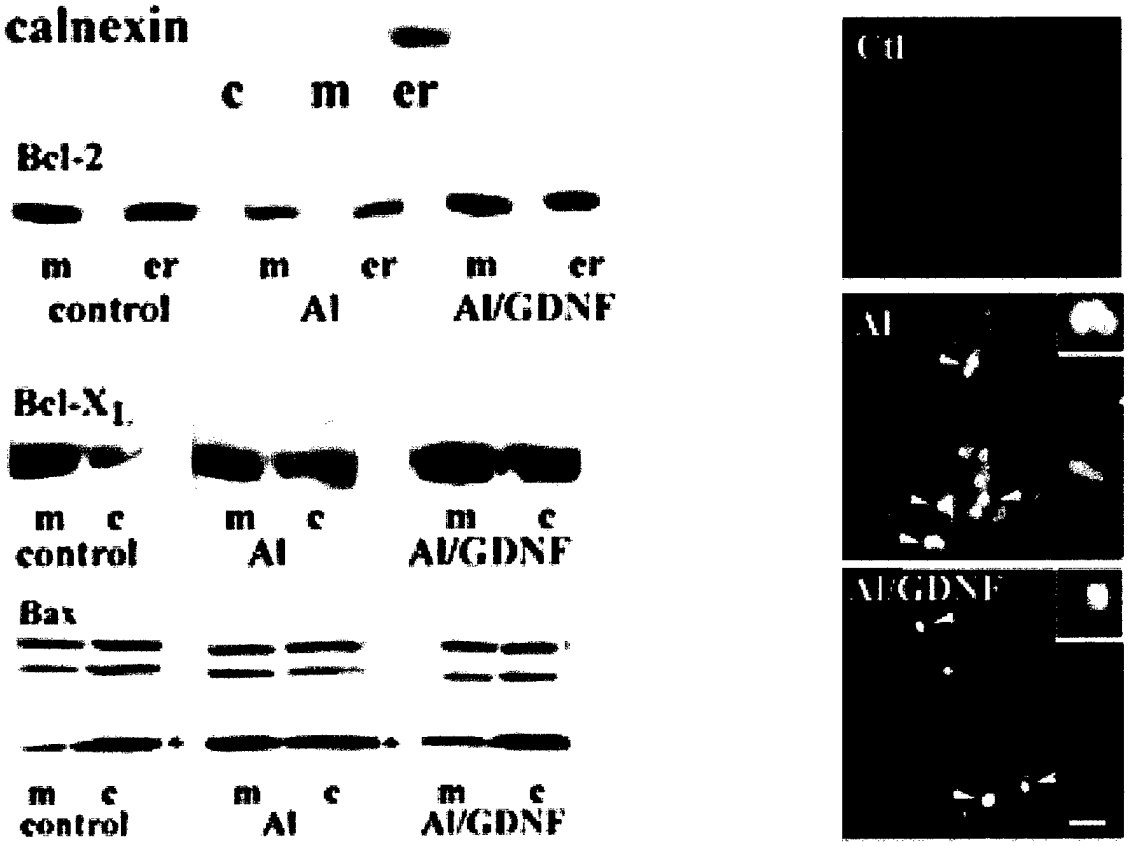

Figure 5. Left: ***Calnexin****, applied as a marker for the endoplasmic reticulum, stains only the endoplasmic reticulum fraction.* ***Bcl-2*** *(27 kDa) in controls is localized in mitochondria and the endoplasmic reticulum. Following Al administration, Bcl-2 levels decrease both in the mitochondria and in the endoplasmic reticulum. Treatment with GDNF maintains Bcl-2 levels at the basal levels observed in the controls, both in the mitochondria and endoplasmic reticulum.* ***Bcl-X_L*** *(31 kDa) immunoreactivity in controls is highly positive in the mitochondrial fraction, and is present to a lesser extent in the cytoplasmic fraction. Aluminum induces a slight decrease in mitochondrial levels, with a subsequent increase in the cytoplasmic levels. GDNF leads to a large increase in Bcl-X_L levels in cytoplasm>mitochondria.* ***Bax*** *(23 kDa) in controls is present at low levels in mitochondria and is highly reactive in the cytoplasm. Aluminum induces an increase in Bax in the mitochondrial fractions, and treatment with GDNF significantly reduces the translocation of Bax into mitochondria.*

Right: *Immunofluorescence images of dual labeling of TUNEL (green) and caspase-3 (red) in the hippocampal CA1 area of control, Al treated and Al/GDNF treated animals. In the Al treated group, the number of neurons showing co-localization of TUNEL and caspase-3 is high (arrows). Treatment with GDNF markedly reduces the number of neurons exhibiting DNA fragmentation and caspase-3 reactivity (arrows).*

Aβ(1-42) and Al induce stress in the ER in rabbit hippocampus, involving nuclear translocation of *gadd 153* and NF-κB and activation of caspase-12:

From the studies described above, it is becoming apparent that the ER, acting in concert with mitochondria, plays a role in regulating apoptosis. In order to evaluate further the role of the ER, we have extended our studies to investigate markers of ER stress and to assess the possible role of the ER apoptosis pathway involving caspase-12 (2;6). We have included in our experiment the intracisternal injection of Aβ(1-42) as well as Al maltolate, since Aβ(1-42) is certainly relevant to Alzheimer's disease and has been shown in vitro to induce ER stress and to activate caspase-12. We have now found that the intracisternal injection of either Al or of Aβ(1-42) into aged rabbits induces nuclear translocation of *gadd 153* and the inducible transcription factor, NF-κB. Translocation of these two proteins is accompanied by decreased levels of Bcl-2 in both the ER and the nucleus. Al induces caspase-12 activation which is a mediator of ER-specific apoptosis; this is the first report of the *in vivo* activation of caspase-12 (7). There is some evidence that Aβ also induces such activation, although this requires additional confirmatory work. The inducible transcription factor, NF-κB, is an important mediator of the human immune and inflammatory response (8), but whether, in our studies, the translocation of NF-κB into the nucleus represents a cellular defensive mechanism or represents an event facilitating neuronal injury, remains unclear. These results are summarized in Figure 6.

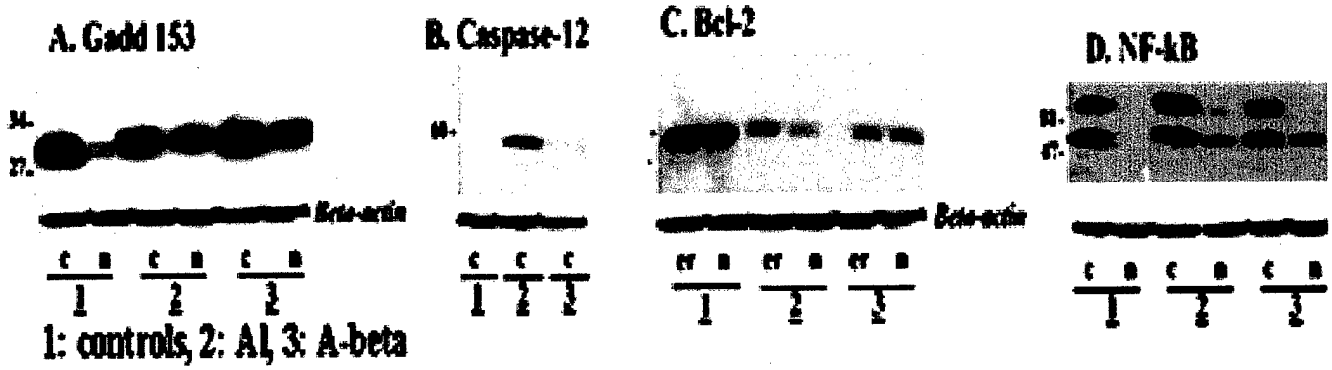

Figure 6 : *Western blot of gadd 153 (**A**), caspase-12 (**B**), Bcl-2 (**C**), and NF-κB (**D**), in cytoplasmic (**c**), nuclear (**n**), or endoplasmic reticulum (**er**) fractions from controls (1), and Al-treated (2) or Aβ(1-42)-treated (3) animals.*

A. *In controls(1), gadd 153 is detected in the cytoplasmic, but not in the nuclear fraction. Following Al (2) or Aβ(1-42) (3) administration, gadd 153 is present in the cytoplasmic fractions and also in the nuclear fractions;* ***B.*** *Caspase-12 is expressed only in the cytoplasmic fraction of Al-treated animal (2), and not in control (1) or Aβ(1-42)-treated (3) animals;* ***C.*** *Bcl-2 staining is intense in both the endoplasmic reticulum and nuclear fractions from controls (1). Al (2) or Aβ(1-42) (3) treatment results in a marked reduction in the staining for Bcl-2 in both the endoplasmic reticulum and nucleus;* ***D.*** *In the cytoplasmic fraction of controls (1), NF-κB is present as a dimer, the two bands corresponding to p52 and p100. Following Al or Aβ(1-42) administration respectively, p52 and p100 are detectable in the cytoplasmic fractions. In the nuclear fraction, while p100 is barely detectable, p52 is present.*

More details of these studies of ER stress induced by Al and Aβ(1-42), are given in a paper that has been submitted to Molecular Brain Research and is attached as **Appendix IV.**

Caspase-3 is primarily localized in the ER when activated as a result of severe Al-induced neurotoxic injury: In addition to caspase-12 activation, and the expression and nuclear translocation of ER-resident proteins, we find (in an ongoing study) that the effector caspase-3 is expressed in the ER of young rabbit brain from animals sacrificed 24 hrs after exposure to Al (Figure 7). This result represents a major finding, since it is the first time that such activity for caspase-3 is reported in the ER. Whether the presence of caspase-3 in the ER is subsequent to its upregulation or is a translocation from the cytoplasm into the ER remains to be clarified. However, this is certainly surprising data, especially in view of the intense activity in the many laboratories worldwide that are studying caspase-3.

Oral lithium treatment inhibits caspase-3 activation in ER: Since we have been successful in achieving neuroprotection with GDNF, presumably by upregulating Bcl-2 in the ER, we have undertaken some studies using lithium treatment, a compound suggested as being a neuroprotective agent due to its ability to increase Bcl-2 levels. We have performed preliminary studies on 6 New Zealand white rabbits pretreated for 14 days with drinking water containing 14 mM lithium carbonate (Sigma Chemical Co, St. Louis, MO). Blood specimens have been obtained from an ear vein at 7, 14 days and at sacrifice. After separation of serum, lithium concentrations were measured using an AVL model 9180 clinical analyzer (Roche Diagnostics, Roswell, GA) which uses a lithium ion selective electrode, and has been evaluated in the P.I.'s laboratory (9). This treatment protocol has resulted in serum lithium concentrations ranging from 0.6 to 1.2 mM/L, levels which are within the therapeutic range for humans treated with lithium for mood stabilization (10). Our preliminary data demonstrate that pretreatment with lithium strongly reduces the Al-induced caspase-3 activation, as assessed by Western blot analysis summarized in Figure 7.

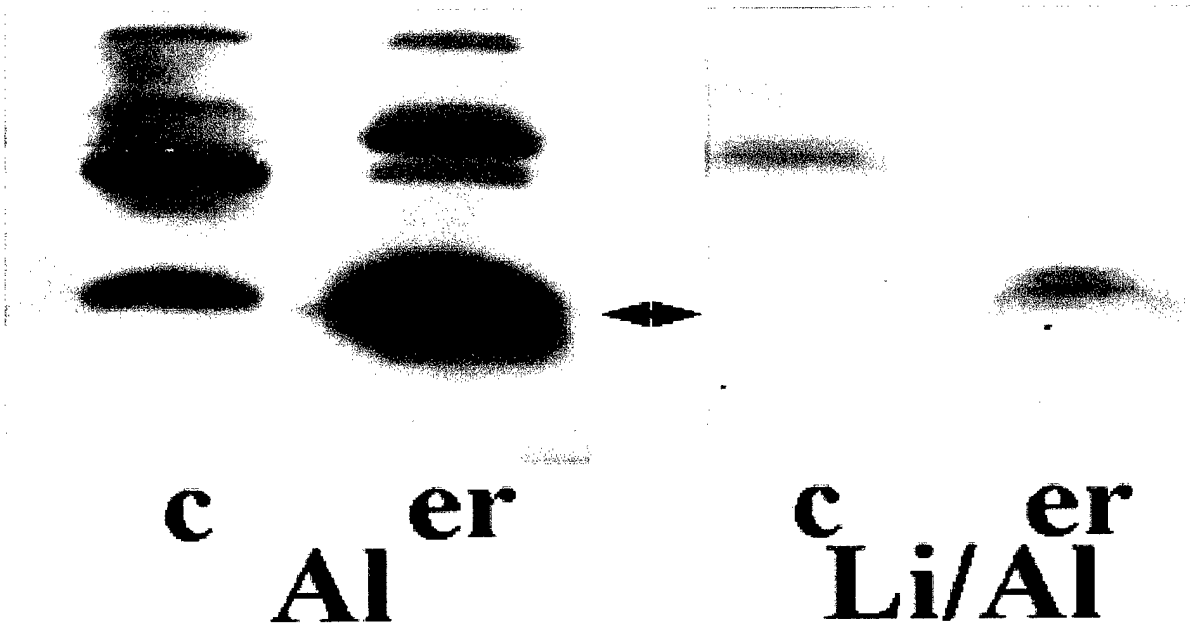

Figure 7: *Western blot analysis of caspase-3 in hippocampus of Al treated rabbits and in animals pretreated with 14 mM of lithium (Li) for 15 days and then injected with Al. Al induces caspase-3 activation in the cytosolic (c) and to a larger extent in the endoplasmic reticulum (er) fractions. Pretreatment with Li completely inhibits the presence of caspase-3 in the cytosol and highly reduces it in the ER.*

Taken together, our preliminary results lead us to the hypothesis that, although mitochondrial apoptotic signals are important in regulating apoptosis following neurotoxic stimuli, the ER and nuclear organelles may also participate in the molecular mechanisms of apoptosis. Studies of the responses of apoptosis-regulatory genes in these organelles promise to uncover important mechanistic information related to neuronal death, and thereby to offer the possibility of major advances in therapy.

Aluminum-induced dendritic pathology revisited: cytochemical and electron microscopic studies of rabbit cortical pyramidal neurons.

We have used material from Al-treated rabbits from some of the above-mentioned studies to further characterize the intraneuronal lesions induced by Al. The primary histological response to aluminum intoxication is the appearance of intensely argyrophilic masses of fibrillar material within many neuronal somata and thickened dendrites. The dendritic thickenings have been beautifully illustrated in silver stains of 50 μm-thick sections at both the light and electron microscopic level. Ultrastructural characterization of these aggregates in both conventionally-prepared and silver-stained sections shows them to be made up of neurofilaments. For this reason, we have elected to call these argyrophilic masses "neurofilamentous arrays (NFAs)". At their zenith, NFAs in cortical pyramidal neurons are composed of thousands of filaments interconnected by periodic crossbridges. NFAs begin their formation within both somata and dendrites as isolated groups of neurofilaments which apparently go on to assemble *en masse* within the cytoplasm. In

symptomatic animals, many cortical neurons are rich in NFAs, yet lack typical cytological signs of degeneration, such as nuclear pyknosis. Though silver staining reveals extensive NFAs only in aluminum-exposed brains, there is a strong degree of immunostaining for phosphorylated neurofilamentous epitopes in both untreated and Al-injected animals. This suggests that protein subunits, already present in the neurons under normal circumstances, are recruited in the presence of aluminum to form NFAs through the directed assembly of masses of oriented filaments, perhaps without any significant mobilization of neuronal synthetic machinery. No evidence has been found within aluminum-induced NFAs for the presence of the microtubule-derived "paired helical filaments" that typify the neurofibrillary tangles of Alzheimer's disease, although immunoreactivity for microtubular proteins has previously been demonstrated in NFAs.

We have prepared a manuscript describing these studies and it is in a final revision stage, although we have not yet selected the journal to which we will submit this paper. We attach this manuscript as **Appendix V**.

Aluminum and neuronal cell injury: inter-relationships between neurofilamentous arrays and apoptosis.

We have summarized some of our work in a mini-review article which is in press in the Journal of Inorganic Biochemistry. This paper is attached as **Appendix VI**.

The rabbit model system for studies of aluminum-induced neurofibrillary degeneration: relevance to human neurodegenerative disorders.

This review article of our animal model system has been published as a book chapter in Aluminum and Alzheimer's Disease. The Science that Describes the Link, C.Exley ed. Elsevier Science B.V. 2001, pp 203-219. A reprint of this chapter is attached as **Appendix VII.**

α-synuclein localization in substantia nigra:

In 14-μm frozen sections of brain from untreated control rabbits, immunocytochemical reactivity indicating the presence of alpha-synuclein was evident in the majority of neurons, with particular localization in nuclei and axons, and in presumptive presynaptic axon terminals. In addition, some regions of the substantia nigra 7-days after Al maltolate demonstrated densely immunoreactive bodies of varying shapes, associated with both nuclei and cytoplasm of the affected neurons. (Figure 8A, B).

***Figure 8A**: Several neurons (arrows) in the reticular portion of the substantia nigra contain pleomorphic dense bodies after immunoreaction for the protein α-synuclein. X 767.* ***Figure 8B:** High magnification of a nigral neuron, which in addition to immunoreactivity for α-synuclein in the cell body, contains intensely positive accumulations in the nucleus (arrow). The immunopositive cytoplasmic bodies are seen to the right of the nucleus. X 1048.*

Studies on the gas chromatography/mass spectrometry detection of 8-hydroxyguanine in DNA from Al-treated rabbits.

Our initial proposal included studies of the assessment of oxidative stress by measuring 8-hydroxyguanine in DNA extracts from rabbit brain using gas chromatography/mass spectrometry. The work that we have carried out on the measurement of 8-hydroxyguanine is summarized as follows:

The method used was that reported by Dizdaroglu (11), and involved DNA extraction from 100 mg of rabbit brain tissue from the temporal cortex. The extraction technique utilized the GenElute mammalian genomic DNA kit (Sigma Chemical Co., St. Louis, MO) which yielded approximately 20 μg of DNA, as determined by UV absorbance measurements. The procedure described by Dizdaroglu's group at NIST applies 2 different stable isotope-labeled analogs of 8-hydroxyguanine as internal standards, the latter obtained from Cambridge Isotope Laboratories (Andover, MA). Unfortunately these standards are no longer available. Therefore, we resorted to the use of 6-azathymine (Sigma) as an internal standard, as used by Spencer *et al.* (12). DNA samples (20 μg) were hydrolyzed for 30 minutes at 140°C with 0.5 mL of 60% formic acid in thick-walled glass tubes sealed under vacuum. The hydrolysates were frozen in vials placed in liquid nitrogen and then lyophilized for 18 hours. For derivatization of DNA hydrolysates, 60 μL of a mixture of nitrogen-bubbled bis(trimethylsilyl)trifluoroacetic acid (BSTFA, Pierce Chemical Co., Rockford, IL) containing 1% trimethylchlorosilane and pyridine (1:1, v/v) were added to the vials. The samples were purged with ultra high purity nitrogen, vortexed and then tightly sealed under nitrogen with Teflon-coated septa. The derivatization was carried out at 23°C for 2

hours by vigorously shaking the vials. A 20 μL aliquot was removed and placed in a vial used for injection onto the gas chromatograph column. The column used was a DB5 0.25 μ thickness capillary, 15 meters long x 0.32mm internal diameter (J & W Scientific, Folsom, CA). A Hewlett Packard model 5890 gas chromatograph (Rockville MD) and a Incos 50 mass spectrometer (Finnigan MAT, San Jose, CA) were used for the final analysis.

The system was initially tested with a standard solution of 8-hydroxyguanine prepared as follows: We dissolved 6 mg of 8-hydroxyguanine (2-amino-6,8-dihydroxypurine; Sigma-Aldrich, Milwaukee, WI) in 6 mL of 0.01N NaOH. In order to dissolve the compound some heating and stirring was needed. 30 μL of this solution (30 μg) was placed in a 1 mL reaction vial, frozen in liquid nitrogen and lyophylized overnight as described above. Derivatization was also as described above. The GC/MS data showed a good yield of product which gave peaks at 455, 440 and 73 atomic mass units (amu), corresponding to the trimethylsilyl derivative of 8-hydroxyguanine reported by Dizdaroglu (13). The mass spectrum is shown in **Appendix VIII A** and the single ion chromatograms in **Appendix VIII B**.

The system was further tested by adding 8-hydroxyguanine to DNA extracted from rabbit brain tissue (temporal cortex). To 20 μg of DNA was added 3 μL of 8-hydroxyguanine and 3 μL of the internal standard 6-azathymine. Each of these solutions were 1 μg/μL. The 8-hydroxyguanine was in a solution of 0.01N NaOH and the 6-azathymine was in methanol. These contents of the tube were dried under vacuum, and 0.5 mL of 60% formic acid were added and the contents sealed under vacuum. Hydrolysis and derivatization were carried out as described above. The major ions detected were as follows:
8-OH guanine: 440 and 455 amu. The intensity of the 440 amu ion is greater than the 455 by ~ 10%.
6-azathymine: 256 and 271 amu. The intensity of the 256 amu ion is greater than the 271 ion by ~ 5-fold.

Using single ion monitoring, we were able to detect 8-hydroxyguanine in the spiked DNA sample with both the 440 and 455 amu ions, as is shown in **Appendix VIII C**.

We then lowered the amount of 6-azathymine internal standard to 1 nmole which is the concentration used by Spencer *et al.* (12). This amount, when undergoing the hydrolysis and derivatization steps, gave no detectable signal by gas chromatography/mass spectrometry analysis. When this experiment was repeated with or without hydrolysis, there was still no observable signal.

We have therefore concluded that this gas chromatography/mass spectrometric procedure was not a viable approach for our needs, both because the sensitivity of the mass spectrometer available to us was a limiting factor, and because excessive amounts of brain tissue were required for the DNA extraction. We will return to a quantitative assay for measuring 8-hydroxyguanine in extracted DNA samples, by collaborating with Dr. Susan Browne of Cornell Medical Center. Dr. Browne has the most advanced HPLC

assay with electrochemical detection, and she has offered to help us with these measurements of 8-hydroxyguanine.

Detection of 8-hydroxyguanine in DNA by immunohistochemistry:

It seems apparent that our future studies of assessment of oxidative stress will be best accomplished by employing immunohistochemical techniques. We have performed some immunohistochemical investigations with serial 14 μm-thick coronal frozen sections from control and Al-treated animals (sacrificed at 7 days following the injection of 2.5 μmole Al maltolate) cut at the level of the hippocampus. We have used a mouse mAb against 8-hydroxyguanine (Trevigen, Gaithersburg, MD) and the Vectastain Elite avidin-biotin complex technique kit (Vector Laboratories, Burlingame, CA), as described in Appendix II. Using this approach we have obtained equivocal results with no definitive staining in the Al-treated animals.

Our future plans are to continue these studies using the OxyDNA fluorometric assay kit (Calbiochem,La Jolla, CA), which should provide us with increased sensitivity over the diaminobenzidine method. We would then use the quantitative HPLC method to verify these results.

KEY RESEARCH ACCOMPLISHMENTS:

- Our initial hypothesis, implicating aging as a factor increasing mitochondrial susceptibility to neurotoxic injury and associated with the opening of the mitochondrial permeability transition pore, has been supported by studies using Cyclosporin A. However, we have failed to see caspase-3 activation following cytochrome *c* translocation into the cytoplasm
- Increasing the dose of Al results in caspase activation in young rabbits, but surprisingly, there appears to be some degree of neuroprotection in the aged animals
- The endoplasmic reticulum (ER) appears to be a key site controlling apoptosis, either through crosstalk with mitochondria or directly via activation of caspase-12. The apoptosis regulatory proteins, Bcl-2 and Bax, are localized in the ER as well as in the mitochondria.
- Agents that increase the antiapoptotic protein Bcl-2 in the ER are neuroprotective. In particular, we have had dramatic results with GDNF and promising results with oral lithium treatment.
- Caspase-3 is primarily localized in the ER in our system, which supports our targeting this organelle in understanding the mechanisms of neuronal cell injury following neurotoxic stress.
- α-synuclein aggregates appear to be localized in the substantia nigra following Al treatment.

REPORTABLE OUTCOMES:

The following papers and abstracts have been either published, or are in press or submitted as a direct result of the research supported by the Department of Defense:

- Ghribi, O., DeWitt, D.A., Forbes, M.S., Herman, M.M., and Savory, J. Co-involvement of mitochondria and endoplasmic reticulum in regulation of apoptosis: changes in cytochrome c, Bcl-2 and Bax in the hippocampus of aluminum-treated rabbits. *Brain Res.* 2001; 903:66-73.

- Ghribi, O., Forbes, M.S., DeWitt, D.A., Herman, M.M., and Savory, J. GDNF protects against aluminum-induced apoptosis in rabbits by upregulating Bcl-2 and Bcl-X_L, and inhibiting mitochondrial Bax translocation. *Neurobiology of Disease*, in press.

- Ghribi O, DeWitt DA, Forbes MS et al. Cyclosporin A inhibits Al-induced cytochrome c release from mitochondria in aged rabbits. *J Alzheimers Disease*. in press.

- Savory, J., Ghribi, O., Forbes, M.S., and Herman, M.M. Aluminum and neuronal injury: inter-relationships between neurofilamentous arrays and apoptosis. *Journal of Inorganic Biochemistry*, in press.

- Savory, J., Ghribi, O., Forbes, M.S. and Herman, M.M. The rabbit model system for studies of aluminum-induced neurofibrillary degeneration: relevance to human neurodegenerative disorders. In: *Aluminum and Alzheimer's Disease*. C. Exley ed. Elsevier 2001 pp. 203-219.

- Ghribi, O., Herman, M.M., Forbes, M.S., DeWitt, D.A., and Savory, J. Aβ and aluminum induce stress in the endoplasmic reticulum in rabbit hippocampus, involving nuclear translocation of gadd 153 aand NF-κB. *Molecular Brain Research*, submitted.

- Ghribi O, DeWitt,DA, Forbes MS, Herman MM and Savory J. MTP opening and expression of cytochrome C, Bcl-2 and Bax in aluminum-treated aged rabbits. Presented at the Society for Neuroscience 30th Annual Meeting, New Orleans, LA. November 4-9, 2000 (abstract).

- Ghribi O, DeWitt,DA, Forbes MS, Herman MM and Savory J. Cyclosporin A prevents cytochrome C release in Al-treated aged rabbit brain. World Alzheimer Congress 2000, Pivotal Research, Washington D.C. July 11, 2000 published in *Neurobiology of Aging* 21: S154, 2000 (abstract).

- Ghribi O, DeWitt,DA, Forbes MS, Herman MM and Savory J. Cross-talk between endoplasmic reticulum and mitochondria regulates apoptosis in

experimental neurodegeneration. Association of Clinical Scientists, Chapel Hill, NC, May 9-12, 2001 (abstract).

- Savory, J. Aluminum and cell suicide: oh what a tangled web we weave. The J.D. Birchall Memorial Lecture presented at the Fourth Keele Meeting on Aluminium, Stoke on Trent, UK February 25-27, 2001 (abstract).

- Forbes MS, Ghribi O, Herman MM, Savory J. Aluminum-induced dendritic pathology revisited: cytochemical and electron microscopic studies of rabbit cortical pyramidal neurons. Manuscript is ready for submission.

CONCLUSIONS:

It is evident from our studies that the ER is an important site for regulating apoptosis either in concert with mitochondria via cytochrome *c* translocation to the cytoplasm, or via caspase-12 activation. Our work has uncovered the unexpected finding that caspase-3 is primarily localized in the ER, at least following Al-induced neurotoxicity. We have provided the first *in vivo* evidence of caspase-12 activation. A most important component of our work on the interaction of the ER and mitochondria has been the assessment of neuroprotective agents and their possible site of action as being in the ER. We have shown for the first time that, in all likelihood, GDNF targets the ER and is remarkably neuroprotective. Of greater significance are our preliminary studies on oral lithium treatment which appears to have the same target as GDNF. Based on our work so far on the mechanisms of mitochondrial and ER pathways leading to apoptosis, we have the following working hypothesis:

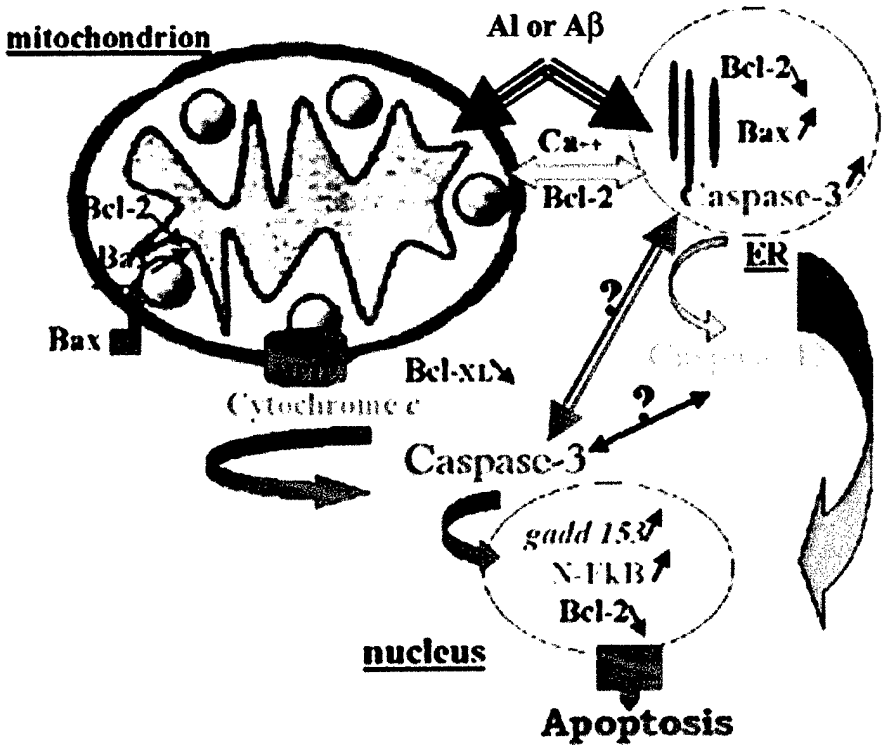

Our hypotheses for the neurotoxic injury that we induce with Al maltolate or Aβ are summarized in the mechanisms depicted in Figure 9. We hypothesize that Al/Aβ are neurotoxic to mitochondria and ER. **(1)** Al/Aβ will induce release of cytochrome *c* from mitochondria by opening of the mitochondrial permeability transition pore (MTP). Release of cytochrome c will be accompanied by dysregulation in the levels of the apoptosis regulatory proteins Bcl-2 and Bax in mitochondria and in the activation of caspase-3 and induction of apoptosis **(Mitochondrial-apoptosis pathway)**. Mitochondrial opening of the MTP may result from either a direct effect of Al/Aβ on mitochondria or from an increase of Ca^{++} entry into mitochondria following the depletion of Ca^{++} storage in the ER **(ER-mitochondria cross-talk)**. **(2)** Al/Aβ will also directly induce stress in the ER leading to, **(a)** dysregulation of the apoptosis regulatory proteins Bax and Bcl-2 in the ER, **(b)** activation of caspase-3 in the ER and activation of the ER-specific apoptosis mediator, caspase-12 **(ER-apoptosis pathway)**, and **(c)** activation of ER resident proteins, including *gadd 153*, and activation of the transcriptional factor, NF-κB, and their translocation into the nucleus **(ER-nucleus signaling)**. The overall result of stress in the mitochondria and in ER will result in caspase-3 damage initiation and in down-regulation of the antiapoptotic Bcl-2 in the nucleus. Consequently, we will assess DNA fragmentation and neuronal death. GDNF and lithium will prevent Al/Aβ - induced apoptosis by increasing the antiapoptotic Bcl-2 levels in the ER and thus preventing ER stress.

REFERENCES CITED:

1. Ghribi O, DeWitt DA, Forbes MS, Arad A, Herman MM, Savory J. Cyclosporin A inhibits Al-induced cytochrome c release from mitochondria in aged rabbits. J Alzheimers Disease 2001;in press.

2. Nakagawa T, Zhu H, Morishima N, Li E, Xu J, Yankner BA, Yuan J. Caspase-12 mediates endoplasmic-reticulum-specific apoptosis and cytotoxicity by amyloid-beta. Nature 2000;403:98-103.

3. Ghribi O, DeWitt DA, Forbes MS, Herman MM, Savory J. Co-involvement of mitochondria and endoplasmic reticulum in regulation of apoptosis: changes in cytochrome c, Bcl-2 and Bax in the hippocampus of aluminum-treated rabbits. Brain Res 2001;903:66-73.

4. He H, Lam M, McCormick TS, Distelhorst CW. Maintenance of calcium homeostasis in the endoplasmic reticulum by Bcl- 2. J Cell Biol 1997;138:1219-28.

5. Ghribi O, Forbes MS, ., DeWitt DA, Herman MM, Savory J. GDNF protects against aluminum-induced apoptosis in rabbits by upregulating Bcl-2 and Bcl-XL and inhibiting mitochondrial Bax translocation. Neurobiol Dis 2001;in press.

6. Nakagawa T, Yuan J. Cross-talk between two cysteine protease families. Activation of caspase-12 by calpain in apoptosis. J Cell Biol 2000;150:887-94.

7. Ghribi O, Herman MM, DeWitt DA, Forbes MS, Savory J. A-β (1-42) and aluminum induce stress in the endoplasmic reticulum in rabbit hippocampus, involving nuclear translocation of *gadd 153* and NF-κB. Mol Brain Res 2001.

8. Baeuerle PA, Henkel T. Function and activation of NF-kappa B in the immune system. Annu Rev Immunol 1994;12:141-79.

9. Bertholf RL, Savory MG, Winborne KH, Hundley JC, Plummer GM, Savory J. Lithium determined in serum with an ion-selective electrode. Clin Chem 1988;34:1500-2.

10. Moyer TP. Therapeutic drug monitoring. In: Burtis, C.A., Ashwood, E.R., eds. Tietz Textbook of Clinical Chemistry. Philadelphia, PA: W.B. Saunders Company, 1999:892.

11. Rodriguez H, Jurado J, Laval J, Dizdaroglu M. Comparison of the levels of 8-hydroxyguanine in DNA as measured by gas chromatography mass spectrometry following hydrolysis of DNA by *Escherichia coli* Fpg protein or formic acid. Nucleic Acids Res 2000;28:E75.

12. Spencer JP, Jenner A, Aruoma OI, Evans PJ, Kaur H, Dexter DT et al. Intense oxidative DNA damage promoted by L-dopa and its metabolites. Implications for neurodegenerative disease. FEBS Lett 1994;353:246-50.

13. Dizdaroglu M. Chemical determination of free radical-induced damage to DNA. Free Radic Biol Med 1991;10:225-42.

Personnel receiving salary support from this grant:

John Savory, Ph.D.

Othman Ghribi, Ph.D.

Michael S. Forbes, Ph.D.

Myxolydia Tyler

Cyclosporin A inhibits Al-induced cytochrome *c* release from mitochondria in aged rabbits

Othman Ghribi[a], David A. DeWitt[d], Michael S. Forbes[a], Ayala Arad[a], Mary M. Herman[c] and John Savory[a,b,*]

[a]*Department of Pathology, University of Virginia, Charlottesville, VA, USA*

[b]*Biochemistry and Molecular Genetics and Chemistry, University of Virginia, Charlottesville, VA, USA*

[c]*IRP, NIMH, NIH, Bethesda, MD, USA*

[d]*Departments of Biology and Chemistry, Liberty University, Lynchburg, VA, USA*

Neurodegenerative diseases including Alzheimer's disease are characterized by a progressive and selective neuronal loss via an apoptosis mechanism, and there is a growing body of evidence which supports a central role of mitochondria in this apoptotic cell death. Release of cytochrome *c* from the mitochondria to the cytosol is considered a critical step in apoptosis. Here we report that aluminum maltolate induces cytochrome *c* translocation into the cytosol as early as 3 hours in aged but not in young rabbit hippocampus. Pretreatment with cyclosporin A, an inhibitor of the mitochondria permeability transition pore (MTP), blocks cytochrome *c* release. Therefore, it appears that aluminum maltolate-induced cytochrome *c* release results from opening of the MTP. This effect implicates aging as a prerequisite factor, since the MTP does not open in young animals. Mitochondrial injury thus may represent a primary initiator of neurodegeneration.

1. Introduction

Recent studies have shown that in Alzheimer's disease, mitochondrial alterations represent a primary event in apoptotic cell death (for review see [3]). Growing evidence suggests that cytochrome *c*, a water-soluble peripheral membrane protein of the mitochondria, is released into the cytoplasm following cytotoxic stimuli [9]. The apoptotic process is then activated and involves regulating proteins such as the anti-apoptotic Bcl-2 and the pro-apoptotic Bax. The release of cytochrome *c* into the cytoplasm is reported to result from opening of the mitochondria transition pore (MTP) in response to cytotoxic insult [22]. Tumor necrosis factor alpha (TNF-∀) [2], transient focal cerebral ischemia [11] and the parkinsonian-related neurotoxin MPP+ [3] have been shown to open the MTP and release cytochrome *c*. Cyclosporin A, an immunosuppressant agent, inhibits MTP opening [14] and has been shown to block cytochrome *c* release by TNF-∀ [2]. In addition, treatment with cyclosporin A ameliorates brain damage resulting from transient forebrain ischemia [10] or traumatic brain injury [13].

Although there is a continuing controversy as to whether aluminum (Al) may play a role in the etiology of Alzheimer's disease, intracisternal administration of the soluble Al maltolate complex have been shown to produce oxidative stress, Aβ deposition, neurofilamentous changes in hippocampal neurons of aged rabbits [15]. On the other hand, we have demonstrated previously that, as early as 3 hr following the intracisternal administration of Al maltolate into aged rabbit brain, there is Bcl-2 upregulation and Bax downregulation. By 72 hrs, apoptosis is strongly evident, Bcl-2 is downregulated and Bax is strongly increased [19]. In the present study, we have investigated changes in the intracellular localization of cytochrome *c* in this same animal model system, testing the hypothesis that Al-induced apoptosis is linked to mitochondrial cytochrome *c* translocation, and that aging is an important factor in this process. We report here that pretreatment with cyclosporin A indeed inhibits translocation of cytochrome *c*, presumably by preventing the opening of the MTP.

*Corresponding author: Dr. John Savory, Department of Pathology, University of Virginia Health Sciences Center, Box 168, Charlottesville, Virginia 22908 USA. Tel.: +1 804 924 5682; Fax: +1 804 924 5718; E-mail: js2r@virginia.edu.

Journal of Alzheimer's Disease 3 (2001) 1–5 JAD112
ISSN 1387-2877 / $8.00

Table 1
Ten groups of 4 animals each were used as follows: One group of aged and 1 of young rabbits received no treatment and were used as controls. Three aged and 3 young groups of animals received saline, followed 1 hour later by Al maltolate and were sacrificed at 3, 24 or 72 hrs. Two groups of aged rabbits were pretreated with cyclosporin A (Cs A) followed at 1 hr by Al and were sacrificed at 3 or 24 hrs later. Experimental design for the groups of animals used per treatment regimen

Treatment regimen					Time of sacrifice
Untreated		Saline/Al		Cs A/Al	
aged	young	aged	young	aged	
4	4				0 hr
		4	4	4	3 hr
		4	4	4	24 hr
		4	4		72 hr

2. Materials and methods

All animal procedures were in accordance with the U.S. Public Health Service Policy on Humane Care and Use of Laboratory Animals, and the National Institutes of Health Guide for the Care and Use of Laboratory animals. The animal protocol was approved by the University of Virginia Animal Care and Use Committee. Aged (4–5 years old) and young (8–12 months old) female New Zealand white rabbits received intracisternal injections of 100 μL physiological saline followed by 100 μL 25 mM Al maltolate, or 250 μg of cyclosporin A (Sandimmune, Novartis Pharmaceuticals Corporation, East Hanover, NJ) in 100 μL of saline, followed by 100 μL 25 mM Al maltolate (see Table 1 for the experimental design). The injections were carried out under ketamine anesthesia as described previously [17]. The quantities of materials injected were the same for the aged and young animals, since preliminary experiments in our laboratory have shown that brain weights are within 10% of each other in both age groups (9.10$\forall$0.61 g in the young, $n = 6$, and 9.80$\forall$0.59 g in the aged, $n = 6$) despite a marked difference in body weight (3.07$\forall$0.73 kg in the young and 5.0$\forall$0.29 kg in the aged). Three groups of 4 aged and 4 young adult rabbits received saline (0 hr) followed by Al maltolate at 1 hr, and were sacrificed 3, 24 or 72 hrs following Al administration. Two groups consisting of 4 aged rabbits received cyclosporin A treatment (0 hr) followed by Al maltolate administration 1 hr later, and animals were sacrificed at 3 or 24 hrs after the Al injection. Two more groups of 4 aged and 4 young adult rabbits received no treatment and served as controls. Rabbits were euthanized and perfused with Dulbecco's phosphate buffered saline (GIBCO, Grand Island, NY) as described previously [8,18]. Brains were removed within 5 minutes after perfusion and tissue from hippocampus and adjacent cortex was rapidly dissected, homogenized and subjected to ultracentrifugation as described below.

Proteins from the mitochondrial and cytosolic fractions were extracted as described previously [9]. Approximately 100 mg of brain tissue from hippocampus was gently homogenized using a teflon homogenizer (Thomas, Philadelphia PA) in 7 volumes of cold suspension buffer (20 mM HEPES-KOH (pH 7.5), 250 mM sucrose, 10 mM KCl, 1.5 mM MgCl2, 1 mM EDTA, 1 mM EGTA, 1 mM DTT, 0.1 mM PMSF, 2 μg/ml aprotinin, 10 μg/ml leupeptin, 5 μg/ml pepstatin and 12.5 μg/ml of N-acetyl-Leu-Leu-Norleu-Al). The homogenates were first centrifuged at 750 g at 4°C for 5 min, and then at 8000 g for 20 min at 4°C. The pellets from the 8000 g centrifugation were resuspended in cold buffer without sucrose, and used as the mitochondrial fraction. The supernatant was further centrifuged at 100,000 g for 60 min at 4°C and used as the cytosolic fraction. Protein concentrations were determined with the BCA protein assay reagent (Pierce, Rockford, Illinois). Samples from both the mitochondrial and cytosolic fractions, containing 7.5 μg of protein, were separated by SDS-PAGE (15% gel) under reducing conditions, followed by transfer to polyvinylidene difluoride membrane (Millipore, Bedford, MD) at 30 mA for 210 min in transfer buffer (20 mM Tris-base, 150 mM glycine, 20% methanol). Following transfer, membranes were incubated with mouse monoclonal antibody to human cytochrome *c* (7H8.2C12, Pharmingen, San Diego, California) at a 1:500 dilution. Monoclonal anti-β-actin (Sigma, Saint Louis, MI) was used at a 1:250 dilution as a gel loading control. Following washes with TBS containing 0.1% Triton X-100, the blots were developed using enhanced chemiluminescence (Immun-Star goat anti-mouse IgG detection kit, Bio-Rad, Hercules, CA). Cytochrome *c* bands on the radiographic films were scanned and densitometrically analyzed using Personal Densiometer SI and Image Quant 5.0 Software (Molecular Dynamics, Sunnyvale, CA).

3. Results

Immunoreactivity of cytochrome *c* in the hippocampus is evident as a single 15 kDa band, thus confirming the specificity of the monoclonal antibody for cytochrome *c*. In aged animals, cytochrome *c* immunoreactivity is strongly reactive in both the cytosolic and mitochondrial fractions at 3 hr and 24 hrs after Al treat-

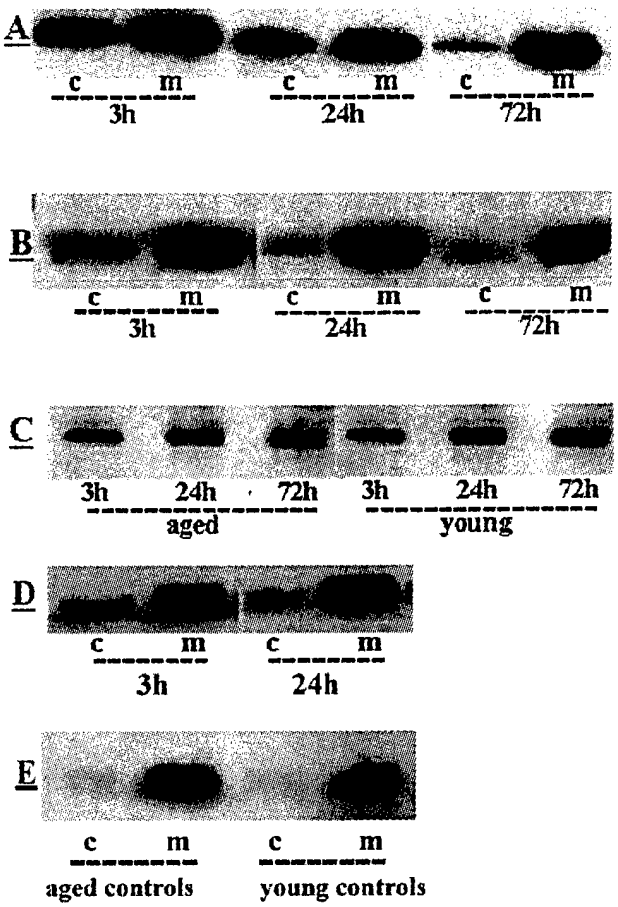

Fig. 1. Representative Western blot analysis of cytosolic (c) and mitochondrial (m) cytochrome *c* in hippocampus of rabbit brain. A: In aged animals, Al maltolate induces cytochrome *c* release into the cytosol at 3 or 24 hrs but not at 72 hr. B: In young animals, cytochrome *c* is barely detectable in the cytosolic fractions at 3, 24 or 72 hrs but is strongly positive in the mitochondrial fractions. C: ∃-actin shows similar protein loading of the cytosolic fractions of aged and young rabbits at 3, 24 and 72 hrs after Al maltolate administration. D: Pretreatment with cyclosporin A inhibits the Al maltolate-induced cytochrome *c* release into the cytosol of aged rabbit hippocampus at 3 or 24 hrs. E: Cytochrome *c* is only detectable in mitochondria and not in the cytosolic fractions of aged and young control hippocampus.

ment. After 72 hrs, mitochondrial cytochrome *c* reactivity is present but the cytosolic fraction contains only a faintly detectable band (Fig. 1(A)). In young animals, cytochrome *c* is intense in the mitochondria but barely detectable in the cytoplasmic fraction at 3, 24 and 72 hrs (Fig. 1(B)). The use of β-actin as a control for the Western blot analysis shows similar amounts of protein loading from the cytosolic fractions in aged and young animals (Fig. 1(C)). Pretreatment with cyclosporin A, 1 hr prior to Al administration, prevents the release of cytochrome *c* into the cytoplasm; this is observed in the aged animals at 3 and 24 hrs (Fig. 1(D)). Figure 1E shows intense immunoreactivity for cytochrome *c* in the mitochondrial fraction but not in the cytosolic fraction of aged and young control brains. The results of the densitometric analysis of cytosolic and mitochondrial cytochrome *c* in aged animals are presented in Fig. 2 showing that pretreatment with cyclosporin A inhibits Al maltolate-induced cytochrome *c* release at 3 and 24 hrs. Results shown above are from hippocampal specimens, however, identical results are obtained using tissue obtained from adjacent cortex (data not shown).

4. Discussion

The current study provides the first in vivo evidence that aging increases susceptibility to stress-induced opening of the MTP, as assessed by cytochrome *c* re-

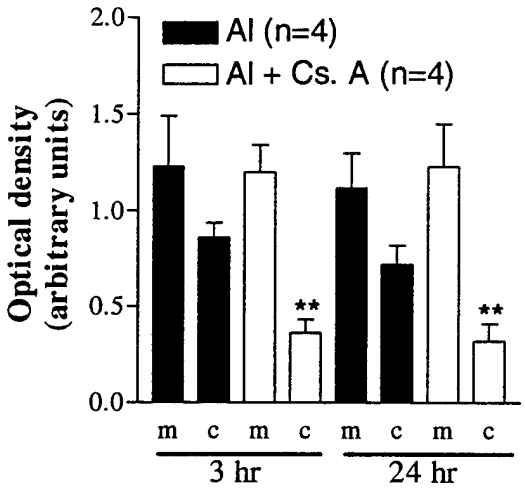

Fig. 2. The results of densitometric analysis of mitochondrial (m), and cytosolic (c) cytochrome *c* in the hippocampus of aged rabbits receiving either Al maltolate or cyclosporin A (Cs A) plus Al-maltolate, animals are sacrificed at 3, 24 hrs. The Al maltolate-induced cytochrome *c* release at 3 and 24 hrs (dark bars) is strongly reduced by pretreatment with cyclosporin A (white bars), $**p < 0.01$ (unpaired Student *t* test).

lease from mitochondria into the cytosol in hippocampus (and cortex) of aged rabbits treated intracisternally with Al-maltolate. The appearance of cytochrome *c* in the cytosol of aged rabbit brain occurs at 3 and 24 hrs following the Al-maltolate treatment, and is dramatically reduced by pretreatment with cyclosporin A, an agent known to block the opening of the MTP [14]. At 72 hrs following Al maltolate administration, the presence of cytochrome *c* in the cytoplasm is no longer evident; it is unclear why this occurs although it could be due to re-closing of the MPTP. In contrast to the response in aged rabbits, young animals barely exhibit cytosolic immunoreactivity for cytochrome *c* following Al administration, and for this reason it was not deemed necessary to perform the experiment of pretreating these young rabbits with cyclosporin A. Release of cytochrome *c* into the cytosol is reported to result from its diffusion following cytotoxic stimuli from its location through the MTP between the inner and outer mitochondrial membranes [1]. Opening of the MTP rapidly causes depolarization, uncoupling of oxidative phosphorylation, and subsequent pronounced mitochondrial swelling [23]. Numerous agents, including Ca^{2+}, inorganic phosphate and oxidant chemicals are known to promote MTP opening [23,24]. Although the exact composition of the MTP is not yet known, it involves proteins from the cytosol, the outer and the inner mitochondrial membranes and the matrix (cyclophilin D) [4,12,24]. Cyclosporin A is reported to block the MTP opening by specifically binding mitochondrial cyclophilin [5,24]. In the present study, inhibition by cyclosporin A of the translocation of cytochrome *c* into the cytosol following Al-maltolate treatment, suggests that the observed cytosolic cytochrome *c* originates from mitochondrial release, as a consequence of opening of the MTP.

Mounting evidence implicates mitochondria as a critical site at which different apoptotic signals converge. Mitochondria are assumed to be involved in apoptosis by opening the MTP which causes the release of cytochrome *c* into the cytoplasm, resulting in caspase activation which in turn has been shown to trigger apoptosis [9]. In the present study, although cytochrome *c* release in aged rabbits is suggested to result from the opening of the MTP, as assessed by the ability of cyclosporin A to inhibit its release, the mechanism by which Al maltolate administration induces the opening of the MTP remains to be determined. Aluminum maltolate-induced cytochrome *c* release may result from an alteration of the mitochondrial membrane potential, generation of reactive oxygen species, or perturbation of Ca^{2+} hemostasis. One other possible mechanism is that Al maltolate may cause an overexpression of the proapoptotic Bax, as we have previously described [19], which then translocates from the cytosol to the mitochondria and leads to cytochrome *c* release. Indeed, in several models of cell death, the overexpression of Bax induces its translocation from the cytosol to the mitochondria [6,21] with a subsequent release of cytochrome *c* [16]. The observation that in young animals cytochrome *c* is not released into the cytosol following Al maltolate administration, indicates that in this case the mitochondria resist opening of MTP. The difference in pore opening between aged and young animals indicates that aging is a facilitating factor in this important event. This difference in the opening of the MTP and subsequent release of cytochrome *c* may account for the more deleterious effects following Al maltolate administration in aged rabbits as compared to the young, as described in our previous report [19].

In conclusion, the present findings implicate mitochondrial injury as assessed by cytochrome *c* release, as an early event in Al-induced neuronal injury. In addition, opening of the MTP as an important component of this process, is implicated. Since the Al-rabbit model system demonstrates many of the biochemical and neurofibrillary changes found in Alzheimer's disease and related neurodegenerative disorders [7], we propose that MTP-related mechanisms of mitochondrial injury may also be important early events in these human diseases.

Acknowledgments

We gratefully acknowledge helpful discussions with Dr. Christos D. Katsetos. Supported by Grant # DAMD 17-99-1-9552 from the US Department of the Army.

References

[1] P. Bernardi and V. Petronilli, The permeability transition pore as a mitochondrial calcium release channel: a critical appraisal, *J Bioenerg Biomembr* **28** (1996), 131–138.

[2] C.A. Bradham, T. Qian, K. Streetz, C. Trautwein, D.A. Brenner and J.J. Lemasters, The mitochondrial permeability transition is required for tumor necrosis factor alpha-mediated apoptosis and cytochrome c release, *Mol Cell Biol* **18** (1998), 6353–6364.

[3] D.S. Cassarino and J.P. Bennett, An evaluation of the role of mitochondria in neurodegenerative diseases: mitochondrial mutations and oxidative pathology, protective nuclear responses, and cell death in neurodegeneration, *Brain Res Rev* **29** (1999), 1–25.

[4] Q. Guo, W. Fu, F.W. Holtsberg, S.M. Steiner and M.P. Mattson, Superoxide mediates the cell- death-enhancing action of presenilin-1 mutations, *J Neuroscience Res* **56** (1999), 457–470.

[5] A.P. Halestrap and A.M. Davidson, Inhibition of Ca^{2+}-induced large-amplitude swelling of liver and heart mitochondria by Cyclosporin is probably caused by the inhibitor binding to mitochondrial-matrix peptidyl-prolyl cis-trans isomerase and preventing it interacting with the adenine nucleotide translocase, *Biochem J* **268** (1990), 153–160.

[6] Y.T. Hsu, K.G. Wolter and R.J. Youle, Cytosol-to-membrane redistribution of Bax and Bcl-X(L) during apoptosis, *Proc Natl Acad Sci USA* **94** (1997), 3668–3672.

[7] Y. Huang, M.M. Herman, J. Liu, C.D. Katsetos, M.R. Wills and J. Savory, Neurofibrillary lesions in experimental aluminum-induced encephalopathy and Alzheimer's disease share immunoreactivity for amyloid precursor protein, Aβ, α_1-antichymotrypsin and ubiquitin-protein conjugates, *Brain Res* **771** (1997), 213–220.

[8] C.D. Katsetos, J. Savory, M.M. Herman, R.M. Carpenter, A. Frankfurter, C.D. Hewitt and M.R. Wills, Neuronal cytoskeletal lesions induced in the CNS by intraventricular and intravenous aluminium maltol in rabbits, *Neuropathol Appl Neurobiol* **16** (1990), 511–528.

[9] X. Liu, C.N. Kim, J. Yang, R. Jemmerson and X. Wang, Induction of apoptotic program in cell-free extracts: requirement for dATP and cytochrome c, *Cell* **86** (1996), 147–157.

[10] K. Meguro, X. Blaizot, Y. Kondoh, C. Le Mestric, J.C. Baron and C. Chavoix, Neocortical and hippocampal glucose hypometabolism following neurotoxic lesions of the entorhinal and perirhinal cortices in the non-human primate as shown by PET. Implications for Alzheimer's disease, *Brain* **122** (1999), 1519–1531.

[11] Y. Morita-Fujimura, M. Fujimura, M. Kawase, S.F. Chen and P.H. Chan, Release of mitochondrial cytochrome c and DNA fragmentation after cold injury-induced brain trauma in mice: possible role in neuronal apoptosis, *Neurosci Lett* **267** (1999), 201–205.

[12] M.D. Neely, K.R. Sidell, D.G. Graham and T.J. Montine, The lipid peroxidation product 4-hydroxynonenal inhibits neurite outgrowth, disrupts neuronal microtubules, and modifies cellular tubulin, *J Neurochem* **72** (1999), 2323–2333.

[13] D.O. Okonkwo, A. Buki, R. Siman and J.T. Povlishock, Cyclosporin A limits calcium-induced axonal damage following traumatic brain injury, *NeuroReport* **10** (1999), 353–358.

[14] V. Petronilli, C. Cola, S. Massari, R. Colonna and P. Bernardi, Physiological effectors modify voltage sensing by the cyclosporin A-sensitive permeability transition pore of mitochondria, *J Biol Chem* **268** (1993), 21939–21945.

[15] K.S.J. Rao, S. Anitha and K.S. Latha, Aluminium-induced neurodegeneration in the hippocampus of aged rabbits mimics Alzheimer's disease, *Alz Reports* **3** (2000), 83–88.

[16] T. Rosse, R. Olivier, L. Monney, M. Rager, S. Conus, I. Fellay, B. Jansen and C. Borner, Bcl-2 prolongs cell survival after Bax-induced release of cytochrome c, *Nature* **391** (1998), 496–499.

[17] J. Savory, Y. Huang, M.M. Herman, M.R. Reyes and M.R. Wills, Tau immunoreactivity associated with aluminum maltolate-induced neurofibrillary degeneration in rabbits, *Brain Res* **669** (1995), 325–329.

[18] J. Savory, Y. Huang, M.M. Herman and M.R. Wills, Quantitative image analysis of temporal changes in tau and neurofilament proteins during the course of acute experimental neurofibrillary degeneration; non-phosphorylated epitopes precede phosphorylation, *Brain Res* **707** (1996), 272–281.

[19] J. Savory, J.K.S. Rao, Y. Huang, P. Letada and M.M. Herman, Age-related hippocampal changes in Bcl-2: Bax ratio, oxidative stress, redox-active iron and apoptosis associated with aluminum-induced neurodegeneration: increased susceptibility with aging, *NeuroToxicol* **20** (1999), 805–818.

[20] H. Uchino, E. Elmer, K. Uchino, O. Lindvall and B.K. Siesjo, Cyclosporin A dramatically ameliorates CA1 hippocampal damage following transient forebrain ischaemia in the rat, *Acta Physiologic Scand* **155** (1995), 469–471.

[21] K.G. Wolter, Y.T. Hsu, C.L. Smith, A. Nechushtan, X.G. Xi and R.J. Youle, Movement of Bax from the cytosol to mitochondria during apoptosis, *J Cell Biol* **139** (1997), 1281–1292.

[22] Z.X. Yao, K. Drieu, L.I. Szweda and V. Papadopoulos, Free radicals and lipid peroxidation do not mediate beta-amyloid-induced neuronal cell death, *Brain Res* **847** (1999), 203–210.

[23] N. Zamzami, S.A. Susin, P. Marchetti, T. Hirsch, I. Gomez-Monterrey, M. Castedo and G. Kroemer, Mitochondrial control of nuclear apoptosis, *J Exp Med* **183** (1996), 1533–1544.

[24] M. Zoratti and I. Szabo, The mitochondrial permeability transition, *Biochimica et Biophysica Acta* **1241** (1995), 139–176.

APPENDIX II

ELSEVIER

Brain Research 903 (2001) 66–73

BRAIN RESEARCH

www.elsevier.com/locate/bres

Research report

Co-involvement of mitochondria and endoplasmic reticulum in regulation of apoptosis: changes in cytochrome *c*, Bcl-2 and Bax in the hippocampus of aluminum-treated rabbits

Othman Ghribi[a], David A. DeWitt[c], Michael S. Forbes[a], Mary M. Herman[d], John Savory[a,b,*]

[a]*Department of Pathology, University of Virginia Health Sciences Center, Box 168, Charlottesville, VA 22908, USA*
[b]*Department of Biochemistry and Molecular Genetics and Chemistry, University of Virginia Health Sciences Center, Box 168, Charlottesville, VA 22908, USA*
[c]*Department of Biology and Chemistry, Liberty University, Lynchburg, VA, USA*
[d]*IRP, NIMH, NIH, Bethesda, MD, USA*

Accepted 13 March 2001

Abstract

Neurodegenerative diseases, including Alzheimer's disease, are characterized by a progressive and selective loss of neurons. Apoptosis under mitochondrial control has been implicated in this neuronal death process, involving the release of cytochrome *c* into the cytoplasm and initiation of the apoptosis cascade. However, a growing body of evidence suggests an active role for the endoplasmic reticulum in regulating apoptosis, either independent of mitochondrial, or in concert with mitochondrial-initiated pathways. Members of the Bcl-2 family of proteins have been shown to either inhibit apoptosis, as is the case with Bcl-2, or to promote it, in the case of Bax. Investigations in our laboratory have focused on neuronal injury resulting from the intracisternal administration of aluminum maltolate to New Zealand white rabbits, an animal system relevant to a study of human disease in that it reflects many of the histological and biochemical changes associated with Alzheimer's disease. Here we report that treatment of young adult rabbits with aluminum maltolate induces both cytochrome *c* translocation into brain cytosol, and caspase-3 activation. Furthermore, as assessed by Western blot analysis, these effects are accompanied by a decrease in Bcl-2 and an increase in Bax reactivity in the endoplasmic reticulum.

Theme: Disorder of the nervous system

Topic: Neurotoxicity

Keywords: Bcl-2; Bax; Mitochondria; Endoplasmic reticulum; Alzheimer's disease; Aluminum

1. Introduction

Apoptosis, which plays a critical role in the normal development and maintenance of tissue homeostasis, plays an important role in neurodegenerative diseases and aging [26]. Alzheimer's disease, a common neurodegenerative disorder, is characterized typically by intraneuronal neurofibrillary tangles, neuritic plaques and selective neuronal death, with evidence of apoptosis being observed as an early event preceding the formation of these classical neuropathological features [32]. Mitochondrial changes following cytotoxic stimuli represent a primary event in apoptotic cell death, since the apoptogenic factor, cytochrome *c*, is released into the cytoplasm [2,15,20,21]. Once this translocation occurs, cytochrome *c* binds to another cytoplasmic factor, Apaf-1, and the formed complex activates the initiator caspase-9 that in turn activates the effector caspases, of which caspase-3 is a prominent member [17,31]. Release of cytochrome *c* from the mitochondria has been shown to involve two distinct pathways. One implicates the opening of the mitochondria permeability transition pore (MTP), and the second, trig-

*Corresponding author. Tel.: +1-804-924-5682; fax: +1-804-924-5718.
E-mail address: js2r@virginia.edu (J. Savory).

0006-8993/01/$ – see front matter
PII: S0006-8993(01)02406-4

gered by the proapoptogenic Bax, is independent of the MTP opening [6]. While Bax has been shown to trigger cell death [7,35], the antiapoptotic Bcl-2 can block cytochrome *c* release and caspase activation [1,25]. Bcl-2 resides in the mitochondria and prevents activation of the effector caspases by mechanisms such as blockade of the MTP opening [19,30], or by functioning as a docking protein [24].

Although Bcl-2 may have a direct action on the mitochondria, it also resides in the endoplasmic reticulum [4,36]. A growing body of evidence suggests an active role for the endoplasmic reticulum in the regulation of apoptosis. Indeed, stress in the endoplasmic reticulum has been shown to induce apoptosis [34] and, furthermore, the endoplasmic reticulum induces activation of caspase-12, an effect not triggered by mitochondrial stress [22]. Recently, it has been reported that the drug brefeldin induces endoplasmic reticulum dilatation and leads to cytochrome *c* release and caspase-3 activation [8]. This effect was blocked by the wild-type Bcl-2 and, surprisingly, a Bcl-2 variant that is exclusively targeted to the endoplasmic reticulum, was also able to accomplish the same task [8]. The authors suggested the existence of 'cross-talk' under Bcl-2 control between the endoplasmic reticulum and mitochondria, and that Bcl-2 may exert its protective effect by controlling calcium homeostasis in the different cell compartments.

Studies in our laboratory have focused on neuronal injury resulting from the intracisternal administration of aluminum (Al) maltolate to New Zealand white rabbits. This animal system is relevant to a study of human disease in that it reflects many of the histological and biochemical changes associated with Alzheimer's disease [10]. In the present study we have investigated the effect of Al maltolate-induced neurotoxic injury on cytochrome *c* release and caspase-3 activation in hippocampus of young adult rabbits. Changes in Bcl-2 and Bax responses in mitochondria and endoplasmic reticulum were further assessed to determine whether cross-talk between these intracellular organelles is also involved in the control of programmed cell death in this animal system.

2. Material and methods

2.1. Animals and treatment

All animal procedures were in accordance with the US Public Health Service Policy on Humane Care and Use of Laboratory Animals, and the National Institutes of Health Guide for the Care and Use of Laboratory Animals. The animal protocol was approved by the University of Virginia Animal Care and Use Committee. Young adult (8–12 months old) female New Zealand white rabbits received either intracisternal injections of 100 μl saline (controls, $n=6$) or 100 μl of 50 mM Al maltolate in saline (treated, $n=6$). Al maltolate is soluble at neutral pH, thus avoiding precipitation of insoluble Al hydroxide as encountered with most of other Al compounds used for neurotoxicological studies [29]. The injection was carried out under ketamine anesthesia according to the method described previously [27]. Al-treated animals and matched controls were sacrificed on days 2 or 3, depending on the time required for the development of severe neurological symptoms in the Al-treated group. Rabbits were euthanized and then perfused with Dulbecco's phosphate-buffered saline (PBS, Gibco, Grand Island, NY) as described previously [10,11,28]. Brains were immediately removed after sacrifice, and a coronal section cut and bisected to yield two symmetrical hippocampal segments, one for immunohistochemistry and the other for immunoblot analysis. The respective sides chosen for these studies were alternated between successive animals. Each brain hemisphere intended for histology was immediately frozen on a liquid nitrogen-cooled surface, placed into a zipper-closure plastic bag, and buried in dry ice pellets until transferring to −80°C before sectioning. For immunoblot analysis, tissue from the hippocampus was rapidly dissected, homogenized and subjected to ultracentrifugation as described below.

2.2. Western blot analysis

Proteins from the mitochondrial, cytosolic and endoplasmic fractions were extracted as described previously [18]. Approximately 100 mg of brain tissue from hippocampus was gently homogenized, using a teflon homogenizer (Thomas, Philadelphia PA), in seven volumes of cold suspension buffer (20 mM Hepes–KOH (pH 7.5), 250 mM sucrose, 10 mM KCl, 1.5 mM $MgCl_2$, 1 mM EDTA, 1 mM EGTA, 1 mM DTT, 0.1 mM PMSF, 2 μg/ml aprotinin, 10 μg/ml leupeptin, 5 μg/ml pepstatin and 12.5 μg/ml of *N*-acetyl-Leu-Leu-Norleu-Al). The homogenates were first centrifuged at 750×*g* at 4°C for 5 min, and then at 8000×*g* for 20 min at 4°C. The 8000×*g* pellets were resuspended in cold buffer without sucrose and used as the mitochondrial fraction. The supernatant was further centrifuged at 100 000×*g* for 60 min at 4°C to separate the cytosolic from the endoplasmic reticulum fractions. Protein concentrations were determined with the BCA protein assay reagent (Pierce, Rockford, IL). Proteins (7.5 μg) from the mitochondrial, cytosolic and endoplasmic fractions were separated by SDS–PAGE (15% gel) under reducing conditions followed by transfer to a polyvinylidene difluoride membrane (Millipore) at 30 mA for 210 min in transfer buffer (20 mM Tris-base, 150 mM glycine, 20% methanol). Following transfer, membranes were incubated with mouse monoclonal antibody (mAb) to human cytochrome *c* (Pharmingen, San Diego, CA) at a 1:250 dilution, or to a 1:100 dilution of mAbs recognizing either Bcl-2 or Bax (Santa Cruz Biotechnology, CA). Cytochrome oxidase subunit IV (COX) mAb obtained

from a commercial source (Molecular Probes, Eugene, OR) was used as a marker of mitochondrial contamination at 1:1000 dilution. A calnexin mAb (Transduction Laboratories, Lexington, MD) was used at 1:500 dilution as an endoplasmic reticulum marker, and a mAb to anti-β actin (Sigma, St. Louis, MO) was used at a 1:250 dilution as a gel loading control. Following washes with Tris-buffered saline (TBS) containing 0.1% Triton X-100, the blots were developed using enhanced chemiluminescence (Immun-Star goat anti-mouse IgG detection kit, Bio-Rad, Hercules, CA). The bands of cytochrome *c*, Bax and Bcl-2 which had been developed on radiographic film, were scanned and densitometrically analyzed using Personal Densitometer SI and Image Quant 5.0 software (Molecular Dynamics, Sunnyvale, CA), and these quantitative analyses were expressed as mean±S.E.M. values. Unpaired Student's *t*-test was used to compare levels of each protein between controls and Al-treated groups in the same subcellular fraction.

2.3. Fluorometric assay of caspase-3 activities

Lysates were prepared by homogenizing hippocampal tissue in 20 mM Hepes–KOH (pH 7.5), 250 mM sucrose, 10 mM KCl, 1.5 mM $MgCl_2$, 1 mM EDTA, 1 mM EGTA, 1 mM DTT, 0.1 mM PMSF. Lysates were centrifuged for 30 min at 160 000×*g* and proteins in the supernatant were quantified using the Bradford method. Lysates (50 μg protein) were incubated for 1 h at 37°C in 1 ml of 1× Hepes buffer containing 10 μl of the fluorogenic substrate Ac-DEVD-AMC (Caspase-3 assay kit, Pharmingen, San Diego, CA). Cleavage of the substrate was monitored at an excitation wavelength of 380 nm and emission wavelength of 440 nm using a Model 450 fluorometer (BioMolecular). Each sample was incubated with or without 10 μl of the caspase-3 inhibitor Ac-DEVD-CHO (Pharmingen, Saint Diego, CA). Caspase-3 activity for each sample was calculated as the difference between the rate of cleavage in the absence and presence of the inhibitor.

2.4. Immunohistochemistry

Serial 14-μm thick coronal frozen sections from control and Al-treated animals were cut at the level of the hippocampus and stored at −80°C prior to immunostaining. The sections were air-dried at room temperature, fixed in cold acetone for 10 min, treated with 1% hydrogen peroxide in PBS and incubated with a blocking solution of 1.5% normal serum, also in PBS. Subsequently, sections were reacted overnight at 4°C with a mouse mAb against caspase-3 (CPP32, Transduction Laboratories, Lexington, KY) at a 1:500 dilution. After washing with 50 mM TBS, and incubating with the biotinylated secondary antibody, sections were processed with a Vectastain Elite avidin–biotin complex technique kit (Vector Laboratories, Burlingame, CA) and visualized by 3,3′-diaminobenzidine/hydrogen peroxide, with light hematoxylin counterstaining. All procedures were performed at room temperature unless otherwise noted.

3. Results

3.1. Western blot analysis

To confirm the purity of the subcellular fractions, we used antibodies against organelle-specific marker proteins; cytochrome *c* oxidase for mitochondria and calnexin for endoplasmic reticulum. As shown in Fig. 1, the fractions were pure, and the β-actin staining, used as a gel loading control, shows similar protein loading in all the wells.

The immunoreactivity of cytochrome *c* is evident as a single band with a molecular weight of 15 kDa. In controls, cytochrome *c* immunoreactivity is not detectable in the cytosolic fraction, but is strongly positive in the mitochondrial and endoplasmic fractions (Fig. 2A). In the Al-treated group, cytochrome *c* is distributed in the cytosolic, mitochondrial, and endoplasmic reticulum fractions (Fig. 2B).

The antibody to Bcl-2 identifies a protein band with an apparent molecular weight of 27 kDa. Bcl-2 is not detected in the cytoplasmic fractions, but relatively intense bands are found in the mitochondrial and endoplasmic fractions in controls (Fig. 2C). In the Al-treated group, Bcl-2 is restricted to the mitochondria and is barely detected in either the cytosolic or endoplasmic reticulum fractions (Fig. 2D). Bax, with an apparent molecular weight of 21 kDa, is distributed in all the fractions, but with a higher intensity in the cytosolic than in the mitochondrial or endoplasmic reticulum fractions (Fig. 2E). In the Al-

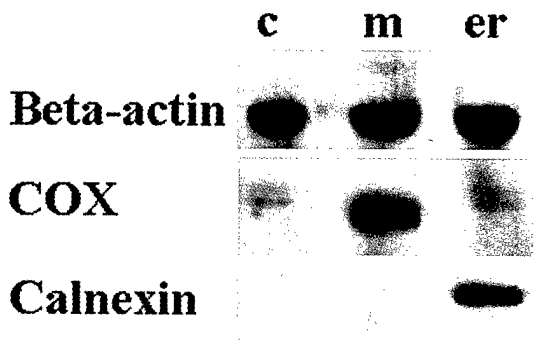

Fig. 1. Western blot analysis for β-actin, cytochrome *c* oxidase subunit IV (COX) and calnexin in cytoplasmic (c), mitochondrial (m) and endoplasmic reticulum (er) fractions from control hippocampal lysates. β-Actin, used as a control loading gel, shows similar protein loading in the mitochondrial, cytoplasmic and endoplasmic reticulum fractions. COX, used as a marker for mitochondrial contamination, is only present in the mitochondrial fractions. Calnexin, used as a marker for the endoplasmic reticulum, stains only the endoplasmic reticulum fractions.

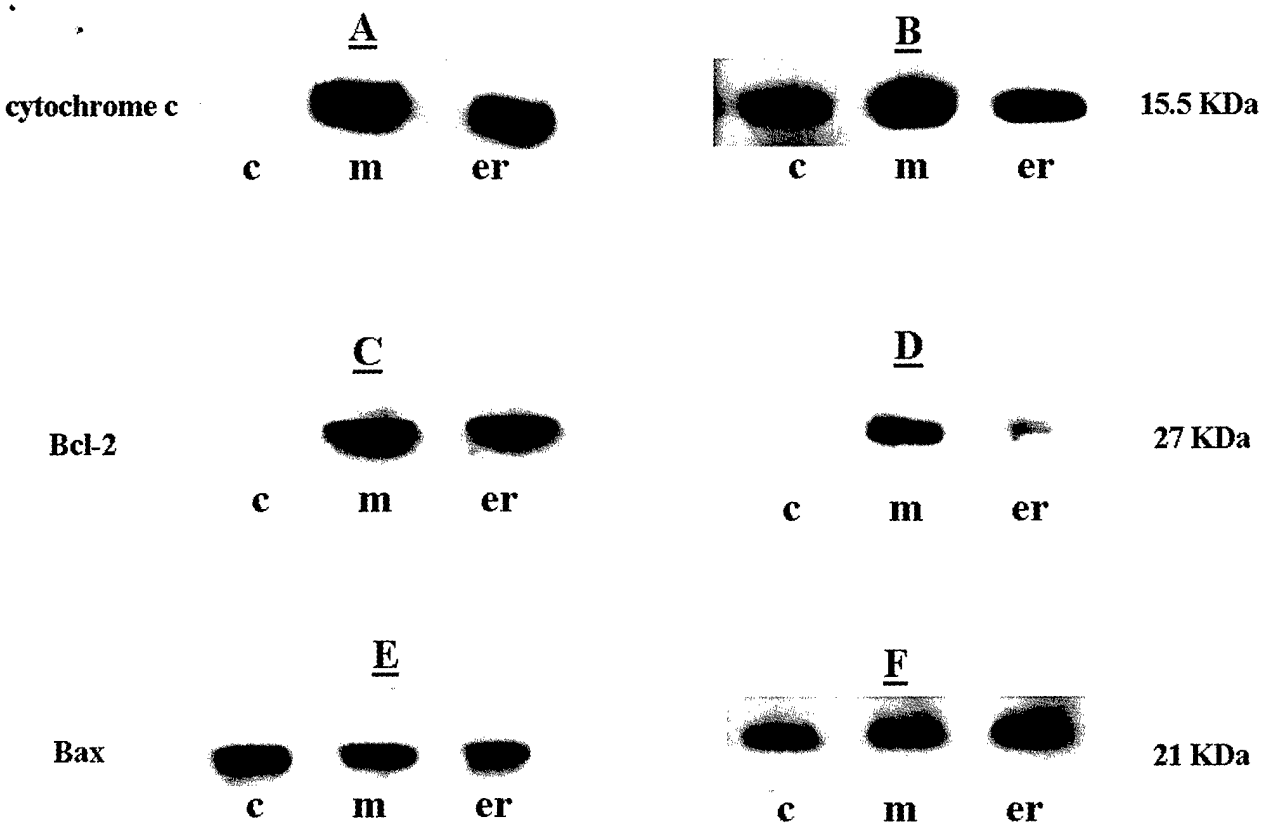

Fig. 2. Representative immunoblots for cytochrome *c*, Bcl-2 and Bax in controls (A,C,E) and in Al-treated groups (B,D,F) in cytoplasmic (c), mitochondrial (m) and endoplasmic reticulum (er) fractions from hippocampus lysates. (A) Cytochrome *c* immunoreactivity is not detected in the cytoplasm but is highly positive in the mitochondria and endoplasmic reticulum in controls. (B) Al treatment induces translocation of cytochrome *c* into the cytoplasm, and positive immunoreactivity for cytochrome *c* is also detected in the mitochondria and endoplasmic reticulum. (C) Bcl-2 staining, which is not detected in the cytoplasm, is highly positive in the mitochondrial and endoplasmic reticulum fractions. (D) Following Al treatment, Bcl-2 is decreased in the mitochondria and is barely detectable in the endoplasmic reticulum. (E) Bax is present in the cytoplasm as well as the mitochondria and endoplasmic reticulum in controls. (F) In the Al-treated group, Bax immunoreactivity is slightly decreased in the cytoplasm and increased in the mitochondria and endoplasmic reticulum.

treated animals, Bax immunoreactivity is detectable also in all the fractions; relative amounts are: endoplasmic reticulum>mitochondria>cytosol (Fig. 2F). The results of the densitometric analysis of cytosolic, mitochondrial and endoplasmic reticulum cytochrome *c*, Bcl-2 and Bax in controls and Al-treated rabbits, are shown in Table 1. Cytochrome *c* is absent in the cytoplasm of controls and its intensities in the other fractions are mitochondria> endoplasmic reticulum. Following Al treatment, cytochrome *c* is distributed as following, cytoplasm= mitochondria>endoplasmic reticulum. In controls, Bcl-2 is not present in the cytoplasmic fraction and levels in the other fractions are mitochondria>endoplasmic reticulum. In the Al-treated group, Bcl-2 is slightly decreased in the mitochondria and barely present in the endoplasmic reticulum. In controls, Bax is present in the three subcellular fractions as follows: cytoplasm>endoplasmic reticulum> mitochondria. Following the administration of Al maltolate the distribution of Bax is endoplasmic reticulm> mitochondria>cytoplasm.

3.2. Caspase-3 activity

The activity of caspase 3-like proteases as assessed by measuring the cleavage of the fluorogenic substrate Ac-DEVD-AMC, demonstrates significant elevations in Al-treated animals approaching 5-fold greater levels than in the controls (Fig. 3).

3.3. Immunohistochemistry

The immunohistochemical localization of caspase-3 in the pyramidal cell layer of the hippocampus of all animals was examined (Fig. 4A). No reaction for caspase-3 is observed in sections processed without incubation with primary antibody (data not shown), or in sections from untreated animals (Fig. 4B). In brains from Al-treated rabbits, there is marked positive immunostaining for caspase-3 in the pyramidal cell layers of the hippocampus (Fig. 4C, arrows).

Table 1
Densitometric scanning analysis of cytochrome *c*, Bcl-2 and Bax in the cytoplasm, mitochondria and endoplasmic reticulum of controls ($n=6$) and of Al-treated rabbits ($n=6$)

	Cytoplasm	Mitochondria	Endoplasmic reticulum
Cytochrome *c*			
Controls	–	2.0±0.15	1.60±0.18
Al-treated	1.75±0.16	1.75±0.22	0.85±0.11
Bcl-2			
Controls	–	1.50±0.10	1.29±0.16**
Al-treated	–	1.10±0.08	0.11±0.06**
Bax			
Controls	1.61±0.22*	0.72±0.13	1.02±0.08*
Al-treated	0.96±0.18*	1.00±0.10	1.42±0.23*

While cytochrome *c* is not detectable in the cytoplasm of controls, it is released into the cytosol following Al treatment. Bcl-2 resides in the mitochondria and endoplasmic reticulum in controls; Al treatment decreases Bcl-2 levels in the endoplasmic reticulum. Bax is distributed in the cytoplasm>endoplasmic reticulum>mitochondria in controls. Following Al administration, Bax is redistributed in the cytoplasm< mitochondria<endoplasmic reticulum.
–, undetectable levels. Data are expressed as mean±S.D. *$P<0.05$; **$P<0.01$ (Student's *t*-test).

4. Discussion

The current study provides evidence that neurotoxic injury, induced in rabbits by the intracisternal administration of Al-maltolate, results in cytoplasmic cytochrome *c* translocation, endoplasmic reticulum Bcl-2 down-regulation and Bax up-regulation, as well as caspase-3 activation. In a previous report from our laboratory [29] we presented immunohistochemical evidence for a similar decrease in the Bcl-2:Bax ratio, together with evidence of apoptosis, in aged rabbits treated with Al maltolate, but this effect was not observed in young adult animals. In the present study, by using a higher concentration of Al maltolate, we now report a dramatic effect following Al administration in young rabbits. There is considerable support for mitochondria playing a key role in the process of cell death, with much attention being focused on cytochrome *c*. When released into the cytoplasm, cytochrome *c* forms a complex with the cytosolic molecule Apaf-1 and activates caspase-9 [33,39]. Subsequently, this complex triggers the activation of effector caspases, in particular caspase-3 [17].

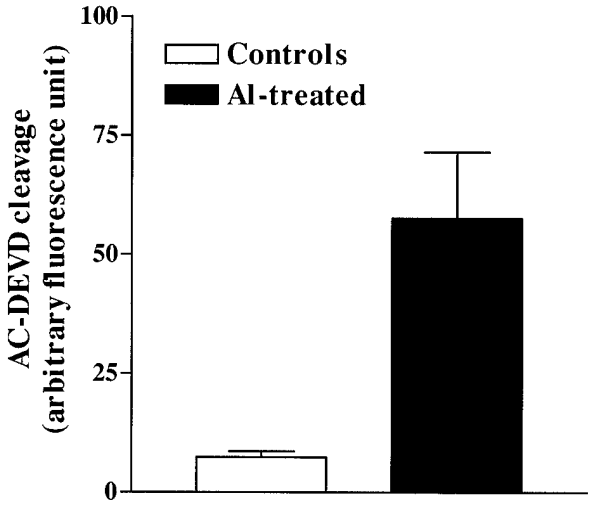

Fig. 3. Caspase-3 activity is shown in hippocampal lysates of controls (white bar) and Al-treated animals (black bar). In controls, low caspase-3 activity is detected. Al treatment induces a 5.5-fold increase in the caspase-3 activity. Data are presented as mean±S.E.M.

Release of cytochrome *c* from mitochondria into the cytosol has been reported following brain injury in mice [21] and addition of the the parkinsonian neurotoxin MPP+ to isolated brain mitochondria [2]. The mechanism by which cytochrome *c* is released from mitochondria to the cytosol is unclear. It has been suggested that following cytotoxic stimuli, the MTP opens and rapidly causes depolarization, uncoupling of oxidative phosphorylation, and subsequent pronounced mitochondrial swelling. Subsequent events are the diffusion of cytochrome *c* into the cytosol through the MTP from its location between the inner and outer mitochondrial membranes [19,38]. On the other hand, cytochrome *c* may also translocate from mitochondria into the cytosol but by a mechanism distinct from the opening of the MTP. Indeed, it has been shown that the pro-apoptotic Bax is able to trigger the release of cytochrome *c* from isolated mitochondria, and that this cytochrome *c* release is not blocked by inhibitors of the MTP opening [6]. Furthermore, it has been reported, in staurosporine-induced apoptosis of HeLa cells, that Bid, a BH3 domain-containing protein, translocates from the cytosol to mitochondria and binds to Bax. This direct binding of Bid to Bax is a prerequisite for Bax structural changes and subsequent cytochrome c release [5]. Our results show that following Al-maltolate treatment, Bax is redistributed to be present at higher levels in endoplasmic reticulum and mitochondria than in the cytosol. Changes in Bax distribution may then initiate cytochrome *c* release and caspase-3 activation. However, whether the cytochrome *c* release we report here results from opening of the MTP, or from an alternate pathway, remains to be determined.

Another interesting finding is the observation of decreased positivity of the anti-apoptotic protein, Bcl-2, in the endoplasmic reticulum following Al treatment. This protein is considered to be a key factor regulating apoptosis. It has been shown that Bcl-2-deficient mice underwent fulminant apoptosis of lymphoid tissue in the thymus and spleen, while mice overexpressing Bcl-2 demonstrated extended cell survival [13]. In other studies of cells treated with staurosporine, overexpression of Bcl-2 has been demonstrated to prevent the efflux of cytochrome *c* from the mitochondria and subsequent initiation of apoptosis [37]. In a cell-free apoptosis system, Bcl-2 over-expression has also been reported to prevent both the release of cytochrome c from mitochondria and activation of cas-

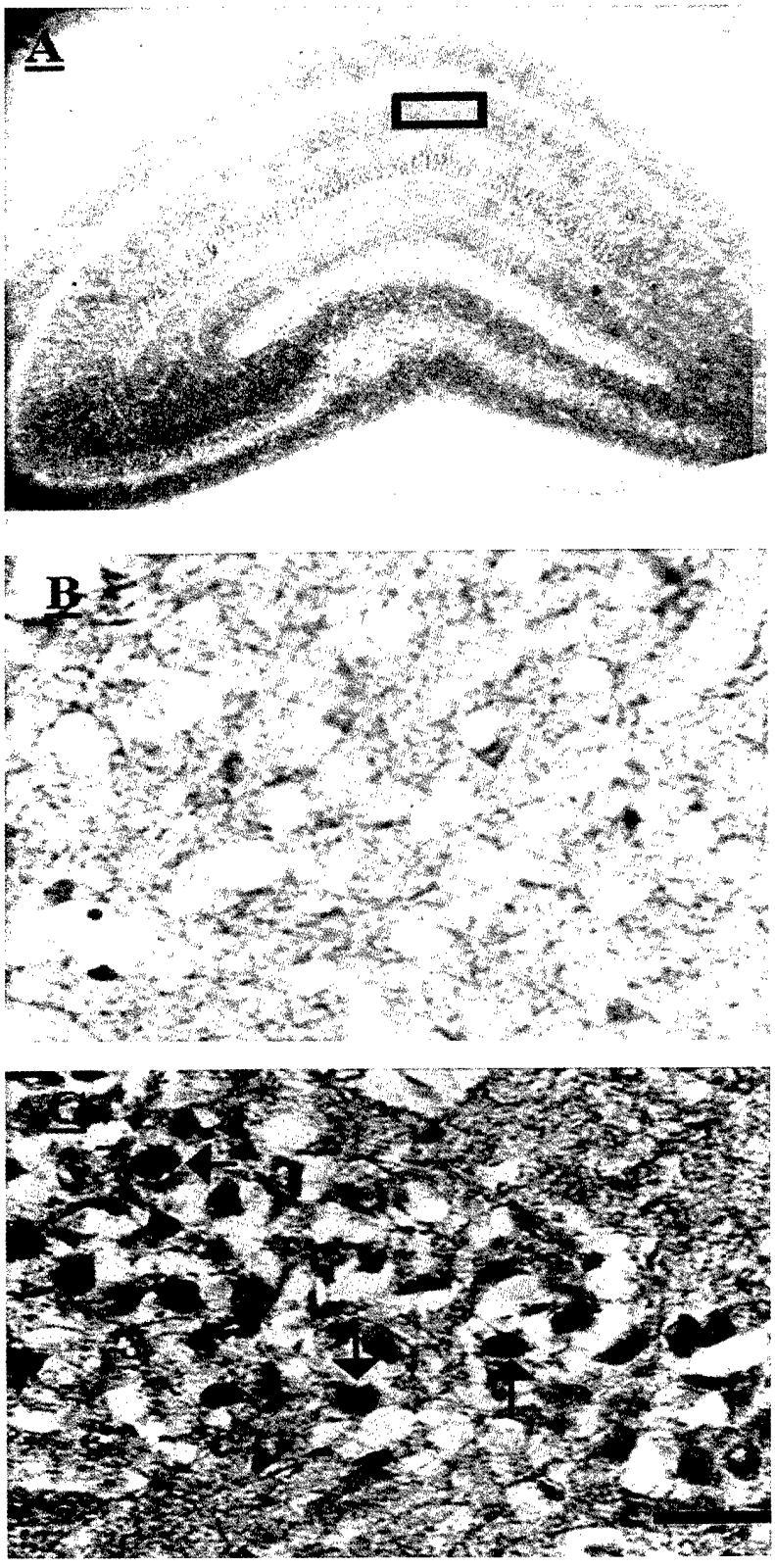

Fig. 4. Immunohistochemical localization of caspase-3 was examined in the pyramidal cell layer of the hippocampus (A, rectangular box). (B) Pyramidal cell layer of controls shows no immunoreactivity for caspase-3 (×400). (C) Positive immunoreactivity for caspase-3 (arrows) in the pyramidal cell layer in Al-treated animals (×400). Bar in (C)=25 μm.

pases [12]. Bcl-2 has also been found to prolong the life of rat neurons subjected to ischemia [3] in haloperidol-induced neuronal death in the hippocampus of mice [16], and in a transgenic mouse model of familial amyotrophic lateral sclerosis [14].

As we report here, the ratio of Bcl-2:Bax could be a key determining factor in the release of cytochrome *c*, the activation of caspase-3 and in the initiation of apoptosis, since these events are accompanied by an up-regulation of the pro-apoptotic Bax and a down-regulation of the anti-apoptotic Bcl-2. Furthermore, as the changes we observed for Bcl-2 and Bax mainly were in the endoplasmic reticulum, we suggest that the Bcl-2:Bax ratio in this cellular organelle regulates the extent of apoptosis. A decrease in this ratio may exacerbate apoptosis, and increasing this ratio may reverse the deleterious effect of cytotoxic stimuli.

The finding of alterations in cytochrome *c*, Bax and Bcl-2 in the present study raises the question as to whether the mitochondria or endoplasmic reticulum trigger apoptosis. Recent evidence now implicates the endoplasmic reticulum in this cell death pathway (for a review see Ref. [23]). In a recent paper, it has been demonstrated that cross-talk between mitochondria and endoplasmic reticulum is controlled by Bcl-2 [8]. Moreover, Bcl-2 is suggested to exert its anti-apoptotic effect by maintaining calcium homeostasis in the endoplasmic reticulum [9].

In conclusion, we have shown that Al maltolate induces cytochrome *c* release and caspase-3 activation in young adult rabbits. These effects are accompanied by a decrease of the anti-apoptotic Bcl-2 and an increase in the pro-apoptotic Bax in the endoplasmic reticulum, but the mechanism by which Al maltolate triggers these changes remains to be determined. Furthermore, whether cytochrome *c* release from mitochondria precedes changes in Bcl-2 and Bax in the endoplasmic reticulum, also remains to be ascertained. Nevertheless, our results demonstrate that in young adult rabbit brain, Al is able to trigger apoptosis via its action as a neurotoxin.

Acknowledgements

Supported by Grant # DAMD 17-99-1-9552 from USA Army to Dr. John Savory.

References

[1] J.M. Adams, S. Cory, The Bcl-2 protein family: arbiters of cell survival, Science 281 (1998) 1322–1326.

[2] D.S. Cassarino, J.K. Parks, W.D. Parker, J.P. Bennett, The parkinsonian neurotoxin MPP+ opens the mitochondrial permeability transition pore and releases cytochrome c in isolated mitochondria via an oxidative mechanism, Biochim. Biophys. Acta (Molecular Basis of Disease) 1453 (1999) 49–62.

[3] J. Chen, S.H. Graham, P.H. Chan, J. Lan, R.L. Zhou, R.P. Simon, Bcl-2 is expressed in neurons that survive focal ischemia in the rat, NeuroReport 6 (1995) 394–398.

[4] S. Cory, Regulation of lymphocyte survival by the Bcl-2 gene family, Annu. Rev. Immunol. 13 (1995) 513–543.

[5] S. Desagher, A. Osen-Sand, A. Nichols, R. Eskes, S. Montessuit, S. Lauper, K. Maundrell, B. Antonsson, J.C. Martinou, Bid-induced conformational change of Bax is responsible for mitochondrial cytochrome c release during apoptosis, J. Cell Biol. 144 (1999) 891–901.

[6] R. Eskes, B. Antonsson, A. Osen-Sand, S. Montessuit, C. Richter, R. Sadoul, G. Mazzei, A. Nichols, J.C. Martinou, Bax-induced cytochrome C release from mitochondria is independent of the permeability transition pore but highly dependent on Mg^{2+} ions, J. Cell Biol. 143 (1998) 217–224.

[7] A. Gross, J. Jockel, M.C. Wei, S.J. Korsmeyer, Enforced dimerization of Bax results in its translocation, mitochondrial dysfunction and apoptosis, EMBO J. 17 (1998) 3878–3885.

[8] J. Hacki, L. Egger, L. Monney, S. Conus, T. Rosse, I. Fellay, C. Borner, Apoptotic crosstalk between the endoplasmic reticulum and mitochondria controlled by Bcl-2, Oncogene 19 (2000) 2286–2295.

[9] H. He, M. Lam, T.S. McCormick, C.W. Distelhorst, Maintenance of calcium homeostasis in the endoplasmic reticulum by Bcl-2, J. Cell Biol. 138 (1997) 1219–1228.

[10] Y. Huang, M.M. Herman, J. Liu, C.D. Katsetos, M.R. Wills, J. Savory, Neurofibrillary lesions in experimental aluminum-induced encephalopathy and Alzheimer's disease share immunoreactivity for amyloid precursor protein, Aβ, α_1-antichymotrypsin and ubiquitin-protein conjugates, Brain Res. 771 (1997) 213–220.

[11] C.D. Katsetos, J. Savory, M.M. Herman, R.M. Carpenter, A. Frankfurter, C.D. Hewitt, M.R. Wills, Neuronal cytoskeletal lesions induced in the CNS by intraventricular and intravenous aluminium maltol in rabbits, Neuropathol. Appl. Neurobiol. 16 (1990) 511–528.

[12] R.M. Kluck, E. Bossy-Wetzel, D.R. Green, D.D. Newmeyer, The release of cytochrome c from mitochondria: a primary site for Bcl-2 regulation of apoptosis, Science 275 (1997) 1132–1136.

[13] S.J. Korsmeyer, X.M. Yin, Z.N. Oltvai, D.J. Veis-Novack, G.P. Linette, Reactive oxygen species and the regulation of cell death by the Bcl-2 gene family, Biochim. Biophys. Acta 1271 (1995) 63–66.

[14] V. Kostic, V. Jackson-Lewis, F. de Bilbao, M. Dubois-Dauphin, S. Przedborski, Bcl-2: prolonging life in a transgenic mouse model of familial amyotrophic lateral sclerosis, Science 277 (1997) 559–562.

[15] J.J. Lemasters, A.L. Nieminen, T. Qian, L.C. Trost, S.P. Elmore, Y. Nishimura, R.A. Crowe, W.E. Cascio, C.A. Bradham, D.A. Brenner, B. Herman, The mitochondrial permeability transition in cell death: a common mechanism in necrosis, apoptosis and autophagy, Biochim. Biophys. Acta 1366 (1998) 177–196.

[16] F. Lezoualc'h, R. Rupprecht, F. Holsboer, C. Behl, Bcl-2 prevents hippocampal cell death induced by the neuroleptic drug haloperidol, Brain Res. 738 (1996) 176–179.

[17] P. Li, D. Nijhawan, I. Budihardjo, S.M. Srinivasula, M. Ahmad, E.S. Alnemri, X. Wang, Cytochrome c and dATP-dependent formation of Apaf-1/caspase-9 complex initiates an apoptotic protease cascade, Cell 91 (1997) 479–489.

[18] X. Liu, C.N. Kim, J. Yang, R. Jemmerson, X. Wang, Induction of apoptotic program in cell-free extracts: requirement for dATP and cytochrome c, Cell 86 (1996) 147–157.

[19] I. Marzo, C. Brenner, N. Zamzami, S.A. Susin, G. Beutner, D. Brdiczka, R. Remy, Z.H. Xie, J.C. Reed, G. Kroemer, The permeability transition pore complex — a target for apoptosis regulation by caspases and Bcl-2-related proteins, J. Exp. Med. 187 (1998) 1261–1271.

[20] T.J. Montine, W.R. Markesbery, W. Zackert, S.C. Sanchez, L.J. Roberts, J.D. Morrow, The magnitude of brain lipid peroxidation correlates with the extent of degeneration but not with density of neuritic plaques or neurofibrillary tangles or with APOE genotype in Alzheimer's disease patients, Am. J. Pathol. 155 (1999) 863–868.

[21] Y. Morita-Fujimura, M. Fujimura, M. Kawase, S.F. Chen, P.H. Chan, Release of mitochondrial cytochrome c and DNA fragmentation after cold injury-induced brain trauma in mice: possible role in neuronal apoptosis, Neurosci. Lett. 267 (1999) 201–205.
[22] T. Nakagawa, H. Zhu, N. Morishima, E. Li, J. Xu, B.A. Yankner, J. Yuan, Caspase-12 mediates endoplasmic-reticulum-specific apoptosis and cytotoxicity by amyloid-beta, Nature 403 (2000) 98–103.
[23] W. Paschen, J. Doutheil, Disturbance of endoplasmic reticulum functions: a key mechanism underlying cell damage?, Acta Neurochir. Suppl. (Wien) 73 (1999) 1–5.
[24] J.C. Reed, Double identity for proteins of the Bcl-2 family, Nature 387 (1997) 773–776.
[25] J.C. Reed, Bcl-2 family proteins, Oncogene 17 (1998) 3225–3236.
[26] P.S. Sastry, K.S. Rao, Apoptosis and the nervous system, J. Neurochem. 74 (2000) 1–20.
[27] J. Savory, Y. Huang, M.M. Herman, M.R. Reyes, M.R. Wills, Tau immunoreactivity associated with aluminum maltolate-induced neurofibrillary degeneration in rabbits, Brain Res. 669 (1995) 325–329.
[28] J. Savory, Y. Huang, M.M. Herman, M.R. Wills, Quantitative image analysis of temporal changes in tau and neurofilament proteins during the course of acute experimental neurofibrillary degeneration; non-phosphorylated epitopes precede phosphorylation, Brain Res. 707 (1996) 272–281.
[29] J. Savory, J.K.S. Rao, Y. Huang, P. Letada, M.M. Herman, Age-related hippocampal changes in Bcl-2:Bax ratio, oxidative stress, redox-active iron and apoptosis associated with aluminum-induced neurodegeneration: increased susceptibility with aging, NeuroToxicology 20 (1999) 805–818.
[30] S. Shimizu, M. Narita, Y. Tsujimoto, Bcl-2 family proteins regulate the release of apoptogenic cytochrome c by the mitochondrial channel VDAC, Nature 399 (1999) 483–487.
[31] S.M. Srinivasula, M. Ahmad, T. Fernandes-Alnemri, E.S. Alnemri, Autoactivation of procaspase-9 by Apaf-1-mediated oligomerization, Mol. Cell 1 (1998) 949–957.
[32] J.H. Su, G.M. Deng, C.W. Cotman, Neuronal DNA damage precedes tangle formation and is associated with up-regulation of nitrotyrosine in Alzheimer's-disease brain, Brain Res. 774 (1997) 193–199.
[33] D.L. Vaux, CED-4 — the third horseman of apoptosis, Cell 90 (1997) 389–390.
[34] A.A. Welihinda, W. Tirasophon, R.J. Kaufman, The cellular response to protein misfolding in the endoplasmic reticulum, Gene Expr. 7 (1999) 293–300.
[35] K.G. Wolter, Y.T. Hsu, C.L. Smith, A. Nechushtan, X.G. Xi, R.J. Youle, Movement of Bax from the cytosol to mitochondria during apoptosis, J. Cell Biol. 139 (1997) 1281–1292.
[36] E. Yang, S.J. Korsmeyer, Molecular thanatopsis: a discourse on the BCL2 family and cell death, Blood 88 (1996) 386–401.
[37] J. Yang, X. Liu, K. Bhalla, C.N. Kim, A.M. Ibrado, J. Cai, T.I. Peng, D.P. Jones, X. Wang, Prevention of apoptosis by Bcl-2: release of cytochrome c from mitochondria blocked, Science 275 (1997) 1129–1132.
[38] N. Zamzami, S.A. Susin, P. Marchetti, T. Hirsch, I. Gomez-Monterrey, M. Castedo, G. Kroemer, Mitochondrial control of nuclear apoptosis, J. Exp. Med. 183 (1996) 1533–1544.
[39] H. Zou, W.J. Henzel, X. Liu, A. Lutschg, X. Wang, Apaf-1, a human protein homologous to *C. elegans* CED-4, participates in cytochrome c-dependent activation of caspase-3, Cell 90 (1997) 405–413.

APPENDIX III

GDNF protects against aluminum-induced apoptosis in rabbits by upregulating Bcl-2 and Bcl-X_L, and inhibiting mitochondrial Bax translocation.

Othman Ghribi[1], Mary M. Herman[3], Michael S. Forbes[1], David A. DeWitt[4], and John Savory[1,2]

Departments of Pathology[1], Biochemistry and Molecular Genetics[2], University of Virginia, Charlottesville, VA, IRP, NIMH, NIH[3], Bethesda, MD and Department of Biology and Chemistry[4], Liberty University, Lynchburg, VA.

Running title: ***GDNF protects against Al neurotoxicity***

Correspondence to: Dr. John Savory, Department of Pathology, University of Virginia Health Sciences Center, Box 168, Charlottesville, Virginia 22908 U.S.A.

(804) 924-5682; FAX (804)924-5718; Email: js2r@virginia.edu

ABSTRACT:

Direct (intracisternal) injection of aluminum complexes into rabbit brain results in a number of similarities with the neuropathological and biochemical changes observed in Alzheimer's disease, and provides the opportunity to assess early events in neurodegeneration. This mode of administration induces cytochrome *c* release from mitochondria, a decrease in Bcl-2 in both mitochondria and endoplasmic reticulum, Bax translocation into mitochondria, activation of caspase-3, and DNA fragmentation. Co-administration of glial cell neuronal-derived factor (GDNF) inhibits these Bcl-2 and Bax changes, upregulates Bcl-X_L and abolishes the caspase-3 activity. Furthermore, treatment with GDNF dramatically inhibits apoptosis, as assessed by the TUNEL technique for detecting DNA damage. Treatment with GDNF may represent a therapeutic strategy to reverse the neuronal death associated with Alzheimer's disease, and may exert its effect on apoptosis-regulatory proteins.

Key Words: cytochrome *c*, Bax, Bcl-2, Bcl-X_L, caspase-3, GDNF, aluminum, endoplasmic reticulum.

INTRODUCTION:

An understanding of the complex events involved in neuronal injury and protection in neurodegenerative diseases requires the availability of animal model systems. The direct injection of aluminum (Al) compounds into the brain of rabbits has been found to result in conditions that mimic a number of neuropathological and biochemical changes present in Alzheimer's and related human neurodegenerative disorders (Huang *et al*, 1997). The use of this animal model should not be confused with the ongoing controversy regarding the possible role of Al in the pathogenesis of Alzheimer's disease, a debate which by no means has been concluded (Savory *et al*, 1996). Here we use this Al/rabbit model system to unravel the events leading to neuronal apoptosis and, most importantly, to demonstrate the antiapoptotic effect of glial cell line-derived neurotrophic factor (GDNF) against fatal Al neurotoxicity.

Alzheimer's disease is a progressive neurodegenerative disorder characterized by three typical pathological features, namely the extracellular deposition of Aβ, the formation of neurofibrillary tangles and selective neuronal loss. However, it is unclear which of these pathological features is the primary event in the initiation and progression of this disease. Selective neuronal death involves vulnerable brain regions, in particular the hippocampus and cerebral cortex, and apoptosis may play a role in the process of cell loss (for review, see Honig & Rosenberg, 2000). Besides inducing intraneuronal neurofilamentous changes in hippocampus, cortex, brainstem and spinal cord which demonstrate many

biochemical features in common with the neurofibrillary tangles seen in Alzheimer's disease (Rao *et al*, 2000; Huang *et al*, 1997), the intracisternal administration of Al maltolate to rabbits also leads to biochemical changes suggestive of apoptosis (Savory *et al*, 1999). Aluminum is highly neurotoxic, and has been shown to accumulate in neurons following cell depolarization (Suarez Fernandez *et al*, 1996) where it inhibits Na^{+}/ Ca^{+2} exchange and thereby induces an excessive accumulation of mitochondrial Ca^{+2} (Szutowicz *et al*, 1998). Increases in intramitochondrial Ca^{+2} levels lead to an opening of the mitochondrial transition pore (MTP), with cytochrome *c* release and subsequent apoptosis resulting from activation of the caspase family of proteases. This mitochondrial pathway is now widely considered to be an important step in controlling and initiating apoptosis in neurodegenerative disorders, and involves regulating proteins such as the anti-apoptotic Bcl-2 and Bcl-X_L, and the pro-apoptotic Bax. The present study was initiated to assess the importance of such apoptosis regulation, especially to see whether agents that up-regulate Bcl-2 and Bcl-X_L will be protective in the Al/rabbit system. Recently, it has been reported that GDNF provides an antiapoptotic effect on primary cultures of the rat mesencephalon (Sawada *et al*, 2000), causing an increase in Bcl-2 and Bcl-X_L. Here we demonstrate that GDNF has indeed markedly antiapoptotic effect in our system, and we have examined factors such as mitochondrial cytochrome *c* release, changes in Bcl-2 in mitochondria and endoplasmic reticulum, Bcl-X_L regulation, Bax translocation into mitochondria, caspase-3 activation and DNA fragmentation.

MATERIALS AND METHODS:

Animals, treatment protocol, clinical monitoring and tissue collection:

All animal procedures were carried out in accordance with the U.S. Public Health Service Policy on the Humane Care and Use of Laboratory Animals, and the National Institutes of Health Guide for the Care and Use of Laboratory Animals. The animal protocol was approved by the University of Virginia Animal Care and Use Committee. Young adult (5-8 months) female New Zealand white rabbits received either intracisternal injections of 100 μL normal saline (n=6; controls), 100 μL 50 mM Al maltolate in saline (n=7; Al treated group), or 100 μl of 500 ng/ml GDNF in saline plus 100 μL 50 mM Al maltolate (n=6; Al/GDNF treated group). The GDNF was obtained commercially (R&D systems, Inc., Minneapolis, MN). The injections were carried out slowly over a period of 2 min under ketamine anesthesia as described previously (Savory *et al*, 1999). All rabbits were monitored daily for clinical symptoms as described by us previously (Huang *et al*, 1997). Rabbits were euthanized 3 days following the intracisternal injection and perfused with Dulbecco's phosphate buffered saline (GIBCO, Grand Island, NY), also as described previously (Savory *et al*, 1999). Brains were immediately removed after sacrifice, and a coronal section cut and bisected to yield two symmetrical hippocampal segments, one for immunohistochemistry and the other for immunoblot analysis and caspase-3-like activity measurements. The respective sides chosen for these studies were alternated between successive animals. Each brain hemisphere intended for tissue sectioning was

immediately frozen rapidly on a liquid nitrogen-cooled surface, placed into a zipper-closure plastic bag, and buried in dry ice pellets until transferring to –80°C before sectioning. For immunoblot and caspase-3-like activity analysis, the hippocampus was rapidly dissected, homogenized and processed as described below.

Western blot analysis:

We examined changes of proteins in the subcellular fractions where they are reported to be localized and/or translocated. Bcl-2 is present in mitochondria and the endoplasmic reticulum and does not translocate into the cytoplasm, unlike cytochrome c; Bax also translocates, but from the cytoplasm to mitochondria (Cassarino *et al*, 1999 ; Cory, 1995 ; Eskes *et al*, 1998). For Bcl-X_L we assessed levels in both mitochondrial and cytoplasmic fractions.

Proteins from the mitochondrial, cytosolic and endoplasmic fractions were extracted as described previously (Liu *et al*, 1996). Tissue from the entire hippocampus was gently homogenized, using a teflon homogenizer (Thomas, Philadelphia PA), in 7 volumes of cold suspension buffer (20 mM HEPES-KOH (pH 7.5), 250 mM sucrose, 10 mM KCl, 1.5 mM $MgCl_2$, 1mM EDTA, 1 mM EGTA, 1 mM DTT, 0.1 mM PMSF, 2 mg/ml aprotinin, 10 mg/ml leupeptin, 5 mg/mL pepstatin and 12.5 mg/mL of N-acetyl-Leu-Leu-Norleu-Al). The homogenates were first centrifuged at 750 g at 4°C for 10 min to first isolate the nuclear fraction, and then at 8000 g for 20 min at 4°C to separate the

mitochondrial from the soluble fraction. The 8000 g pellets were resuspended in cold buffer without sucrose and used as the mitochondrial fraction. The supernatant was further centrifuged at 100,000 g for 60 min at 4°C to separate the cytosolic from the endoplasmic reticulum fractions. Protein concentrations were determined with the BCA protein assay reagent (Pierce, Rockford, Illinois). Proteins (7.5 μg) from the mitochondrial, cytosolic and endoplasmic reticulum fractions were separated by SDS-PAGE (15% gel) under reducing conditions, followed by transfer to a polyvinylidene difluoride membrane (Millipore, Bedford, MD) at 300 mA for 210 min in transfer buffer (20 mM Tris-base, 150 mM glycine, 20% methanol). Following transfer, membranes were incubated with mouse monoclonal antibody (mAb) to human cytochrome *c*, Bcl-2 (C-2), Bax (B-9), or Bcl-X_L (H-5), all at a dilution of 1:100. All of these mAbs were obtained from a commercial source (Santa Cruz Biotechnology, Santa Cruz, CA). Cytochrome oxidase subunit IV mAb obtained from a commercial source (Molecular Probes, Eugene, OR) was used as a marker of mitochondrial contamination at 1:1000 dilution, and a calnexin mAb (Transduction Laboratories, Lexington, MD) was applied at 1:500 dilution as an endoplasmic reticulum marker. Following washes with Tris buffered saline (TBS) containing 0.1% Triton X-100, the blots were developed with enhanced chemiluminescence (Immun-Star goat anti-mouse IgG detection kit, Bio-Rad, Hercules, CA). The bands representing cytochrome *c*, Bax, Bcl-2 and Bcl-X_L were developed on radiographic film and analyzed by densitometry with Personal Densitometer SI and Image Quant 5.0 software (Molecular Dynamics, Sunnyvale, CA).

Caspase-3 like activity assay:

Lysates were prepared by homogenizing hippocampal tissue in 20 mM HEPES-KOH (pH 7.5), 250 mM sucrose, 10 mM KCl, 1.5 mM $MgCl_2$, 1mM EDTA, 1 mM EGTA, 1 mM DTT, 0.1 mM PMSF. Lysates were centrifuged at 4°C for 30 min at 160,000 g, and the protein concentration in the supernatant was determined using the Bradford method. Lysates (50 μg protein) were incubated for 1 hr at 37°C in 1 mL of 1x HEPES buffer containing 10 μL of the fluorogenic substrate Ac-DEVD-AMC, with and without 10 μL of the caspase-3 inhibitor Ac-DEVD-CHO (Caspase -3 assay kit, Pharmingen, San Diego, CA). Cleavage of the substrate was monitored at an excitation wavelength of 380 nm and emission wavelength of 440 nm using a Model 450 fluorometer (BioMolecular Inc). Caspase-3 activity for each sample was calculated as the difference between the rate of cleavage in the absence and presence of the inhibitor.

DNA fragmentation and immunohistochemistry:

Frozen coronal brain sections (14 μm thick) from the hippocampal level were fixed and permeabilized as described previously (Henshall *et al*, 2000). Detection of DNA fragmentation was performed using the terminal deoxynucleotidyl transferase-mediated dUTP nick end labeling (TUNEL) technique. In brief, tissue sections from controls, Al-treated and Al/GDNF-treated animals were dried for 15 min at room temperature and fixed in 10% formalin for 15 min, followed by 10 min incubation in 1:2 vol/vol

ethanol/acetic acid. Sections were washed three times in PBS for 5 min each, permeabilised with 3% Triton X-100 for 20 min and immersed in 3% hydrogen peroxide for 15 min. Sections were then washed three times in PBS buffer for 5 min each, then processed for apoptosis detection using an Apoptosis Detection System, Fluorescein (Promega, Madison, WI). Positive control fixed sections were incubated with 1 unit/ml of Dnase I for 5 min. All steps were conducted at room temperature.

For dual-labeled caspase-3 immunostaining, brain sections previously stained with the TUNEL from controls, Al-treated, and Al/GDNF-treated animals were blocked with 2% goat serum and incubated for 2 hrs at 37°C in a 1:200 dilution of the caspase-3/CPP 32 mouse mAb, specific for activated caspase-3 (Transduction Laboratories, Lexington, KY). Sections were then washed three times in PBS for 5 min and incubated for 2 h at 37°C in a 1:500 dilution of the Cy3-conjugated goat anti-mouse IgG (Jackson ImmunoResearch Laboratories, West Grove, PA). Sections were subsequently washed in PBS buffer, mounted in Vectashield, coverslipped and evaluated and recorded digitally with a fluorescence microscope. TUNEL and caspase-3 positive neurons were counted at a magnification of 400X with an Olympus BH2 microscope (Melville, NY) and Image Pro Plus 4.1 analysis software (Media Cybernetics,
Baltimore, MD) . Five fields were captured from the CA 1 region of the hippocampus from each animal, and results were compared between the Al-treated and the Al/GDNF-treated animals. Results from the Al-treated rabbits were assigned a value of 100%. The GDNF effect was then expressed as the percent reduction in the number of positive

neurons in the Al/GDNF group when compared to the Al-treated rabbits.

Statistical analysis:

Densitometric analysis for cytochrome *c*, Bcl-2, Bax and Bcl-X_L were expressed as mean ± SEM values. Differences in densitometric levels of these proteins in mitochondrial, cytoplasmic and endoplasmic fraction were statistically compared between the controls, Al-treated or Al/GDNF-treated animals, using ANOVA with the posthoc Fisher's PLSD test. Changes in caspase-3 protease activity in the different animal groups were compared using one-way ANOVA and the Student's *t* test. A value <0.05 was considered significant.

RESULTS:

By the day 3 following Al maltolate administration, all animals with this treatment alone develop neurological symptoms characterized by forward head tilt, hemiplegic gait, loss of appetite, splaying of the extremities and paralysis. These symptoms were so severe at this time that the rabbits had to be sacrificed. Treatment with GDNF protected the animals against this Al-induced toxicity, and no neurological symptoms were evident up to day 3.

Western blot analysis:

Cytochrome *c* immunoreactivity, as shown by Western blot and densitometric analysis of these blots (Figure 1A), is faintly detectable in the cytosolic fraction in the control brains and is strongly positive in the mitochondrial fractions. Aluminum treatment induces cytochrome *c* release into the cytoplasm and GDNF administration fails to inhibit the Al-induced translocation of cytochrome *c* into the cytoplasm.

Bcl-2 (Figure 1B) is detectable in controls in the mitochondrial and endoplasmic reticulum fractions. In the Al-treated group, Bcl-2 reactivity is decreased both in the mitochondria and in the endoplasmic reticulum, but treatment with GDNF maintains the Bcl-2 levels. As shown in Figure 1B, densitometric analysis of Bcl-2 demonstrates that Al dramatically decreases Bcl-2 levels in both the mitochondrial and endoplasmic reticulum fractions, and that this effect is reversed by GDNF.

Bax (Figure 1C) is distributed with higher intensity in the cytosolic than in the mitochondrial fractions of controls. Following Al treatment, Bax immunoreactivity is markedly increased at the mitochondrial level. Treatment with GDNF significantly decreases Bax intensity in the mitochondria.

Bcl-X_L immunoreactivity (Figure 1D) in controls is highly positive in the mitochondrial fraction, and is present to a lesser extent in the cytoplasmic fraction. Aluminum treatment, while having no significant effect on Bcl-X_L in mitochondria, slightly increases these levels in the cytoplasmic fraction. GDNF administration results in an

enhancement of Bcl-X_L in both the mitochondrial and cytoplasmic fractions.

Cytochrome c oxidase subunit IV and calnexin antibodies, used respectively as specific markers for mitochondria and endoplasmic reticulum proteins, confirm the purity of the subcellular fractionation carried out in the present experiments. As shown in Figure 2, cytochrome *c* oxidase subunit IV stains only the mitochondrial fraction and calnexin stains only the endoplasmic reticulum fractions.

Caspase-3 like activity:

The activity of caspase 3-like proteases in hippocampal lysates, assessed by measuring the cleavage of the fluorogenic substrate Ac-DEVD-AMC in the presence and absence of an inhibitor, demonstrates significant elevations in the Al-treated animals. This increase in caspase-3-like activity approaches 5-fold greater levels in the Al-treated animals as compared to controls. Treatment with GDNF strongly reduces the caspase-3-like activity (Figure 3).

DNA fragmentation and caspase-3 immunoreactivity:

Sections from control animals treated with DNAse I (positive control) show widespread TUNEL-positive staining in the pyramidal layer (CA1) of the hippocampus (Figure 4A), while in a similar area in the control untreated group no TUNEL (Figure 4B) or caspase-3

positive neurons (Figure 4C) are seen. Aluminum administration induces a large number of TUNEL positive (Figure 4D) and caspase-3 stained (Figure 4E) neurons in the same region of the hippocampus. There are also TUNEL and caspase-3-positive neurons in the nearby temporal cortex but to a lesser extent (data not shown). Treatment with GDNF dramatically reduces TUNEL positivity (Figure 4G), and the caspase-3 staining (Figure 4H) in these neurons. No positivity for either TUNEL or caspase-3 is observed in the temporal cortex (data not shown). Quantitation of TUNEL positive (Figure 5 A and B) and caspase-3 positive (figure 5 D and E) neurons, carried out at a magnification of 400X, shows that the Al-induced TUNEL staining and caspase-3 activity increase are markedly reduced by GDNF treatment (Figure 5C and F respectively).

DISCUSSION:

Hippocampal tissue from Al maltolate-treated rabbits exhibits cytochrome *c* translocation into the cytoplasm, accompanied by a decrease in Bcl-2 and an increase in Bax. Furthermore, changes in the levels of these proteins are accompanied by evidence of activation of caspase-3 and DNA fragmentation, suggestive of the initiation of apoptosis. Treatment with GDNF reverses the increase in levels of the proapoptotic protein Bax, and enhances levels of the antiapoptotic proteins Bcl-2 and Bcl-X_L, thus abolishing the caspase-3-like activity and dramatically inhibiting apoptosis.

Mitochondrial cytochrome *c* is considered to play a pivotal role in the initiation of

apoptosis when released into the cytoplasm. On the other hand, members of the Bcl-2 family of proteins are believed to determine cell life or death by inhibiting (as in the case of Bcl-2 and Bcl-X_L), or promoting (as in the case of Bax), the release of cytochrome *c* (for a review see Graham *et al*, 2000). Opening of the MTP has been proposed to lead to cytochrome *c* release; however, it may not represent the unique mechanism for this release (for review, see Gottlieb, 2000). Indeed, it has been suggested that Bax, when translocated into mitochondria following neurotoxic stimuli, can by itself form a channel, or can interact with the voltage-dependent anion channel (VDAC) to form a larger channel which is permeable to cytochrome *c* (Shimizu *et al*, 2000). In the present work it remains to be determined whether the release of cytochrome *c* induced by Al occurs through opening of the MTP and/or as a result of the increase in mitochondrial Bax. Since Al perturbs Ca^{2+} homeostasis in mitochondria (Szutowicz *et al*, 1998), it may then open the MTP and release cytochrome *c*. We recently have reported such a mechanism in aged rabbit brains where the Al-induced cytochrome *c* release was supressed by cyclosporin A, a blocker of the MTP (Ghribi *et al*, 2001).

Treatment with GDNF greatly reduces Bax translocation into mitochondria and increases the levels of the antiapoptotic Bcl-2 and Bcl-X_L, but does not inhibit cytochrome *c* release into the cytoplasm. However, the GDNF-treated animals show no caspase-3-like activity, and have a markedly reduced number of apoptotic cells when compared to animals receiving Al. Also, these GDNF-treated rabbits do not demonstrate neurological symptoms for up to the first 3 days, whereas within this time period, those receiving Al

alone develop severe symptoms and must be sacrificed. The mechanism by which GDNF exhibits its protective effect in the present study is unknown and, based on present results, it appears that the antiapoptotic effect is independent of the blockade of cytochrome *c* release. It also seems unlikely that the observed cytochrome *c* release originates from a putative Bax channel, since GDNF treatment inhibits mitochondrial Bax translocation and increases mitochondrial Bcl-2 levels, a process normally capable of inhibiting cytochrome *c* release via a Bax-dependent pathway (for review see Tsujimoto & Shimizu, 2000). However, it has been shown recently that during tumor necrosis-related apoptosis-inducing ligand (TRAIL)-induced apoptosis in Jurkat cells, Bcl-2 overexpression fails to block mitochondrial dysfunction and does not inhibit cytochrome *c* release (Kim *et al*, 2001). It is known that formation of the cytochrome *c*-Apaf-1 complex (for a review see Gottlieb, 2000), rather than the presence *per se* of cytochrome *c* in the cytoplasm, is the determining factor in the activation of caspases and in the triggering of apoptosis. Indeed, it has been reported that the antiapoptogenic protein Bcl-X_L has the ability, when overexpressed, to sequester Apaf-1, and thereby to inhibit Apaf-1 dependent caspase-9 activation (Hu *et al*, 1998; Pan *et al*, 1998). Interestingly, the GDNF-induced increase in mitochondrial and cytoplasmic Bcl-X_L levels we report here may provide, at least in part, an explanation for the antiapoptotic effect of GDNF. By upregulating Bcl-X_L levels in the cytoplasm, this protein can bind to Apaf-1, leaving cytochrome *c* free but now unable to initiate caspase-9 activation.

Although mitochondrial alterations represent a major step in the initiation of apoptosis,

increasing evidence now implicates the endoplasmic reticulum as an important organelle in the regulation of apoptosis. The endoplasmic reticulum-mediating apoptosis occurs either in concert with mitochondria and is controlled by Bcl-2 (Hacki *et al*, 2000), or occurs by a mechanism independent of the mitochondrial pathway (Nakagawa *et al*, 2000). Interestingly, our results show that Al administration leads to a decrease in the Bcl-2 levels also in the endoplasmic reticulum, and that these Bcl-2 levels are restored by GDNF treatment. Thus, it appears that the endoplasmic reticulum may play an important role in the initiation or the exacerbation of apoptosis induced by Al, with the possibility that a key event is an increase in Bcl-2 in this organelle, coupled with a concomitant increase in Bcl-X_L which could sequester Apaf-1 and thereby contribute to the antiapoptotic effect of GDNF. Such findings have been reported, suggesting that Bcl-2 targeted to the endoplasmic reticulum is capable of blocking certain types of apoptosis (Lee *et al*, 1999; Zhu *et al*, 1996). However, it remains unclear how Bcl-2 in the endoplasmic reticulum exerts such an antiapoptotic effect. More recently it has been demonstrated that stress in the endoplasmic reticulum activates a specific apoptosis pathway mediated by caspase-12 that is independent from the mitochondrial apoptosis pathway (Nakagawa *et al*, 2000). Investigations of this caspase-12-mediated endoplasmic reticulum apoptosis in our Al-model of neurodegeneration is important, and such studies are underway in our laboratory.

The activity most often attributed to GDNF is that of promoting neuronal survival. GDNF binds to the GDNF family receptor α (GFRα), with a higher affinity to GFRα1

than to GFRα2 (Klein *et al*, 1997; Sanicola *et al*, 1997) to form a complex that subsequently activates the receptor tyrosine kinase, c-ret (Jing *et al*, 1996). Upregulation of GDNF mRNA in rat brains has been shown to occur following excitotoxicity induced by glutamate (Ho *et al*, 1995) or kainate (Humpel *et al*, 1994). GDNF has been shown to protect neurons against oxidative stress in cultured mesencephalic neurons and glial cells (Iwata-Ichikawa *et al*, 1999), against ischemic/hypoxic-induced brain injury in neonatal rats (Ikeda *et al*, 2000), after brain injury following permanent middle cerebral artery occlusion in rats (Kitagawa *et al*, 1998), and in primate models of Parkinson's disease (Kordower *et al*, 2000). The mechanisms by which GDNF exerts its neuroprotective effect are diverse, and recent evidence demonstrates that the rescue and repair of injured neurons is a consequence of an antiapoptotic action of GDNF. Indeed, GDNF has been shown to up-regulate Bcl-2 and Bcl-X_L levels in rat mesencephalic neurons subjected to apoptosis, resulting in a reduction of caspase activation (Kitagawa *et al*, 1998;Sawada *et al*, 2000). The present investigation not only confirms these antiapoptotic properties of GDNF, but further elucidates the cell organelles in which the apoptosis-regulatory proteins are controlled.

Apoptosis in neurodegenerative disorders, including Alzheimer's disease, may be responsible for the neuronal losses associated with these diseases. Therefore, the elucidation of the mechanisms of cell death could culminate in the development of novel therapeutic strategies for prevention and therapy. We conclude that the intracisternal administration of the neurotoxin, Al maltolate, induces changes in the level of proteins

regulating apoptosis, and that GDNF regulates the increases in Bcl-2 and Bcl-X_L, both of which are antiapoptotic. This regulation, coupled with decreases in the proapoptotic Bax, serves to inhibit apoptosis. Most importantly, these changes dramatically protect against the development of the acute, severe and invariably fatal neurological symptoms associated with Al administration. Further experiments are needed to examine the long-term effects of GDNF treatment on Al-induced fatal neurological symptoms. We have performed a preliminary experiment with 9 animals treated with Al maltolate and GDNF, and allowed to survive longer than the 3 days reported in the present study. Five of these rabbits developed neurological symptoms after 8-9 days, and the remaining 4 rabbits were asymptomatic up to 2 months. Because experimentally-induced neurofibrillary degeneration resulting from Al administration shares many features of the neurofibrillary pathology in a number of human neurodegenerative disorders, particularly in Alzheimer's disease, our results support proposed treatments with GDNF or related compounds as approaches to provide protection against the neuronal loss associated with these conditions.

ACKNOWLEDGMENTS:

We gratefully acknowledge helpful statistical analysis discussions with Dr. James Boyd, Department of Pathology, Health Sciences System, University of Virginia. Supported by Grant # DAMD 17-99-1-9552 from the US Department of the Army.

REFERENCES:

Cassarino,D.S., Parks,J.K., Parker,W.D., & Bennett,J.P. (1999) The parkinsonian neurotoxin MPP+ opens the mitochondrial permeability transition pore and releases cytochrome c in isolated mitochondria via an oxidative mechanism. *Biochimica et Biophysica Acta - Molecular Basis of Disease*, **1453**, 49-62.

Cory,S. (1995) Regulation of lymphocyte survival by the bcl-2 gene family. *Annu.Rev.Immunol.*, **13**, 513-543.

Eskes,R., Antonsson,B., Osen-Sand,A., Montessuit,S., Richter,C., Sadoul,R., Mazzei,G., Nichols,A., & Martinou,J.C. (1998) Bax-induced cytochrome C release from mitochondria is independent of the permeability transition pore but highly dependent on Mg2+ ions. *J.Cell Biol.*, **143**, 217-224.

Ghribi,O., DeWitt,D.A., Forbes,M.S., Arad,A., Herman,M.M., & Savory,J. (2001) Cyclosporin A inhibits Al-induced cytochrome c release from mitochondria in aged rabbits. *J Alz.Dis.* in press.

Gottlieb,R.A. (2000) Mitochondria: execution central. *FEBS Lett.* **482**, 6-12.

Graham,S.H., Chen,J., & Clark,R.S. (2000) Bcl-2 family gene products in cerebral ischemia and traumatic brain injury. *J Neurotrauma*, **17**, 831-841.

Hacki,J., Egger,L., Monney,L., Conus,S., Rosse,T., Fellay,I., & Borner,C. (2000) Apoptotic crosstalk between the endoplasmic reticulum and mitochondria controlled by Bcl-2. *Oncogene* **19**, 2286-2295.

Henshall,D.C., Chen,J., & Simon,R.P. (2000) Involvement of caspase-3-like protease in the mechanism of cell death following focally evoked limbic seizures. *J Neurochem.* **74**, 1215-1223.

Ho,A., Gore,A.C., Weickert,C.S., & Blum,M. (1995) Glutamate regulation of GDNF gene expression in the striatum and primary striatal astrocytes. *NeuroReport* **6**, 1454-1458.

Honig,L.S. & Rosenberg,R.N. (2000) Apoptosis and neurologic disease. *Am.J.Med.* **108**, 317-330.

Hu,Y., Benedict,M.A., Wu,D., Inohara,N., & Nunez,G. (1998) Bcl-XL interacts with Apaf-1 and inhibits Apaf-1-dependent caspase-9 activation. *Proc. Natl. Acad. Sci.U.S.A* **95**, 4386-4391.

Huang,Y., Herman,M.M., Liu,J., Katsetos,C.D., Wills, M.R., & Savory,J. (1997) Neurofibrillary lesions in experimental aluminum-induced encephalopathy and Alzheimer's disease share immunoreactivity for amyloid precursor protein, Ab, a_1-antichymotrypsin and ubiquitin-protein conjugates. *Brain Res.* **771**, 213-220.

Humpel,C., Hoffer,B., Stromberg,I., Bektesh,S., Collins,F., & Olson,L. (1994) Neurons of the hippocampal formation express glial cell line-derived neurotrophic factor messenger RNA in response to kainate-induced excitation. *Neuroscience* **59**, 791-795.

Ikeda,T., Xia,X.Y., Xia,Y.X., Ikenoue,T., Han,B., & Choi,B.H. (2000) Glial cell line-derived neurotrophic factor protects against ischemia/hypoxia-induced brain injury in neonatal rat . *Acta Neuropathol.(Berl)* **100**, 161-167.

Iwata-Ichikawa,E., Kondo,Y., Miyazaki,I., Asanuma,M., & Ogawa,N. (1999) Glial cells protect neurons against oxidative stress via transcriptional up-regulation of the glutathione synthesis. *J Neurochem.* **72**, 2334-2344.

Jing,S., Wen,D., Yu,Y., Holst,P.L., Luo,Y., Fang,M., Tamir,R., Antonio,L., Hu,Z., Cupples,R., Louis,J.C., Hu,S., Altrock,B.W., & Fox,G.M. (1996) GDNF-induced activation of the ret protein tyrosine kinase is mediated by GDNFR-alpha, a novel receptor for GDNF. *Cell* **85**, 1113-1124.

Kim,E.J., Suliman,A., Lam,A., & Srivastava,R.K. (2001) Failure of Bcl-2 to block mitochondrial dysfunction during TRAIL- induced apoptosis. Tumor necrosis-related apoptosis-inducing ligand. *Int.J.Oncol.* **18**, 187-194.

Kitagawa,H., Hayashi,T., Mitsumoto,Y., Koga,N., Itoyama,Y., & Abe,K. (1998) Reduction of ischemic brain injury by topical application of glial cell line-derived neurotrophic factor after permanent middle cerebral artery occlusion in rats. *Stroke* **29**, 1417-1422.

Klein,R.D., Sherman,D., Ho,W.H., Stone,D., Bennett,G.L., Moffat,B., Vandlen,R., Simmons,L., Gu,Q., Hongo,J.A., Devaux,B., Poulsen,K., Armanini,M., Nozaki,C., Asai,N., Goddard,A., Phillips,H., Henderson,C.E., Takahashi,M., & Rosenthal,A. (1997) A GPI-linked protein that interacts with Ret to form a candidate neurturin receptor. *Nature* **387**, 717-721.

Kordower,J.H., Emborg,M.E., Bloch,J., Ma,S.Y., Chu,Y., Leventhal,L., McBride,J., Chen,E.Y., Palfi,S., Roitberg,B.Z., Brown,W.D., Holden,J.E., Pyzalski,R., Taylor,M.D., Carvey,P., Ling,Z., Trono,D., Hantraye,P., Deglon,N., & Aebischer,P. (2000) Neurodegeneration prevented by lentiviral vector delivery of GDNF in primate models of Parkinson's disease. *Science* **290**, 767-773.

Lee,S.T., Hoeflich,K.P., Wasfy,G.W., Woodgett,J.R., Leber,B., Andrews,D.W., Hedley,D.W., & Penn,L.Z. (1999) Bcl-2 targeted to the endoplasmic reticulum can inhibit apoptosis induced by Myc but not etoposide in Rat-1 fibroblasts. *Oncogene* **18**,

3520-3528.

Liu,X., Kim,C.N., Yang,J., Jemmerson,R., & Wang,X. (1996) Induction of apoptotic program in cell-free extracts: requirement for dATP and cytochrome c. *Cell* **86**, 147-157.

Nakagawa,T., Zhu,H., Morishima,N., Li,E., Xu,J., Yankner,B.A., & Yuan,J. (2000) Caspase-12 mediates endoplasmic-reticulum-specific apoptosis and cytotoxicity by amyloid-beta. *Nature* **403**, 98-103.

Pan,G., O'Rourke,K., & Dixit,V.M. (1998) Caspase-9, Bcl-XL, and Apaf-1 form a ternary complex. *J.Biol.Chem.* **273**, 5841-5845.

Rao,J.K.S., Anitha,S., & Latha,K.S. (2000) Aluminum-induced neurodegeneration in the hippocampus of aged rabbits mimics Alzheimer's disease. *Alzheimer's Reports* **3**, 83-87.

Sanicola,M., Hession,C., Worley,D., Carmillo,P., Ehrenfels,C., Walus,L., Robinson,S., Jaworski,G., Wei,H., Tizard,R., Whitty,A., Pepinsky,R.B., & Cate,R.L. (1997) Glial cell line-derived neurotrophic factor-dependent RET activation can be mediated by two different cell-surface accessory proteins. *Proc. Natl. Acad. Sci.U.S.A* **94**, 6238-6243.

Savory,J., Exley,C., Forbes,W.F., Huang,Y., Joshi,J.G., Kruck,T., McLachlan,D.R., & Wakayama,I. (1996) Can the controversy of the role of aluminum in Alzheimer's disease be resolved? What are the suggested approaches to this controversy and methodological issues to be considered?. *J. Toxicol. Environ. Health* **48**, 615-635.

Savory,J., Rao,J.K.S., Huang,Y., Letada,P., & Herman,M.M. (1999) Age-related hippocampal changes in Bcl-2:Bax ratio, oxidative stress, redox-active iron and apoptosis associated with aluminum-induced neurodegeneration: increased susceptibility with aging. *NeuroToxicol.* **20**, 805-818.

Sawada,H., Ibi,M., Kihara,T., Urushitani,M., Nakanishi,M., Akaike,A., & Shimohama,S. (2000) Neuroprotective mechanism of glial cell line-derived neurotrophic factor in mesencephalic neurons. *J.Neurochem.* **74**, 1175-1184.

Shimizu,S., Ide,T., Yanagida,T., & Tsujimoto,Y. (2000) Electrophysiological study of a novel large pore formed by Bax and the voltage-dependent anion channel that is permeable to cytochrome c. *J Biol.Chem.* **275**, 12321-12325.

Suarez Fernandez,M.B., Torreblanca Pacios,A., Goenaga Infante,H., Soldado,A.B., Sanz Mendel,A., Vega,J.A., & Novelli,A. (1996) Aluminum accumulation and toxicity in cultured neurons and astrocytes. Metal Ions in Biology and Medicine (ed. by P. Callery, J. Corbella, J. L. Domingo, J. C. Etienne, & J. M. Llabet), pp. 284-286. John

Libbey Eurotext, Paris.

Szutowicz,A., Bielarczyk,H., Kisielevski,Y., Jankowska,A., Madziar,B., & Tomaszewicz,M. (1998) Effects of aluminum and calcium on acetyl-CoA metabolism in rat brain mitochondria. *J Neurochem.* **71**, 2447-2453.

Tsujimoto,Y. & Shimizu,S. (2000) Bcl-2 family: life-or-death switch. *FEBS Lett.* **466**, 6-10.

Zhu,W., Cowie,A., Wasfy,G.W., Penn,L.Z., Leber,B., & Andrews,D.W. (1996) Bcl-2 mutants with restricted subcellular location reveal spatially distinct pathways for apoptosis in different cell types. *EMBO J.* **15**, 4130-4141.

FIGURES AND LEGENDS:

Figure 1: Representative immunoblot and densitometric analyses for cytochrome *c*, Bcl-2, Bax and Bcl-X_L proteins of mitochondrial (m), cytoplasmic (c) or endoplasmic fractions (er) from hippocampus in controls (n=6), the Al-treated group (n=7) and Al/GDNF-treated group (n=6). **A**: **Cytochrome *c*** (15.5 kDa) is localized in the mitochondria and is barely detectable in the cytoplasm of controls. Aluminum administration induces translocation of cytochrome *c* into the cytoplasm, and co-perfusion with GDNF does not inhibit the Al-induced cytochrome *c* translocation (***$p<0.01$; versus controls). **B: Bcl-2** (27 kDa) in controls is localized in mitochondria and the endoplasmic reticulum. Following Al administration, Bcl-2 levels decrease both in the mitochondria and in the endoplasmic reticulum. Treatment with GDNF maintains Bcl-2 levels to the basal levels observed in the controls, both in the mitochondria and endoplasmic reticulum (*$p<0.05$, **$p<0.01$ versus controls; +$p<0.05$ versus Al treated). **C: Bax** (23 kDa) in controls is present at low levels in mitochondria and highly reactive in the cytoplasm. Aluminum induces an increase in Bax in the mitochondrial fractions, and treatment with GDNF significantly reduces the translocation of Bax into mitochondria (**$p<0.01$ versus controls; +$p<0.05$ versus Al treated). Note that Bax immunoblotting results in three distinct bands: the upper band is approximately 54 kDa and the lower band is 23 kDa. **D: Bcl-X_L** (31 kDa) immunoreactivity in controls is highly positive in the mitochondrial fraction, and is present to a lesser extent in the cytoplasmic fraction. Aluminum induces a slight decrease in mitochondrial levels, with a

subsequent increase in the cytoplasmic levels. GDNF leads to a large increase in Bcl-X_L levels in cytoplasm>mitochondria (*p<0.05, **p<0.01 versus controls; +p<0.05 versus Al treated).

Figure 2: A representative Western blot analysis for cytochrome *c* oxidase subunit IV (Cyt.OX) and calnexin in cytoplasmic (c), mitochondrial (m) or endoplasmic reticulum (er). Cytochrome *c* oxidase subunit IV, used as a marker for mitochondrial contamination, is only present in the mitochondrial fraction, and calnexin, applied as a marker for the endoplasmic reticulum, stains only the endoplasmic reticulum fraction.

Figure 3: Caspase-3-like activity in hippocampal lysates of control (white bar), Al-treated (black bar) and Al/GDNF-treated animals (hatched bar). In the controls, the level of caspase-3 activity detected is low. Aluminum treatment induces a large increase (5-fold) in caspase-3 activity; GDNF treatment completely abolishes the Al-induced caspase-3 like activity. Data are presented as mean ± SEM (***p<0.001versus controls; +++p<0.001 versus Al- treated group). A value of 70 arbitrary fluorescence units corresponds to 50 percent inhibition of the initial reading when the caspase-3 inhibitor Ac-DEVD-CHO is added.

Figure 4: Immunofluorescence images of TUNEL labeling and caspase-3 protein in the hippocampal CA1 area of control, Al treated and Al/GDNF treated animals. Magnification scale bar in I represents 50 μm. **A:** TUNEL-positive labeling (positive

control) induced by treatment of tissue section from a naive rabbit with Dnase I. **B:** TUNEL labeling of DNA fragmentation from control brain with no positively-stained neurons **C:** Caspase-3 immunoreactivity in control. **D:** TUNEL labeling demonstrates the emergence of DNA fragmentation following Al administration (arrows). **E:** Distinct caspase-3 immunoreactivity is enhanced in the same neurons as in D, from Al-treated rabbits (arrows). **F:** Image overlay of D and E showing co-localization of positive TUNEL labeling with caspase-3 immunoreactivity. Box in F: higher power magnification of a neuron double-stained with TUNEL and caspase-3. **G:** TUNEL labeling following treatment with GDNF shows a reduced number of neurons exhibiting DNA fragmentation. **H:** Caspase-3 immunoreactivity in the CA 1 sector is greatly reduced in rabbits treated with GDNF. **I:** overlay image of G and H demonstrates a reduced number of positive neurons, in comparison to F; TUNEL labeling and caspase-3 immunoreactivity are colocalized. Box in I: higher power magnification of a neuron double-stained with TUNEL and caspase-3.

Figure 5: TUNEL-positive (A and B) and caspase-3 positive (D and E) cells in the CA1 region of the hippocampus, with quantitation of the results, in Al treated and in Al/GDNF treated animals. The Al-induced TUNEL labeling (A) and caspase-3 activation (D), are markedly reduced by GDNF treatment, (B) and (E) respectively. C and F are quantitative analyses showing the neuroprotective effect of GDNF which reduces the number of TUNEL-positive (C) and caspase-3 positive (F) neurons in comparison to Al-treated animals. (A, B, D, and E 400X).

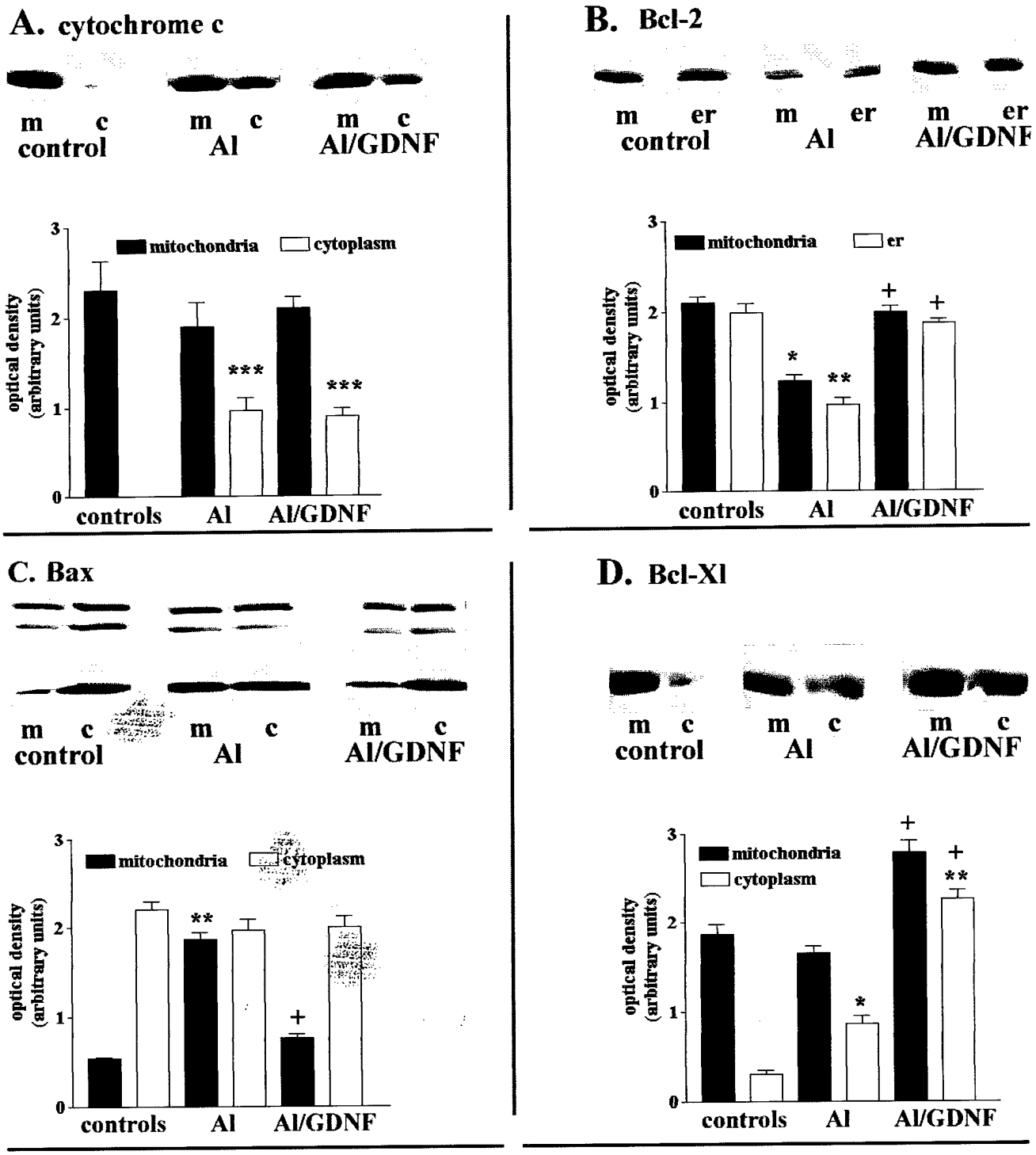
A. cytochrome c
m c
control
m c
Al
m c
Al/GDNF
mitochondria
cytoplasm
optical density (arbitrary units)
***
***
controls
Al
Al/GDNF
B. Bcl-2
m er
control
m er
Al
m er
Al/GDNF
mitochondria
er
optical density (arbitrary units)
*
**
+
+
controls
Al
Al/GDNF
C. Bax
m c
control
m c
Al
m c
Al/GDNF
mitochondria
cytoplasm
optical density (arbitrary units)
**
+
controls
Al
Al/GDNF
D. Bcl-Xl
m c
control
m c
Al
m c
Al/GDNF
mitochondria
cytoplasm
optical density (arbitrary units)
*
+
+
**
controls
Al
Al/GDNF

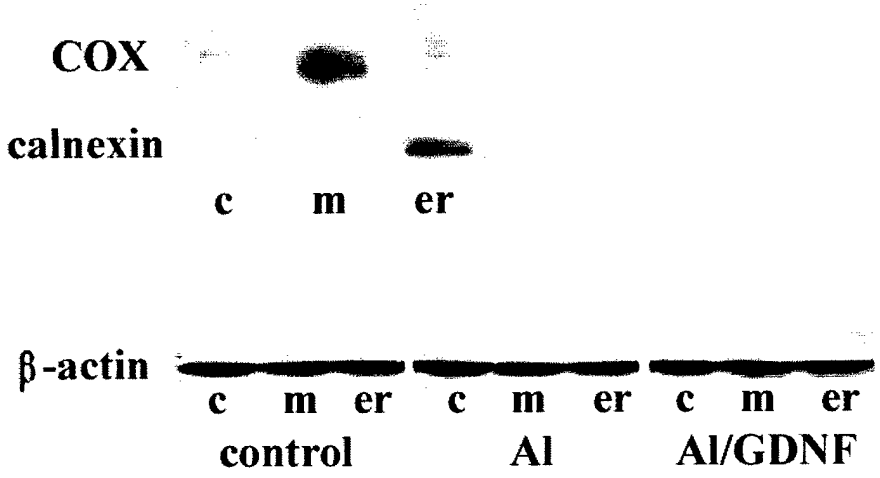
COX
calnexin
c
m
er
β-actin
c
m
er
c
m
er
c
m
er
control
Al
Al/GDNF

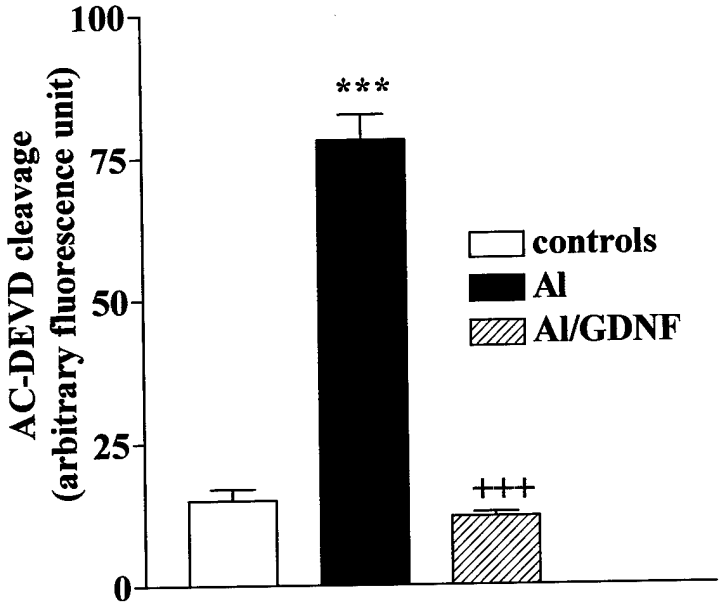
100
75
50
25
0
AC-DEVD cleavage
(arbitrary fluorescence unit)
***
+++
controls
Al
Al/GDNF

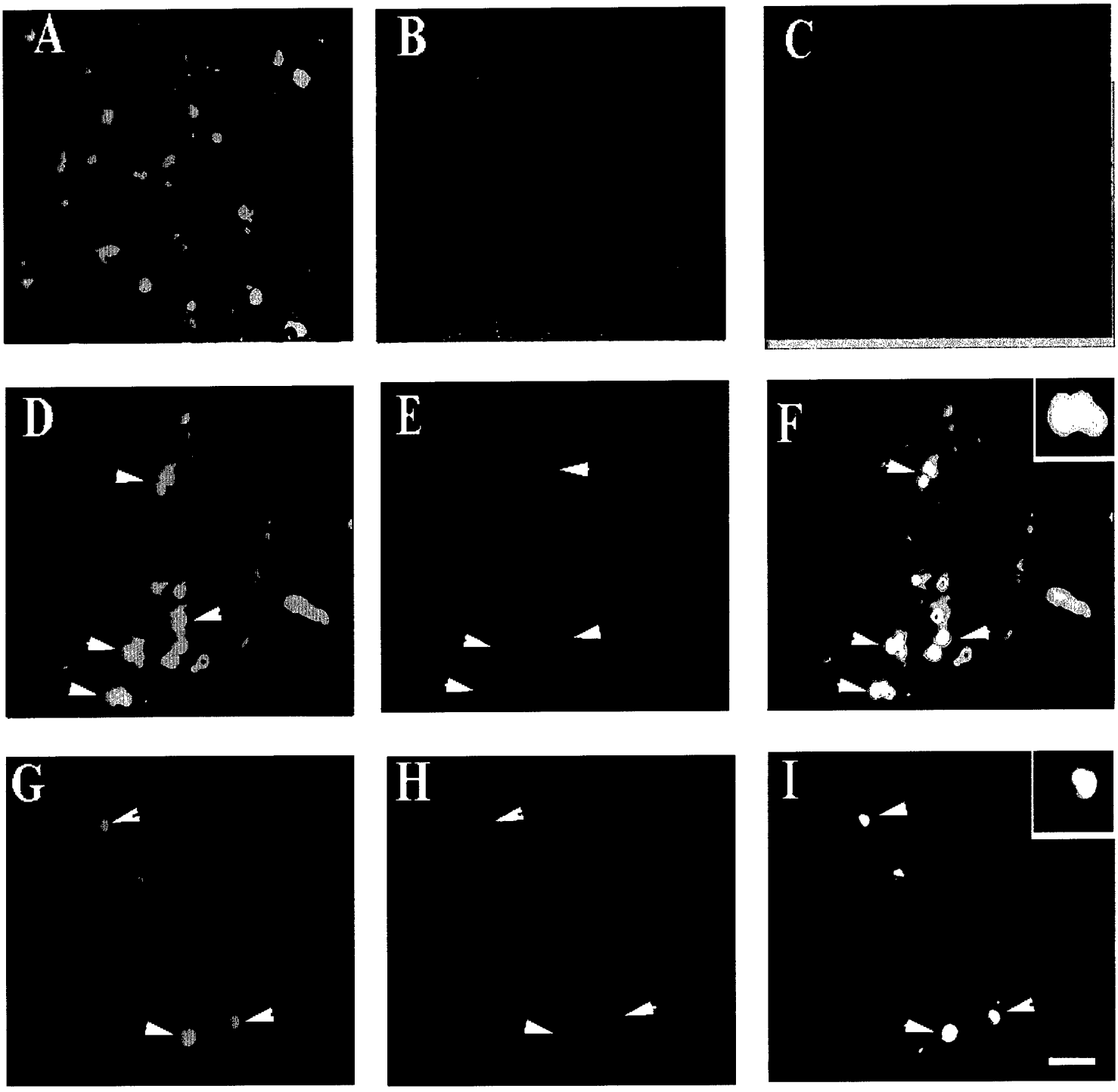
A
B
C
D
E
F
G
H
I

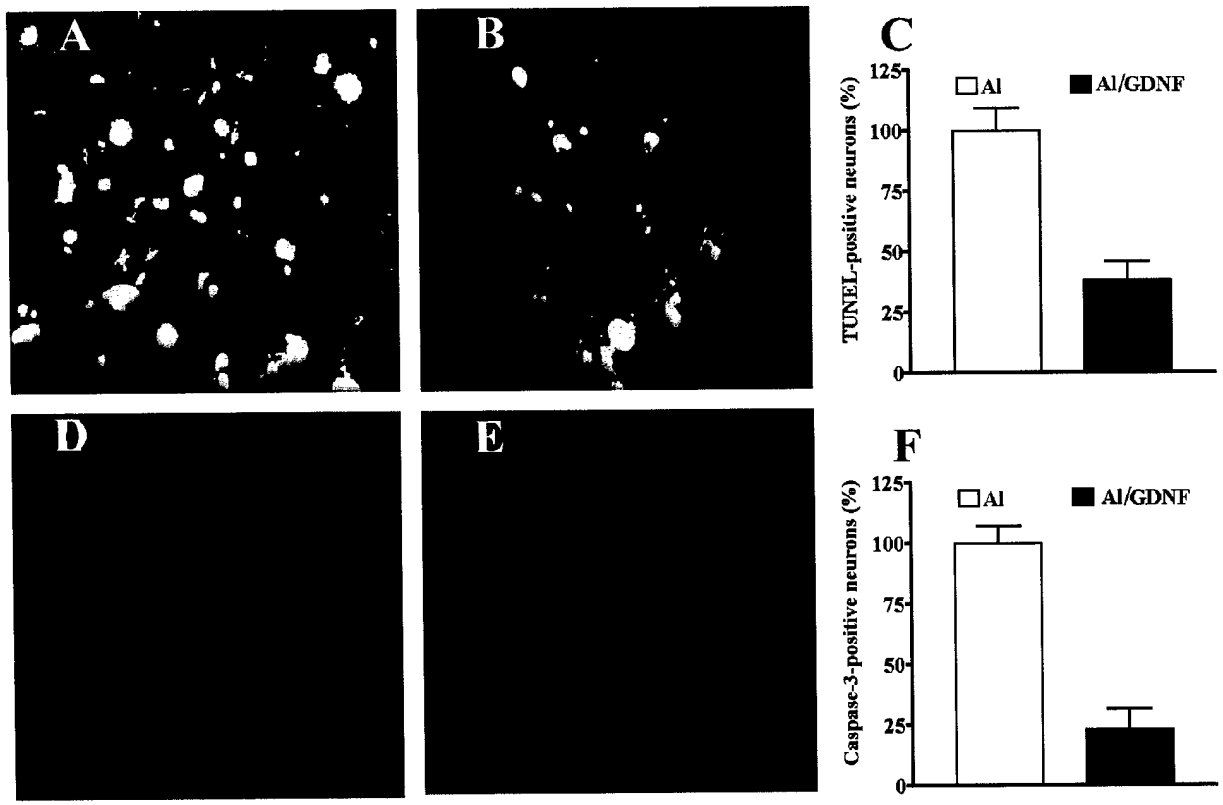
A
B
C
D
E
F
TUNEL-positive neurons (%)
Caspase-3-positive neurons (%)
AI
AI/GDNF
125
100
75
50
25
0

APPENDIX IV

Aβ(1-42) and aluminum induce stress in the endoplasmic reticulum in rabbit hippocampus, involving nuclear translocation of *gadd 153* and NF-κB.

Othman Ghribi [a], Mary M. Herman [c], David A. DeWitt [d], Michael S. Forbes [a], and John Savory [a,b]

Departments of Pathology [a], Biochemistry and Molecular Genetics and Chemistry [b], University of Virginia, Charlottesville, VA; IRP, NIMH, NIH, Bethesda, MD [c], and Department of Biology and Chemistry, Liberty University [c], Lynchburg, VA.

Running title: Al and Aβ induce stress in the ER

Grant: # DAMD 17-99-1-9552 from The US Department of the Army

Correspondence to: Dr. John Savory, Department of Pathology, University of Virginia Health Sciences Center, Box 168, Charlottesville, Virginia 22908 U.S.A.
(804) 924-5682; FAX (804)924-5718; Email: js2r@virginia.edu

Abstract

Apoptosis may represent a prominent form of neuronal death in chronic neurodegenerative disorders such as Alzheimer's disease. Although apoptosis under mitochondrial control has received considerable attention, mechanisms utilized within the endoplasmic reticulum (ER) and the nucleus in mediating apoptotic signals are not well understood. A growing body of evidence is emerging from different studies which suggests an active role for the ER in regulating apoptosis. Disturbances of ER function have been shown to trigger two different apoptotic pathways; one involves cross-talk with mitochondria and is regulated by the antiapoptotic Bcl-2, and the second is characterized by the activation of caspase-12. Also, stress in the ER has been suggested to result in the activation of a number of proteins such as *gadd 153* and NF-κB, and downregulation of the antiapoptotic Bcl-2. In the present study, intracisternal injection of either the neurotoxin aluminum maltolate or of Aβ(1-42) in aged rabbits has been found to induce nuclear translocation of *gadd 153* and the inducible transcription factor, NF-κB. Translocation of these two proteins is accompanied by decreased levels of Bcl-2 in both the ER and nucleus. Aluminum maltolate, but not Aβ, induces caspase-12 activation which is a mediator of ER-specific apoptosis; this is the first report of the *in vivo* activation of caspase-12. These findings indicate that the ER may play a role in regulating apoptosis *in vivo*, and could be of significance in the process of neurodegeneration and related disorders.

Theme Neurotoxicity

Keywords Aβ(1-42), aluminum, *gadd 153*, caspase-12, NF-κB, endoplasmic reticulum.

1. Introduction

Evidence is accumulating that apoptotic cell death is a major factor in human neurodegenerative diseases, including Alzheimer's disease, and that this event may precede the formation of intraneuronal neurofibrillary tangles and neuritic plaques [38]. Although mitochondrial alterations may represent an important step in the mechanisms underlying this neuronal cell death, mitochondria may not be the only cellular organelle which control neuronal loss in neurodegeneration. There is now evidence suggesting that the endoplasmic reticulum (ER) also may play an important role in regulating neuronal cell death, thereby raising the question whether the cell death pathway in neurodegenerative disorders is triggered by mitochondria or the ER [29;37]. Studies of involvement of the ER in neuronal death have, however, lagged behind those of mitochondria, and it may be found that the ER occupies an important role in the pathogenesis of neurodegenerative diseases. Indeed, in addition to its physiological role as a calcium and protein store, the ER is the site of localization for the presenilin-1 mutation which has been linked to the early onset of familial Alzheimer's disease [1]. The ER has also been identified as the site of formation of the peptide Aβ(1-42), which may be the earliest event to take place in Alzheimer's disease [11]. In addition, ER stress-inducing agents have been shown to activate the expression of various genes, such as those coding for the growth arrest and DNA damage-induced gene *gadd 153* [30], and the inducible transcription factor NF-κB [4;36]. Several lines of evidence suggest that NF-κB plays an important role in the survival of neurons by its translocation from the

cytoplasm into the nucleus [3;24;27]. Moreover, members of the *Bcl-2* family of proteins, Bcl-2 and Bcl-X_L, reside in the ER, and it has been established that they are also important in determining cellular and neurological outcomes in neurodegenerative disorders (for review see [8]). Recently, stress in the ER has been shown to result in a specific type of apoptosis, independent of mitochondrial-targeted apoptotic signals; this novel pathway is mediated by caspase-12 [23]. Procaspase-12 resides in the ER, and upon its activation by ER stress is released to the cytoplasm in an active form (caspase-12) which initiates apoptosis.

Previous studies in our laboratory have utilized the neurotoxin, aluminum (Al) maltolate, injected into rabbit brain as a means for investigating mechanisms of neurodegeneration, since this system demonstrates cytoskeletal changes that share a number of biochemical similarities with those found in Alzheimer's disease [12;33]. Having observed these results with the highly neurotoxic Al maltolate, we now extend our studies to Aβ, which also has been demonstrated to be neurotoxic and is now considered to play a central role in the pathogenesis of Alzheimer's disease, a hypothesis supported by genetic, biochemical, histopathological and animal modeling data [35]. In the present experiments carried out on aged male New Zealand White rabbits, we have examined Al maltolate-induced stress in the ER, as assessed by the activation of *gadd 153* and its translocation into the nucleus, and have compared the results to changes produced by the administration of Aβ(1-42). We have also examined the effect of these two treatment regimens on caspase-12 activation, Bcl-2 protein levels in ER and in the nuclear

fractions, and on NF-κB translocation. Since the hippocampus is particularly vulnerable in Alzheimer's disease, we have focused our studies on this area of the brain.

2. Material and methods

2.1 Materials

Aβ(1-42) was obtained from American Peptide Company (Sunnyvale, CA). Mouse monoclonal antibody (mAb) specific to human *gadd 153* (B-3), Bcl-2 (C-2), and NF-κB (C-5), were obtained from Santa Cruz Biotechnology (Santa Cruz, CA). Caspase-12 mAb was a gift from Dr. Junying Yuan, Harvard Medical School, Boston, MA; β-actin and α-mouse IgG FITC were obtained from Sigma Chemical Co. (Saint Louis, MO) and Cy3-conjugated goat anti-mouse IgG from Jackson ImmunoResearch Laboratories (West Grove, PA).

2.2 Animals, treatment protocol and tissue collection

All animal procedures were carried out in accordance with the U.S. Public Health Service Policy on the Humane Care and Use of Laboratory Animals, and the National Institutes of Health Guide for the Care and Use of Laboratory Animals. The animal protocol was approved by the University of Virginia Animal Care and Use Committee. Aged (4.5-5 years) male New Zealand white rabbits received either intracisternal injections of 100 μL

normal saline (n=5; controls), 100 μL of 25 mM Al maltolate in saline (n=6; Al-treated group), or 100 μl of 1 mg/ml Aβ(1-42) in saline (n=7; Aβ treated group). Aggregate Aβ(1-42) was prepared by incubating freshly solubilized Aβ(1-42) at a concentration of 1 mg/ml in saline at 37°C for 3 days. The injections were carried out under ketamine anesthesia as described previously [34]. All rabbits were euthanized after 15 days, at which time the Al-treated animals had developed severe neurological symptoms requiring their sacrifice, including forward head tilt, hemiplegic gait, loss of appetite, splaying of the extremities and paralysis. The controls and Aβ(1-42) animals did not display clinical symptoms. At the time of sacrifice the rabbits were perfused with Dulbecco's phosphate buffered saline (GIBCO, Grand Island, NY), also as described previously [34]. Brains were immediately removed, and a coronal section cut and bisected to yield two symmetrical hippocampal segments, one for immunohistochemistry and the other for immunoblot analysis. Each brain hemisphere intended for histochemistry was immediately frozen rapidly on a liquid nitrogen-cooled surface, placed into a zipper-closure plastic bag, and buried in dry ice pellets until transferring to –80° C for storage before sectioning. For immunoblot analysis, tissue from the hippocampus was rapidly dissected, homogenized and processed as described below.

2.3 Western blot analysis

Proteins from the subcellular fractions were extracted as described previously [19]. Approximately 50 mg of brain tissue from hippocampus was gently homogenized, using

a teflon homogenizer (Thomas, Philadelphia PA), in 7 volumes of cold suspension buffer (20 mM HEPES-KOH (pH 7.5), 250 mM sucrose, 10 mM KCl, 1.5 mM $MgCl_2$, 1mM EDTA, 1 mM EGTA, 1 mM DTT, 0.1 mM PMSF, 2 mg/ml aprotinin, 10 mg/ml leupeptin, 5 mg/mL pepstatin and 12.5 mg/mL of N-acetyl-Leu-Leu-Norleu-Al). The homogenates were centrifuged at 900 g at 4°C for 10 min to isolate the nuclear fraction, and then at 8000 g for 20 min at 4°C to separate the mitochondrial fraction from the soluble fraction. The supernatant was further centrifuged at 100,000 g for 60 min at 4°C to separate the cytoplasmic from the ER fractions. We examined changes of proteins in the subcellular fractions where they are reported to be localized and/or translocated; *gadd 153* and NF-κB in the cytoplasmic and nuclear fractions, Bcl-2 in the endoplasmic reticulum and nuclear fractions, and caspase-12 in cytoplasmic fractions. Protein concentrations were determined with the BCA protein assay reagent (Pierce, Rockford, Illinois). Proteins (7.5 μg) were separated by SDS-PAGE (15% gel) under reducing conditions, followed by transfer to a polyvinylidene difluoride membrane (Millipore, Bedford, MD) at 300 mA for 210 min in transfer buffer (20 mM Tris-base, 150 mM glycine, 20% methanol). Following transfer, membranes were incubated overnight at 4°C with mouse mAb to human *gadd 153* and NF-κB at 1:250 dilution, caspase-12 at a 1:10 dilution, and Bcl-2 at a dilution of 1:100. β-Actin was used at a 1:500 dilution as a gel-loading control. The blots were developed with enhanced chemiluminescence (Immun-Star detection kit, Bio-Rad, Hercules, CA). The bands of *gadd 153*, caspase-12, Bcl-2 and NF-κB, were scanned and densitometrically analyzed using Personal Densitometer SI and Image Quant 5.0 software (Molecular Dynamics, Sunnyvale, CA),

and these quantitative analyses were expressed as mean ± SEM values. Unpaired Student's *t* test was used to compare levels of each protein between controls and Al-treated or Aβ(1-42)-treated animals in the same subcellular fraction.

2.4 Immunohistochemistry

Serial 14 μm-thick coronal frozen sections from controls, Al-treated, and Aβ(1-42)-treated animals were cut at the level of the hippocampus and stored at -80° C prior to immunostaining. The sections were air-dried at room temperature, fixed in cold acetone for 10 min, treated with 1% hydrogen peroxide in PBS and incubated with a blocking solution of 1.5% normal serum, also in PBS. Subsequently, sections were reacted overnight at 4°C with a mouse mAb against *gadd 153* or NF-κB at a 1:250 dilution. After washing with 50 mM TBS and incubating with the biotinylated secondary antibody, sections were processed with a Vectastain Elite Avidin-Biotin complex technique kit (Vector Laboratories, Burlingame, CA). Immunostaining for *gadd 153* was visualized by the use of Vector SG substrate and a Nuclear Fast Red counterstain kit (Vector Laboratories, Burlingame, CA). Sections incubated with NF-κB antibody were visualized with DAB Chromogen (Dako Corporation, Carpinteria, CA) and counterstained with methyl green (Sigma, Saint Louis, MO).

For double labeling of NF-kB and *gadd 153*, frozen coronal brain sections (14 μm thick) from the hippocampal level of controls, Al-treated and Aβ(1-42)-treated animals were dried for 15 min at room temperature (RT) and fixed in 10% formalin for 15 min, followed by a 10 min incubation in 1:2 vol/vol ethanol/acetic acid. Sections were washed three times in PBS for 5 min each and permeabilised with 0.3% Triton X-100 for 20 min at RT. Sections were then washed three times in PBS buffer for 5 min each, blocked with 2% goat serum and incubated for 2 hrs at 37°C in a 1:200 dilution of the *gadd 153* mouse mAb. Sections were then washed three times in PBS for 5 min and incubated for 2 h at 37°C in a 1:500 dilution of the Cy3-conjugated goat anti-mouse IgG. Sections were washed in PBS buffer and then in distilled H_2O, blocked with 2% goat serum and incubated for 2 hrs at 37°C in a 1:250 dilution of NF-κB mouse mAb, then incubated for 2 h at 37°C in a 1:250 dilution of α-mouse IgG FITC. After 3x 5 min washes in PBS and a 5 min wash in distilled H_2O, sections were coverslipped and examined with a fluorescence Olympus BH2 microscope (Melville, NY) and Image Pro Plus 4.1 analysis software (Media Cybernetics, Baltimore, MD) .

3. Results

3.1 Western blot analysis

As shown in Figure 1A and Table I, *gadd 153* (~ 30KDa) is only detected in the

cytoplasmic fraction in control animals, but is present as well in the nuclear fraction in the Al- and Aβ(1-42)-treated group. Caspase-12 (~60KDa) is detected in the cytoplasmic fractions from Al-treated rabbits but is not expressed in the cytoplasmic fractions from controls (Figure 1B and Table I). A very faint band corresponding to caspase-12 is seen in the Aβ-treated animals (Figure 1B), but its significance is inconclusive. Bcl-2 can be identified by a protein band having an apparent molecular weight of 27 kDa both in the ER and nuclear fractions in controls (Figures 1C). In comparison to these control animals, Al maltolate and Aβ(1-42) administration induce a decrease in Bcl-2 levels, both in the ER and nuclear fractions (Figures 1C and Table I). Two bands are detected for NF-κB (Figure 1D) corresponding to p52 and p100; these are observed only in the cytoplasmic fraction of controls, with no bands being detected in the nuclear fraction. In the Al maltolate and Aβ(1-42)-treated animals, the two bands corresponding to p52 and p100 are also detected in the cytoplasmic fractions; in these animals there is an intense band in the nuclear fraction corresponding to p52, and a lighter band for p100 (Table I).

3.2 Immunohistochemistry

The immunohistochemical localization of NF-κB and *gadd 153* in the pyramidal cell layer of the hippocampus (CA1) of all animals was examined (Figure 2A). A faint immunostaining for NF-κB (Figure 2 B) or *gadd 153* (Figure 2 C) appears in sections from control rabbits. However, in sections from Al-treated (Figures 2D and F) and Aβ(1-

42)-treated animals (Figures 2E and G), positive immunostaining for NF-κB (purple reaction product) and *gadd 153* (brown-black reaction product) is present in association with the nuclei of most neurons.

Sections dual-labeled for NF-κB and *gadd 153* from control animals demonstrate a very few scattered, positive-staining neurons in the pyramidal layer (CA1) of the hippocampus (Figure 3 A-C), while Al maltolate administration induces a large number of NF-κB-positive (Figure 3D) and *gadd 153*-stained (Figure 3E) neurons in the same region. As shown in Figure 3F, NF-κB coexists with *gadd 153* in several neurons. Treatment with A-β(1-42) also induces positive immunostaining for both NF-κB (Figure 3 G) and *gadd 153* (Figure 3 H) and, as with Al maltolate treatment, several neurons exhibit both NF-κB and *gadd 153* staining (Figure 3I). Positivity for NF-κB and *gadd 153* are also observed in neurons in the temporal cortex (data not shown).

4. Discussion

Disturbances of ER function have been shown to trigger different apoptotic pathways. The first involves cross-talk between the ER and mitochondria, and is regulated by the antiapoptotic Bcl-2 [10]. A second pathway, distinct from that involving mitochondria, has recently been demonstrated and involves activation of caspase-12 [22;23]. In these studies it has been shown in mouse cortical neurons that Aβ(1-40) triggers an ER-specific

apoptosis mediated by active caspase-12, and that a reduction in caspase-12 provides protection from apoptosis. The authors suggest that cleavage of procaspase-12 (which resides in the ER) to active cytoplasmic caspase-12 is accomplished by the cysteine family member, m-calpain [22]. In addition, factors that induce ER stress activate the expression of various genes that code for ER resident proteins; examples include *gadd 153* [30] and activation of the inducible transcription factor NF-κB [26]. Activation of *gadd 153* or NF-κB leads to their translocation into the nucleus, where they may play a role in neuronal survival or death. It has been demonstrated that the *gadd 153* gene is specifically activated by agents that disturb ER function. mRNA levels for *gadd 153* are increased both during hypoxia and after exposure of cells to agents that elevate the levels of glucose-regulated proteins [31]. Activation of *gadd 153* expression has also been confirmed following transient cerebral ischemia in rat [30]. Furthermore, the magnitude of *gadd 153* expression appears to be proportional to the extent of damage, as in homocysteine-induced death in neuronal cell culture [2].

In the present report, we show that both Al and Aβ(1-42) administration induce stress in the ER, as demonstrated by the activation of *gadd 153* and its translocation into the nucleus, which we have confirmed both by immunohistochemistry and Western blot analysis. We also report for the first time the *in vivo* activation of caspase-12; this is clearly seen following Al treatment, but is inconclusive when we administer Aβ(1-42).

Bcl-2 possesses an antiapoptotic function and is located in membranes of mitochondria, ER, and nucleus of different cell types and (for review see[6]). Overexpression of Bcl-2 has been demonstrated to prevent the efflux of cytochrome *c* from the mitochondria and the subsequent initiation of apoptosis in staurosporine treated cells [39]; it prolongs the life of neurons in rat subjected to ischemia [5] or in a transgenic mouse model of familial amyotrophic lateral sclerosis [16]. Bcl-2 targeted to the endoplasmic reticulum has been shown to block certain types of apoptosis [18;40;40]. We have recently demonstrated that in mitochondrial and ER fractions derived from brain, levels of Bcl-2 are decreased following Al maltolate administration to young adult rabbits [7]. Recent reports have shown that neuronal apoptosis induced by the Alzheimer's disease Aβ peptide is related to an alteration of the proapoptotic Bax/antiapoptotic Bcl-2 ratio [28], and that transgenic murine cortical neurons expressing human Bcl-2 exhibit increased resistance to Aβ(1-42) [32]. Treatment of human neuron primary cultures with Aβ(1-40) provokes a down-regulation of Bcl-2 expression [28]. In the present experiments, we have measured levels of Bcl-2 protein in the ER and in the nucleus, and our results show that treatment with either Al or Aβ(1-42) induces a marked decrease in Bcl-2 levels in both organelles.

The inducible transcription factor, NF-κB, is an important mediator of the human immune and inflammatory response [3]. Exposure of cells to various pathological stimuli activate NF-κB; activated NF-κB dimer is rapidly released from the cytoplasm, where it is normally sequestered by the inhibitory unit IκB, and then translocates to the nucleus, where it activates transcription of different genes (for a review see [26]). Various agents

that induce stress in the ER have been shown to activate NF-κB [9;25;27]. The role of NF-κB in regulating neuronal death is complex. In some cases it has been demonstrated to promote neuronal survival, and in other cases to promote neuronal death. NF-κB, activated by low doses of Aβ(1-40) has been demonstrated to be neuroprotective in cerebellar granule cells [15]. NF-κB has also been reported to be involved in the survival of cerebellar granule neurons subjected to different potassium concentrations [17]. In global ischemia and traumatic spinal cord injury, however, NF-κB promoted neuronal death (for review see [20]). Moreover, increased levels in NF-κB activity have been observed in the brain of patients with various neurodegenerative disorders, including Alzheimer's disease[14], Parkinson's disease [13], and amyotrophic lateral sclerosis [21]. Thus, it appears that whether NF-κB acts as a promoter or inhibitor of neuronal loss depends on the cell type and the nature of the toxic stimuli. In our study, we show that NF-κB is activated in response to the administration of either Al or Aβ (1-42). Whether the translocation of NF-κB into the nucleus represents a cellular defensive mechanism, or represents an event facilitating neuronal injury, remains unclear.

In summary, our data show that both Al maltolate and Aβ(1-42) induce stress in the ER of rabbit brain. In response to the induced stress, the ER resident protein *gadd 153*, and the inducible transcriptional factor, NF-κB, are both translocated into the nucleus. Furthermore, Al- and Aβ(1-42)–induced stress is also marked by a decrease in the antiapoptotic Bcl-2 protein, both in the ER and in the nucleus. In addition, Al activates

caspase-12, a process specific to the ER-mediated apoptosis pathway. We propose that, although mitochondrial apoptotic signals are important in regulating apoptosis, ER and nuclear organelles may also participate in the molecular mechanisms of apoptosis following neurotoxic stimuli.

Acknowledgements

Supported by Grant # DAMD 17-99-1-9552 from the US Department of the Army. We gratefully acknowledge the generous gift of the capase-12 antibody from the laboratory of Dr. Junying Yuan.

References

1. The structure of the presenilin 1 (S182) gene and identification of six novel mutations in early onset AD families. Alzheimer's Disease Collaborative Group, Nat. Genet. 11 (1995) 219-222.

2. S.Althausen and W.Paschen, Homocysteine-induced changes in mRNA levels of genes coding for cytoplasmic- and endoplasmic reticulum-resident stress proteins in neuronal cell cultures, Brain Res Mol. Brain Res. 84 (2000) 32-40.

3. P.A.Baeuerle and T.Henkel, Function and activation of NF-kappa B in the immune system, Annu. Rev. Immunol. 12 (1994) 141-179.

4. B.Baumann, B.Kistler, A.Kirillov, Y.Bergman, and T.Wirth, The mutant plasmacytoma cell line S107 allows the identification of distinct pathways leading to NF-kappaB activation, J Biol. Chem. 273 (1998) 11448-11455.

5. J.Chen, S.H.Graham, P.H.Chan, J.Lan, R.L.Zhou, and R.P.Simon, Bcl-2 is expressed in neurons that survive focal ischemia in the rat, NeuroReport, 6 (1995) 394-398.

6. B.Fadeel, B.Zhivotovsky, and S.Orrenius, All along the watchtower: on the regulation of apoptosis regulators, FASEB J. 13 (1999) 1647-1657.

7. O.Ghribi, D.A.DeWitt, M.S.Forbes, M.M.Herman, and J.Savory, Co-involvement of mitochondria and endoplasmic reticulum in regulation of apoptosis: changes in cytochrome c, Bcl-2 and Bax in the hippocampus of aluminum-treated rabbits, Brain Res. in press.

8. S.H.Graham, J.Chen, and R.S.Clark, Bcl-2 family gene products in cerebral ischemia and traumatic brain injury, J Neurotrauma, 17 (2000) 831-841.

9. L.Guerrini, F.Blasi, and S.Denis-Donini, Synaptic activation of NF-kappa B by glutamate in cerebellar granule neurons in vitro, Proc. Natl. Acad. Sci. U.S.A, 92 (1995) 9077-9081.

10. J.Hacki, L.Egger, L.Monney, S.Conus, T.Rosse, I.Fellay, and C.Borner, Apoptotic crosstalk between the endoplasmic reticulum and mitochondria controlled by Bcl-2, Oncogene, 19 (2000) 2286-2295.

11. T.Hartmann, S.C.Bieger, B.Bruhl, P.J.Tienari, N.Ida, D.Allsop, G.W.Roberts, C.L.Masters, C.G.Dotti, K.Unsicker, and K.Beyreuther, Distinct sites of intracellular

production for Alzheimer's disease A beta 40/42 amyloid peptides, Nat. Med. 3 (1997) 1016-1020.

12. Y.Huang, M.M.Herman, J.Liu, C.D.Katsetos, M.R.Wills, and J.Savory, Neurofibrillary lesions in experimental aluminum-induced encephalopathy and Alzheimer's disease share immunoreactivity for amyloid precursor protein, Aβ, α_1-antichymotrypsin and ubiquitin-protein conjugates, Brain Res. 771 (1997) 213-220.

13. S.Hunot, B.Brugg, D.Ricard, P.P.Michel, M.P.Muriel, M.Ruberg, B.A.Faucheux, Y.Agid, and E.C.Hirsch, Nuclear translocation of NF-kappaB is increased in dopaminergic neurons of patients with Parkinson's disease, Proc. Natl. Acad. Sci. U.S.A. 94 (1997) 7531-7536.

14. B.Kaltschmidt, M.Uherek, B.Volk, P.A.Baeuerle, and C.Kaltschmidt, Transcription factor NF-kappaB is activated in primary neurons by amyloid beta peptides and in neurons surrounding early plaques from patients with Alzheimer disease, Proc. Natl. Acad. Sci. U.S.A, 94 (1997) 2642-2647.

15. B.Kaltschmidt, M.Uherek, H.Wellmann, B.Volk, and C.Kaltschmidt, Inhibition of NF-kappaB potentiates amyloid beta-mediated neuronal apoptosis, Proc. Natl. Acad. Sci. U.S.A, 96 (1999) 9409-9414.

16. V.Kostic, V.Jackson-Lewis, F.de Bilbao, M.Dubois-Dauphin, and S.Przedborski, Bcl-2: prolonging life in a transgenic mouse model of familial amyotrophic lateral sclerosis, Science, 277 (1997) 559-562.

17. E.Koulich, T.Nguyen, K.Johnson, C.Giardina, and S.D'mello, NF-kappaB is involved in the survival of cerebellar granule neurons: association of Ikappabeta phosphorylation with cell survival, J. Neurochem. 76 (2001) 1188-1198.

18. S.T.Lee, K.P.Hoeflich, G.W.Wasfy, J.R.Woodgett, B.Leber, D.W.Andrews, D.W.Hedley, and L.Z.Penn, Bcl-2 targeted to the endoplasmic reticulum can inhibit apoptosis induced by Myc but not etoposide in Rat-1 fibroblasts, Oncogene, 18 (1999) 3520-3528.

19. X.Liu, C.N.Kim, J.Yang, R.Jemmerson, and X.Wang, Induction of apoptotic program in cell-free extracts: requirement for dATP and cytochrome c, Cell, 86 (1996) 147-157.

20. M.P.Mattson, C.Culmsee, Z.Yu, and S.Camandola, Roles of nuclear factor kappaB in neuronal survival and plasticity, J. Neurochem., 74 (2000) 443-456.

21. A.Migheli, R.Piva, C.Atzori, D.Troost, and D.Schiffer, c-Jun, JNK/SAPK kinases and transcription factor NF-kappa B are selectively activated in astrocytes, but not motor neurons, in amyotrophic lateral sclerosis, J. Neuropathol. Exp. Neurol. 56 (1997)

1314-1322.

22. T.Nakagawa and J.Yuan, Cross-talk between two cysteine protease families. Activation of caspase-12 by calpain in apoptosis, J. Cell Biol. 150 (2000) 887-894.

23. T.Nakagawa, H.Zhu, N.Morishima, E.Li, J.Xu, B.A.Yankner, and J.Yuan, Caspase-12 mediates endoplasmic-reticulum-specific apoptosis and cytotoxicity by amyloid-beta, Nature, 403 (2000) 98-103.

24. H.L.Pahl and P.A.Baeuerle, A novel signal transduction pathway from the endoplasmic reticulum to the nucleus is mediated by transcription factor NF-kappa B, EMBO J. 14 (1995) 2580-2588.

25. H.L.Pahl and P.A.Baeuerle, A novel signal transduction pathway from the endoplasmic reticulum to the nucleus is mediated by transcription factor NF-kappa B, EMBO J. 14 (1995) 2580-2588.

26. H.L.Pahl and P.A.Baeuerle, The ER-overload response: activation of NF-kappa B, Trends Biochem. Sci. 22 (1997) 63-67.

27. H.L.Pahl, M.Sester, H.G.Burgert, and P.A.Baeuerle, Activation of transcription factor NF-kappaB by the adenovirus E3/19K protein requires its ER retention, J. Cell Biol. 132 (1996) 511-522.

28. E.Paradis, H.Douillard, M.Koutroumanis, C.Goodyer, and A.LeBlanc, Amyloid beta peptide of Alzheimer's disease downregulates Bcl-2 and upregulates Bax expression in human neurons, J. Neurosci. 16 (1996) 7533-7539.

29. W.Paschen and J.Doutheil, Disturbance of endoplasmic reticulum functions: a key mechanism underlying cell damage? Acta Neurochir. Suppl (Wien), 73 (1999) 1-5.

30. W.Paschen, C.Gissel, T.Linden, S.Althausen, and J.Doutheil, Activation of gadd153 expression through transient cerebral ischemia: evidence that ischemia causes endoplasmic reticulum dysfunction, Brain Res. Mol. Brain Res. 60 (1998) 115-122.

31. B.D.Price and S.K.Calderwood, Gadd45 and Gadd153 messenger RNA levels are increased during hypoxia and after exposure of cells to agents which elevate the levels of the glucose-regulated proteins, Cancer Res. 52 (1992) 3814-3817.

32. C.Saille, P.Marin, J.C.Martinou, A.Nicole, J.London, and I.Ceballos-Picot, Transgenic murine cortical neurons expressing human Bcl-2 exhibit increased resistance to amyloid beta-peptide neurotoxicity, Neurosci. 92 (1999) 1455-1463.

33. J.Savory, Y.Huang, M.M.Herman, M.R.Reyes, and M.R.Wills, Tau immunoreactivity associated with aluminum maltolate-induced neurofibrillary degeneration in rabbits,

Brain Res. 669 (1995) 325-329.

34. J.Savory, J.K.S.Rao, Y.Huang, P.Letada, and M.M.Herman, Age-related hippocampal changes in Bcl-2:Bax ratio, oxidative stress, redox-active iron and apoptosis associated with aluminum-induced neurodegeneration: increased susceptibility with aging, NeuroToxicol. 20 (1999) 805-818.

35. D.J.Selkoe, Alzheimer's disease results from the cerebral accumulation and cytotoxicity of amyloid β-protein, Journal of Alzheimer's Disease, 3 (2001) 75-81.

36. V.A.Shatrov, V.Lehmann, and S.Chouaib, Sphingosine-1-phosphate mobilizes intracellular calcium and activates transcription factor NF-kappa B in U937 cells, Biochem. Biophys. Res Commun. 234 (1997) 121-124.

37. B.K.Siesjo, B.Hu, and T.Kristian, Is the cell death pathway triggered by the mitochondrion or the endoplasmic reticulum? J. Cereb. Blood Flow Metab. 19 (1999) 19-26.

38. J.H.Su, G.M.Deng, and C.W.Cotman, Neuronal DNA damage precedes tangle formation and is associated with up-regulation of nitrotyrosine in Alzheimer's-disease brain, Brain Res. 774 (1997) 193-199.

39. J.Yang, X.Liu, K.Bhalla, C.N.Kim, A.M.Ibrado, J.Cai, T.I.Peng, D.P.Jones, and X.Wang, Prevention of apoptosis by Bcl-2: release of cytochrome c from mitochondria blocked, Science, 275 (1997) 1129-1132.

40. W.Zhu, A.Cowie, G.W.Wasfy, L.Z.Penn, B.Leber, and D.W.Andrews, Bcl-2 mutants with restricted subcellular location reveal spatially distinct pathways for apoptosis in different cell types, EMBO J. 15 (1996) 4130-4141.

Legends for figures

Figure 1 : Western blot of *gadd 153* (**A**), caspase-12 (**B**), Bcl-2 (**C**), and NF-κB (**D**), in cytoplasmic (**c**), nuclear (**n**), or endoplasmic reticulum (**er**), fractions from controls (1), and Al-treated (2) or Aβ(1-42)-treated (3) animals.

A. In controls(1), gadd 153 is detected in the cytoplasmic, but not in the nuclear, fraction. Following Al (2) or Aβ(1-42) (3) administration, *gadd 153* is present in the cytoplasmic fractions and also in the nuclear fractions; **B**. Caspase-12 is expressed only in the cytoplasmic fraction of Al-treated animal (2), and not in control (1) or Aβ(1-42)-treated (3) animals; **C.** Bcl-2 staining is intense in both the endoplasmic reticulum and nuclear fractions from controls (1). Al (2) or Aβ(1-42) (3) strongly reduce the staining for Bcl-2 in both the endoplasmic reticulum and nucleus; **D**. In the cytoplasmic fraction of controls (1), NF-κB is present as a dimer, the two bands corresponding to p52 and p100. Following Al or Aβ(1-42) administration respectively, p52 and p100 are detectable in the cytoplasmic fractions. In the nuclear fraction, while p100 is barely detectable, p52 is present.

Figure 2 : Photomicrographs for NF-κB (**B,D** and **E**) and *gadd 153* (**C, F** and **G**) labeling in the CA1 pyramidal cell layer of hippocampus (**A**) in controls, Al-treated and

Aβ(1-42)-treated animals. Control sections are immunostained with NF-κB (**B**) or *gadd 153* (**C**). Positive brown-black reactivity for NF-κB is localized in the nucleus in sections from Al-treated (**D**) or Aβ(1-42)-treated (**E**) animals (methyl green nuclear counterstain); insets in D and E are at a higher magnification. G*add 153* antibody also demonstrates nuclear localization (purple) in Al-treated (**F**) and Aβ(1-42)-treated (**G**) animals, (nuclear fast red counterstain); insets in F and G are at a higher magnification. Note the cytoplasmic reaction product with NF-κB (brown-black) and *gadd 153* (purple) staining. Scale bars: in B-G, 50μm; insets in D-G, 10μm.

Figure 3.

Immunofluorescence images of NF-κB (green) and *gadd 153* (red) labeling in the hippocampal CA1 area of control (top column), Al-treated (middle column), and Aβ(1-42)-treated (lower column) animals. NF-κB (**A**) and *gadd 153* (**B**) labeling in control. **C:** is an overlay of A and B. NF-κB labeling demonstrates the emergence of increased staining following Al administration (**D**) or Aβ(1-42)-treatment (**G**). *Gadd 153* immunoreactivity is also enhanced in neurons from an Al-treated (**E**) or Aβ(1-42)-treated animal (**H**). **F:** Image overlay of D and E, showing co-localization (arrow, yellow reaction product) of positive NF-κB labeling with *gadd 153* in Al-treated animal (arrows, yellow reaction product). **I**: overlay image of G and H demonstrates a number of positive neurons double-stained with NF-κB and *gadd 153* (arrows) in an Aβ(1-42)-treated animal. Scale bars represent 20 μm.

Tables

Table I. Densitometric analysis of *gadd 153*, caspase-12, Bcl-2, and NF-κB Western blots in controls (n=5), Al-treated (n=6), and Aβ(1-42)-treated (n=7) animals. Al or Aβ(1-42) treatment induces release of *gadd 153* and NF-κB into the nucleus, and reduces the expression of Bcl-2 protein in endoplasmic reticulum and nuclear fractions in comparison to control levels. Aluminum, but not Aβ(1-42), activates caspase-12.

A. Gadd 153

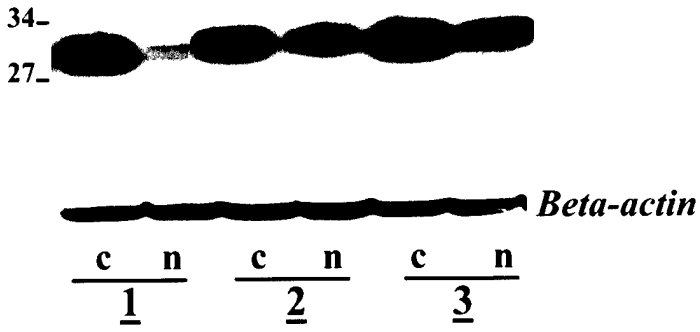

B. Caspase-12

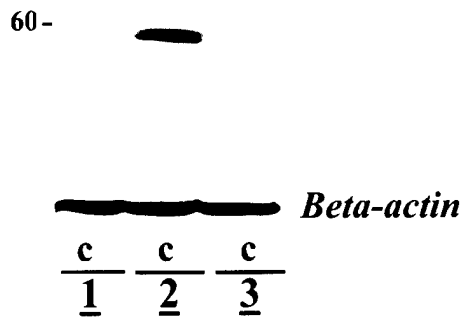

C. Bcl-2

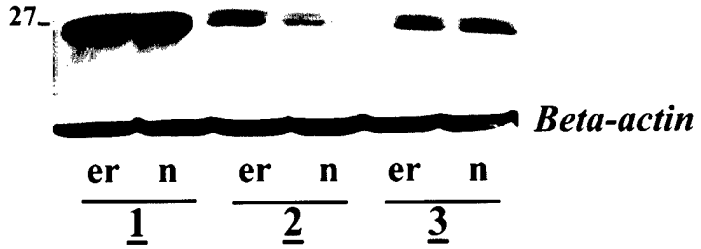

D. NF-kB

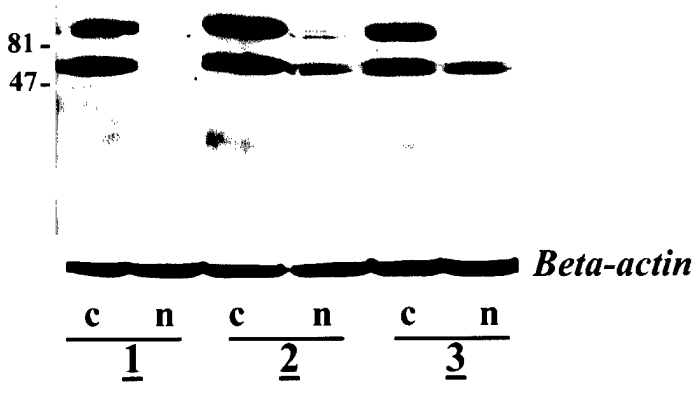

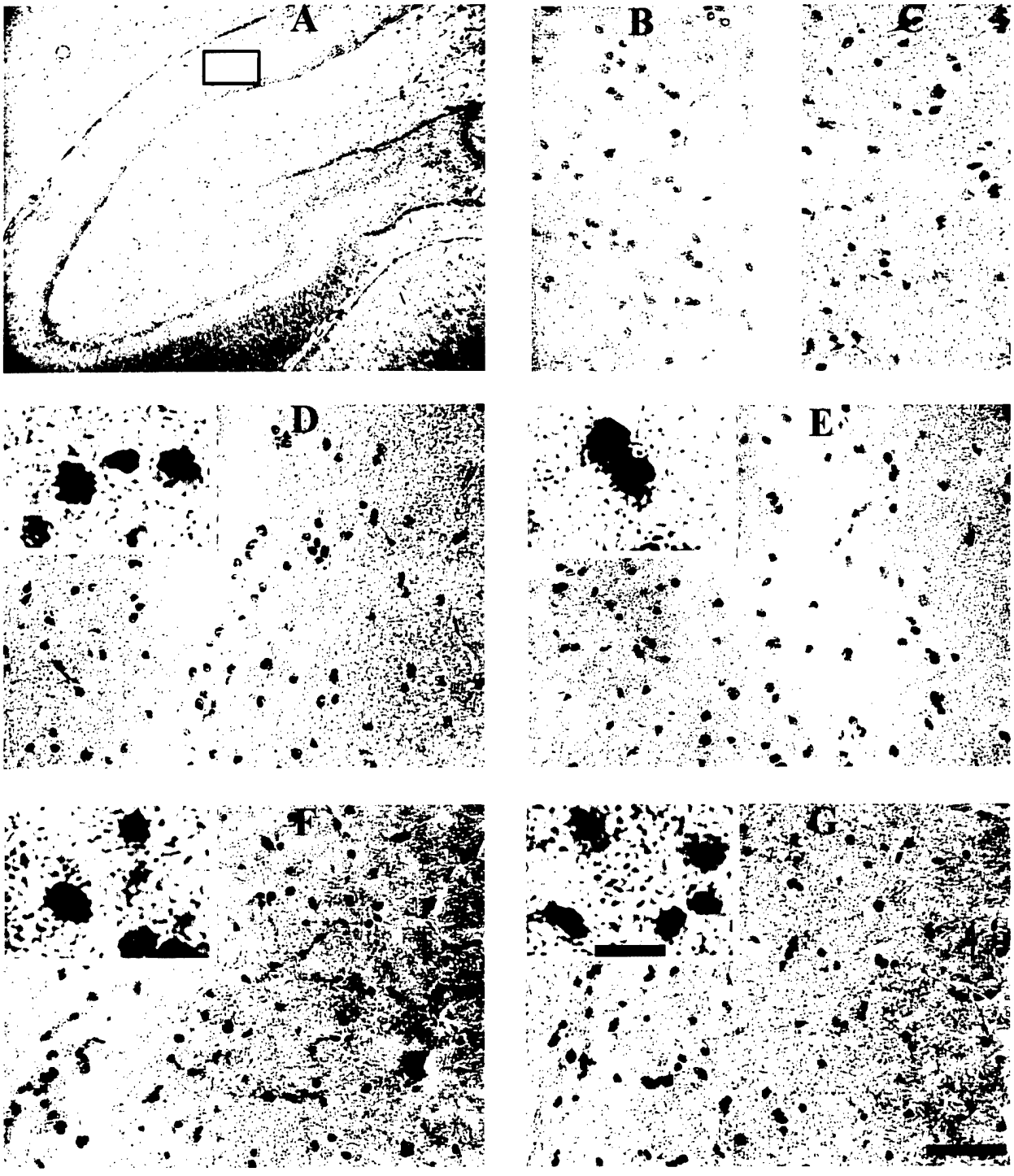
A
B
C
D
E
F
G

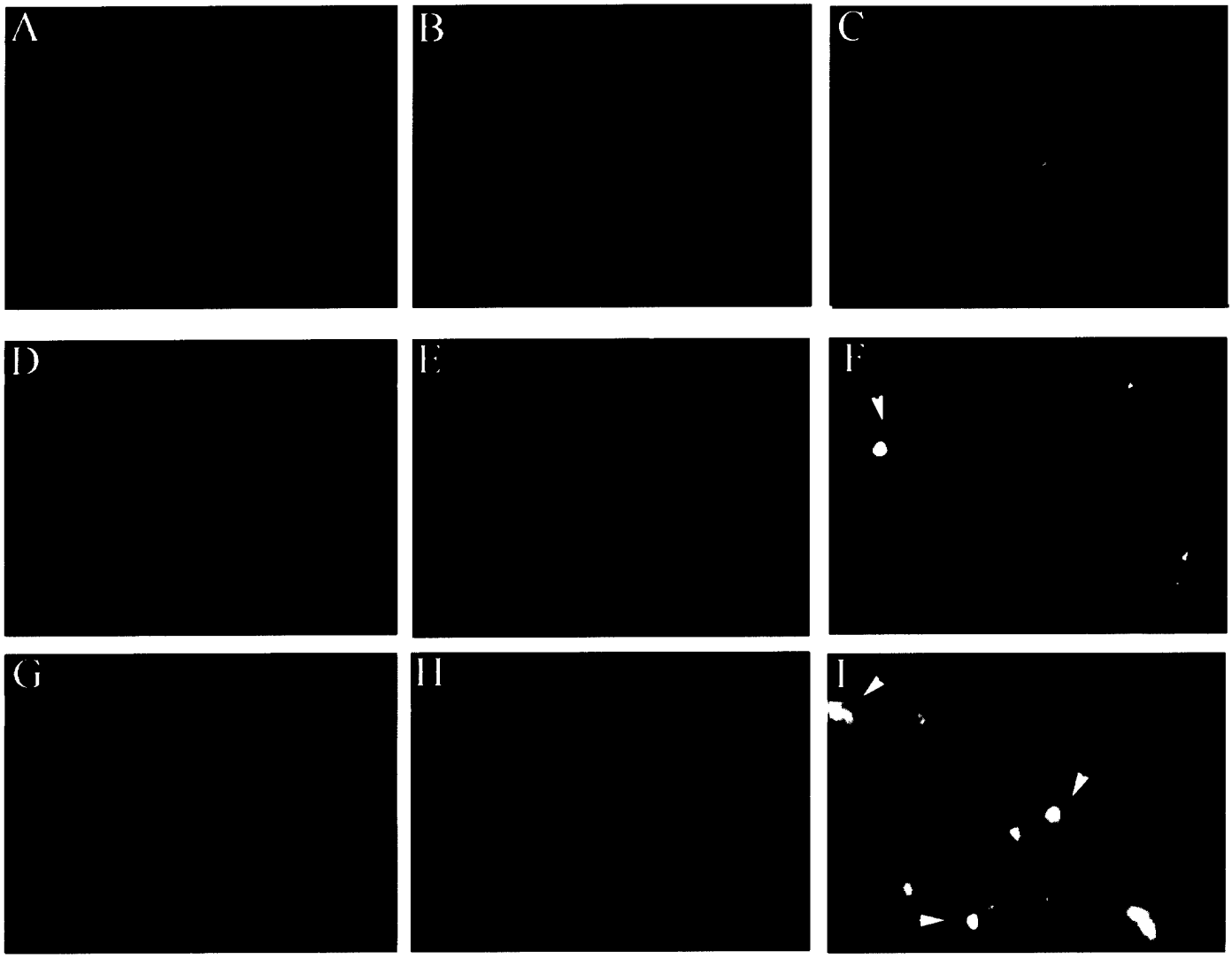
A
B
C
D
E
F
G
H
I

Table I. Densitometric analysis of *gadd 153*, caspase-12, Bcl-2, and NF-κB blots in controls, Al-treated, and Aβ(1-42)-treated rabbits.

		Cytoplasm		ER	Nucleus	
	Controls	3.17 ± 0.23			-	
Gadd 153	**Aluminum**	2.98 ± 0.33			1.60 ± 0.18	
	A-β(1-42)	2.85 ± 0.11			1.75 ± 0.16	
	Controls	-				
Caspase-12	**Aluminum**	1.12 ± 0.12				
	A-β(1-42)	±				
	Controls			2.50 ± 0.11	2.29 ± 0.22	
Bcl-2	**Aluminum**			0.82 ± 0.17**	0.75 ± 0.12**	
	A-β(1-42)			0.91 ± 0.18**	0.78 ± 0.26**	
		p 52	***p 100***		***p 52***	***p 100***
	Controls	1.61 ± 0.22	1.48 ± 0.22		-	-
NF-κB	**Aluminum**	1.78 ± 0.10	1.88 ± 0.13		0.66 ± 0.11	0.24 ± 0.09
	A-β(1-42)	1.66 ± 0.18	1.60 ± 0.18		0.72 ± 0.13	0.16 ± 0.08

- : undetectable levels; ± : barely detectable; empty columns: not measured.
**$p < 0.01$ (Student's *t* test, in comparison to controls).

APPENDIX V

Aluminum-induced dendritic pathology revisited: cytochemical and electron microscopic studies of rabbit cortical pyramidal neurons.

M. S. Forbes[1], O. Ghribi[1], M. M. Herman[3], and J. Savory[1,2]

*Departments of Pathology[1] and Biochemistry and Molecular Genetics[2], University of Virginia Health Sciences Center, Charlottesville, Virginia

[3]IRP, NIMH, NIH, Bethesda, Maryland

Running Title: NFAs in Brain of Al-treated Rabbit

ABSTRACT

Intracisternal administration of aluminum maltolate induces both biochemical and histological changes in the rabbit brain. The primary histological response to aluminum intoxication is the appearance within many neuronal somata and dendrites of intensely argyrophilic masses of fibrillar material. Ultrastructural characterization of these bodies in both conventionally-prepared and silver-stained sections shows them to be made up of neurofilaments. For this reason, we have elected to call these argyrophilic masses "neurofilamentous arrays (NFAs)". At their zenith, NFAs in cortical pyramidal neurons are composed of thousands of filaments interconnected by periodic crossbridges. NFAs begin their formation within both somata and dendrites as isolated groups of neurofilaments which apparently go on to assemble *en masse* within the cytoplasm. In symptomatic animals, many cortical neurons are rich in NFAs, yet lack typical cytological signs of degeneration such as nuclear pyknosis. Though silver staining reveals extensive NFAs only in aluminum-exposed brains, there is a strong degree of immunostaining for phosphorylated neurofilamentous epitopes in both untreated and Al-injected animals. This suggests that protein subunits, already present in the neurons under normal circumstances, are recruited in the presence of aluminum to form NFAs through the directed assembly of masses of oriented filaments, perhaps without any significant mobilization of neuronal synthetic machinery. No evidence has been found within aluminum-induced NFAs for the presence of the microtubule-derived "paired helical filaments" that typify the neurofibrillary tangles of Alzheimer's disease, although immunoreactivity for microtubular proteins has previously been demonstrated in NFAs.

INTRODUCTION

The neurotoxicity of aluminum ion has long been established, and the rapidity with which profound symptomatology can be induced by the direct introduction of aluminum into the brain has recommended this procedure as a potential model system for other neurological diseases (such as Alzheimer's) which have less obvious etiologies and far longer time-courses of development. A seminal finding in aluminum neurointoxication has been the presence in certain neurons of highly-visible cytoplasmic inclusions, which upon examination by various cytological staining regimens and electron microscopy prove to be masses of filaments. This observation has lent further credence to the concept of an Alzheimer's model, since a characteristic of Alzheimer's disease is the appearance of intraneuronal bodies called "neurofibrillary tangles," that also are composed of filamentous elements. Although there are distinct differences between the aluminum-induced inclusions and the Alzheimer "tangles," there nevertheless remains between the two pathologies a similarity that involves considerable alteration to the cytoskeletal components of neurons. There are other features of the aluminum-rabbit model system which render it applicable to the study of certain aspects of neuronal injury and death in human neurodegenerative disorders. We have previously demonstrated certain biochemical similarities between this rabbit system and the neuropathological lesions of Alzheimer's disease {Huang, Herman, et al. 1997 1178 /id}. Apoptosis also is a feature associated with severe aluminum neurotoxicity in rabbit brain {Savory, Rao, et al. 1999 1196 /id}, and this same cell-death pathway may play a role in the neuronal loss observed in Alzheimer's disease {Behl 2000 2220 /id}{Honig & Rosenberg 2000 2218 /id}. It remains to be clarified, however, just how the

various abnormalities seen in Alzheimer's disease brain come eventually to result in neuronal loss.

Although a considerable body of earlier work has been devoted to the presence, regional distribution, and general structural and staining characteristics of aluminum-induced neuronal inclusions {Kowall, Pendlebury, et al. 1989 74 /id}{Klatzo, Wisniewski, et al. 1965 931 /id}{Wisniewski, Karczewski, et al. 1966 2325 /id}{Yates, Gordon, et al. 1976 2326 /id}{Boni, Otvos, et al. 1976 2323 /id}, we have initiated a closer examination of their microscopic architecture and the steps by which their development might proceed. We have chosen to term these bodies "neurofilamentous arrays" (or simply "NFAs") to distinguish them from superficially similar aggregates found in other neuropathologies, We have concluded, furthermore, that NFA formation is not part of a degenerative process per se, but in fact may represent an attempt on the part of the individual neurons to defend against the presence of a neurotoxic insult. Accordingly, it seems that cells that develop these inclusions are not necessarily condemned to death, but under certain circumstances can survive, perhaps by dint of the very presence of NFAs, which after time disappear from the cells. That is to say, although NFAs may serve as an obvious marker for an ongoing neuropathologic event, they are not in and of themselves indicators of unavoidable cell death.

MATERIALS AND METHODS

Animals: Young female white rabbits of the New Zealand strain were used for this study. The animals ranged from 8-12 months in age and 2.4-3.6 kg in weight. Although older animals were examined in earlier studies {Ghribi, DeWitt, et al. 2001 2234 /id}, it was found that the most profound histological changes occur in younger animals following aluminum administration. Experimental animals were administered a single dose of 50 mM aluminum maltolate in 100 µl of sterile saline, injected directly into the cisterna magna with a sterile 25-gauge infusion apparatus. Control animals were left untreated in order to provide an appreciation of baseline "normal" ultrastructure of rabbit brain. Both in this and our previous biochemical studies it was determined that one week of survival is sufficient for histological alterations to become visible in spinal cord, brainstem and cortex. By that time, aluminum-treated animals usually evince as well a distinct symptomatology that consists of loss to some degree of motor function, particularly in the hind limbs, with accompanying lethargy and loss of appetite.

Tissue processing: Brains from control and experimental animals were prepared for microscopic examination by vascular perfusion with aldehyde fixative. Following administration via the ear vein of a euthanizing dose of pentobarbital, each animal was rapidly thoracotomized, its descending aorta clamped, and a 16-gauge needle inserted into the apex of the left ventricle. The right atrium was then cut and a gravity-feed perfusion begun, consisting in sequence of 300 ml of glucose/sucrose/saline solution (0.4%/0.8%/0.8%, respectively) followed immediately by 500 ml of a solution containing 0.05% glutaraldehyde, 4% paraformaldehyde, 15% (v/v) saturated

aqueous picric acid, and 0.1 M sodium phosphate buffer, pH 7.4. Total perfusion time was approximately 10 min, after which time the brain was quickly exposed, removed from the skull, and immersed for 3 hr in fresh fixative solution. The brain was then sliced into four separate coronal segments (forebrain/midbrain/cerebellum + brainstem/spinal cord), which were reimmersed in fixative solution at 4°C overnight. The segments were washed in several changes of 0.1 M sodium phosphate and stored in phosphate buffer with 0.01% sodium azide added to prevent microbial contamination.

For sectioning, the individual segments were encapsulated in 15% gelatin, and this stabilizing coating further hardened by immersion for 24-48 hr in the aldehyde fixative. Selected segments were cut into 50-μm coronal sections with injector-type razorblades mounted in a vibrating microtome (DSK Microslicer DTK-3000, Ted Pella, Inc., Redding, CA), and returned to azide-phosphate solution until further processing was undertaken. All sections were processed in free-floating form, and not until the conclusion of each procedure were those sections intended for light microscopy mounted on slides (see details, below).

Bielschowsky's silver staining of neurofilamentous arrays: Selected 50-μm sections were stained in free-floating form by a protocol used in this laboratory to reveal argyrophilic components in neurons. In summary, sections were immersed in darkness in 20% aqueous silver nitrate at 37°C for 30 minutes, followed by 15 minutes incubation in "ammoniacal silver" (prepared by adding concentrated ammonium hydroxide to the silver nitrate, while stirring, until a clear solution appears). The silver reaction was developed by adding ca. 10 drops/50 ml solution

of a "developer" consisting of 2% formalin and 0.4% citric acid in distilled water acidified with concentrated nitric acid (2 drops/250 ml). Whereas in our experience fourteen-micrometer-thick, formaldehyde-fixed sections mounted on slides require only about 15-20 minutes to show a suitable degree of staining in this solution, the considerably thicker sections used in this study required as much as 2 hr to display a thorough argyrophilia of neuronal cytoskeletal elements (as monitored, during the development step, by light-microscopic examination of the wet sections). The reaction was stopped by transfer of sections into 1% aqueous ammonium hydroxide, with a subsequent "fix" in 5% sodium thiosulfate. Some sections were washed in distilled water, affixed to gelatin-coated slides, allowed to dry down, and then cleared in xylenes and coverslipped for light microscopic examination, while others were directed to a plastic-embedment regimen detailed below ("Electron Microscopic Examination").

Immunocytochemical staining of cytoskeletal components: Pre-embedding immunocytochemistry on brain sections was carried out as previously described {Alheid, Beltramino, et al. 1998 2301 /id}. To summarize, sections were infiltrated 30 min with a cryoprotectant solution (2% DMSO and 20% glycerol in 0.1 M sodium cacodylate) and collected on segments of glass microscope slides. These were placed into aluminum weighing dishes, which were set on a liquid-nitrogen surface for two cycles of freezing and thawing; this procedure renders sections more permeable to antibody penetration. The sections were washed thoroughly in phosphate buffer, blocked with 10% normal horse serum and 1% BSA (Sigma 7030) in 0.1 M sodium phosphate, pH 7.4, and then incubated in vials of primary antibody solution (see primary antibody concentrations below; carrier solution consisted of 1% BSA in 0.1 M sodium phosphate

buffer, pH 7.4). Incubation continued overnight at 4°C with constant agitation on a Nutator (Model 1105, Clay-Adams, Parsippany, NJ). The next morning sections was washed in buffer and then exposed to secondary antibody in carrier (1:200 biotinylated horse anti-mouse IgG, Vector BA-2000) at RT for 2 hr, followed by rinses and incubation in avidin-solution (Vector Vectastain ABC Elite Kit) for 2 hr at RT. Sections were then rinsed and the reaction developed for 30 min by the glucose oxidase-diaminobenzidine method of Itoh et al. {Itoh, Konishi, et al. 1979 2303 /id}. As with the silver-stained sections that were intended for light microscopic examination alone, immunostained sections were affixed to gelatin-coated slides, allowed to dry, cleared in a series of xylene solutions, and coverslipped.

A monoclonal antibody which reacts with phosphorylated neurofilament epitopes (SMI-31, Sternberger Monoclonals, Inc., Lutherville, MD) was tested on sections at dilutions of 1:1000 and 1:5000.

Electron microscopic examination: For conventional TEM examination, the 50-μm sections were washed in 0.1 M Na cacodylate solution and postfixed gradually (to minimize section curling) in ascending concentrations of osmium tetroxide (final concentration of 1%) in cacodylate buffer (pH 7.4) for a total postfixation period of 30 min. *En bloc* contrasting with saturated aqueous uranyl acetate was carried out for 30 min. Some of the silver-stained sections were prepared without either osmium postfixation or uranium block-staining. All sections were dehydrated in an ascending series of ethanols, passed through propylene oxide, and infiltrated under vacuum in Poly/Bed 812 resin (Polysciences, Warrington, PA, U.S.A.). The free-floating sections were transferred to microscope slides coated with liquid-release agent (Electron

Microscopy Sciences, Ft. Washington, PA, U.S.A.) and topped with similarly-coated coverslips, which were weighed down with coins to flatten the sections. The embedments were then cured at 60°C for two days. Sections were examined on the slides with a light microscope and areas of interest selected. The coverslip portions over these regions were removed with a scribing tool and dissecting pin, and a trapezoidal portion of the brain section cut out with a razorblade and glued with cyanoacrylate to an epoxy capsule. Semi-thin (0.25-1.0 μm) sections were prepared with glass knifes on a Sorvall MT-2B ultramicrotome and stained with 1% toluidine blue in 1% sodium borate for orientation and detailed light microscopic documentation; for the TEM, 70-100 "ultrathin" sections were cut with a DuPont diamond knife. Sections were collected on copper-mesh grids and stained with saturated uranyl acetate in 50% acetone (1-2 min) and 0.5% alkaline lead citrate (1-2 min). All sections were examined in a Zeiss EM-10CA transmission electron microscope operated at an accelerating voltage of 60 keV. This instrument was calibrated for crucial magnifications against a replica of an optical grating, and measurements of cell structures were made directly from high-magnification photographs with a vernier caliper.

RESULTS

Light microscopic observations: The cytoskeletal elements of neurons are clearly delineated with a silver staining procedure such as the Bielschowsky's method, and their three-dimensional interrelationships are particularly well demonstrated in 50-micrometer-thick sections stained with this procedure (Figs. 1-6). While in parietal cortex of untreated animals the cytoskeleton is revealed as dark threadlike profiles located primarily in axons (Figs. 1, 3), equivalent sections of aluminum-intoxicated brain offer a striking contrast, with numerous pyramidal cell bodies standing out in silhouette because of the prominent silver-stained profiles within them (Figs. 2, 4-6); cells affected in this manner are found in varying numbers throughout the cerebral cortex, but are particularly numerous in the more caudal cortical midline. ***(Mary: see accompanying diagram of W. atlas coronal sections, w. NFA locations indicated by outlines, yellow highlighting, and white arrows)***

In cortical cells from aluminum-exposed brains, a pattern of staining emerges that consists of elongated apical dendritic aggregates, accompanied by short, thick basal dendritic arrays (Figs. 2, 4-6). The apical dendritic masses may display "corkscrewed" profiles (Fig. 5) that in many cases can be resolved into several separate, parallel helical skeins within the same process. In the "whole-mount" sort of display afforded by the thick-section, Bielschowsky's-stained preparations, some cells (Fig. 6) demonstrate continuity between the apical and basal argyrophilic masses. This can be confirmed in toluidine-blue-stained, "semi-thin" sections of plastic-embedded material (Fig. 7), where because of a lack of osmiophilia the neuronal inclusions appear unstained against the

darker background of contrasted nucleus and cytoplasm. Although nuclei are difficult to detect in Bielschowsky's-stained cortex of aluminum-treated rabbits, being largely obscured by the intensely silver-stained masses superimposed on them, they appear normal in semi-thin and ultrathin sections (Figs. 7-9).

Electron microscopic studies: In the electron microscope, the cytoplasmic inclusions appear in thin section as lucent profiles of variable size and shape (Fig. 8). TEM examination of Bielschowsky's silver-stained sections shows, furthermore, that these bodies are selectively and specifically marked by the deposition of silver particles (Fig. 9). Each inclusion is composed primarily of filaments, which in some cases number in the thousands within in a single group, with only an occasional mitochondrion and a few vesicles or tubules captured within the filamentous confines (Fig. 10). Inspection at high magnification reveals the filaments to be closely packed and uniform in appearance (Figs. 11, 12). On the basis of their 14-nm diameter (14.1 ± 1.7 nm, n =15) , similar to that of neurofilaments that form sparse populations in dendrites of untreated animals (14.9 ± 0.9 nm, n = 15) and to axonal filaments (13.2 ± 0.9 nm, n = 15), they can be identified as belonging to the cytoskeletal fibril category commonly known as "neurofilaments." Because of this, we have chosen to refer to these particular argyrophilic masses as "neurofilamentous arrays" or "NFAs." While neurofilaments and glial filaments alike are considered to belong to the general category known as "10-nanometer" or "intermediate" filaments, it is clear that the neurofilaments, whether found in unaffected dendrites, axons, or NFAs, are typically larger in diameter than their glial counterparts, which--more in keeping to the traditional nomenclature--average about 10 nm in diameter (10.2 ± 1.0 nm, n = 15).

The closely-packed neurofilaments that compose NFAs are joined together by numerous cross-bridging structures (Fig. 12) that hook the filaments together in a lattice-like array, in which adjacent filaments commonly observe both parallel orientation and a center-to-center spacing of ca. 33 nm (33.4 ± 2.6 nm, n = 17) (Fig. 11). The degree of NFA development is not the same in all cortical neurons, even at the same coronal level; while fully-formed populations of NFAs may be evident in one neuron, only small somatic and dendritic filament groups may appear in nearby cells (Figs. 13, 14). Regardless of the extent of NFAs, there is no overt ultrastructural sign of degeneration in any of the cells that contain them. That is, the NFA-containing cells, absent the masses of filaments, are qualitatively identical to their unaffected neighbors and display no sign of nuclear pyknosis, Golgi swelling, or visible alterations to the ER and mitochondria.

Immunocytochemical observations: Despite the profound differences in the histological picture of normal vs. aluminum-treated cortical cells, the pattern of immunological staining for the phosphorylated epitope of neurofilaments is quite similar, with abundant staining in both cases throughout the dendrites and somata of cortical pyramidal neurons (Figs. 15, 16). The overall staining appears more intense in the aluminum-treated animal, and close examination shows this to result from the density of immunoreactive material within the apical and basal dendrites (Fig. 17).

DISCUSSION

Fibrillar neuronal inclusions, often called "neurofibrillary tangles," are considered a hallmark of neurodegeneration in a variety of pathological situations, Alzheimer's disease and aluminum toxicity among them. In the case of aluminum-treated rabbits, development of these fibrillar inclusions (*neurofilamentous arrays* or *NFAs*) is well-documented, predictable in timing and age-responsive. However, the presence of NFAs seems more indicative of a synthetic event than necessarily of an intrinsically degenerative process. While we do not believe the presence of NFAs necessarily to signify impending cell death, their development in certain brain cells (here cortical pyramidal neurons) is nevertheless a bellwether, signalling the occurrence of a neurological insult (in this case exposure to aluminum maltolate). The resulting biochemical changes in such proteins as cytochrome *c*, Bax and Bcl-2 are virtually identical in both cortex and neighboring hippocampus {Ghribi, DeWitt, et al. 2001 2240 /id}, despite the lack of NFAs in hippocampal neurons. The time-course of development of cortical NFAs is consistent, even when neuroprotection is bestowed by glial cell-derived nerve growth factor (GDNF), which protein--when injected simultaneously with aluminum--allows the animals to survive, while many of the NFAs eventually wane {Ghribi, Forbes, et al. 2001 2241 /id}; this indicates NFA formation to be a largely transitory event, which may embody a defensive, "filtering" response by certain cells to the presence of aluminum ion.

NFAs in aluminum-treated rabbit brain are composed of normal-appearing neurofilaments. The same three polypeptide species (68, 150-160, and 200 kDa) are found in both "normal" and NFA-component neurofilaments {Selkoe, Liem, et al. 1979 207 /id}{Ghetti & Gambetti 1983 163 /id},

and all such neurofilaments are immunologically distinct from glial cell filaments, {Dahl & Bignami 1978 999 /id}, which are composed primarily of glial fibrillary acidic protein (GFAP). Commercially available monoclonal antibodies for the phosphorylated and non-phosphorylated epitopes of neurofilaments have been utilized in several studies of NFAs in the aluminum-rabbit neuropathy model {Kowall, Pendlebury, et al. 1989 74 /id}{Pendlebury, Perl, et al. 1988 2045 /id}{Strong, Wolff, et al. 1991 918 /id}{Katsetos, Savory, et al. 1990 18 /id}{Savory, Huang, et al. 1996 1 /id}. In all of these, SMI-31 (which detects phosphorylated NF antigens) intensely stained NFAs of aluminum-exposed brain, while in equivalent neurons of control animals, SMI-31 immunoreactivity was restricted to the axons, with no reactivity at all appearing in either dendrites or perikarya. Our experience with this same antibody, however, demonstrates a considerable presence of phosphorylated NF epitope throughout cortical pyramidal neurons in control and aluminum-treated rabbit brain alike. This finding seems at odds with the studies mentioned above, and the difference may be attributable to our immunohistochemical technique.

Interestingly, it has been found that topical application of SMI-31 antibody to acetone-fixed cultured spinal neurons gave results similar to the other studies–i.e., axons were strongly labeled, but cell bodies were not {Durham 1990 2317 /id}. However, actual injection of antibody into the living cells or immunoreaction of Triton-extracted cells prior to fixation both resulted in positive staining of perikaryal and dendritic filament complements {Durham 1990 2317 /id}. In that report it was proposed that the question of SMI-31 immunoreactivity is not dictated by the actual degree of neurofilament phosphorylation, but rather by the relative *accessibility* of the epitopes {Durham 1990 2317 /id}. These findings are consistent with previous findings from our laboratory

{Savory, Herman, et al. 1993 12 /id} which detected no significant changes between control and aluminum-exposed rabbit brain, either in the total amounts or the degree of phosphorylation and gene expression of any of the neurofilament isoforms. The immunohistochemical method used in this and other laboratories for "permeabilization" of sections, then, assumes special significance. As noted in our Methods section, we utilize a process of repeated freeze/thaw cycles, in the presence of an infiltrated cryoprotectant solution. It is thought that this procedure produces submicroscopic fissures in cell membranes, which enhance penetration of the subsequent reagent solutions, in particular the antibodies. This regimen, then, may optimize the immunological reactivity of phosphorylated neurofilament epitopes, whether they are incorporated into actual filaments or not.

By and large, neuronal dendrites, despite their newly-appreciated functionalities {Matus 2000 2304 /id}{Hausser, Spruston, et al. 2000 2314 /id}{Segev & London 2000 2305 /id}, are not under ordinary circumstances particularly striking in terms of their architecture. However, upon exposure of the CNS to aluminum there rapidly appear, within both apical and basal dendrites of cortical pyramidal neurons, populations of oriented neurofilaments tightly bound together in massive rods or bundles that may nearly fill the dendritic processes, and occupy substantial somatic cytoplasm besides. The groups of filaments appear to begin forming in situ from nucleating points in both soma and dendrites to create tightly-organized skeins of parallel neurofilaments. These aluminum-induced cytoskeletal changes may result largely from utilization of the proteinaceous material--already present in non-filamentous form--which is induced to adopt fibrillar configuration and create large three-dimensional aggregates. Overall, this indicates that phosphorylated neurofilament epitopes are already in place, and abundantly so, in the normal

brain. The fundamental difference between control neurons and aluminum-exposed, NFA-containing cells is the structural form taken by the majority of neurofilament proteins; i.e., they are primarily "globular" or in some short-chain-subunit form in the control animal, while in the aluminum-exposed rabbit they exist mainly as masses of filaments. In essence, then, there appears to occur a rapid and extensive *reconfiguration* of existing cytoskeletal subunits into fully-formed cytoskeletal fibrils that are interconnected by numerous crossbridge structures. Treatment of neuroblastoma cells with aluminum salts has been shown {Shea, Clarke, et al. 1989 84 /id} to produce Bielschowsky-silver positive accumulations consisting of neurofilaments; these filamentous whorls were not seen in the somata of untreated cells, however. This fits in well with our observations on intact brain, where it also appears that aluminum elicits the formation of great numbers of "assembled" neurofilaments. Since even in the dendrites of the untreated brain there is a certain amount of "default" silver staining (e.g., see Fig. 3), one may conclude that this is associated with the relatively few neurofilaments that exist there in true fibrillar form. Our finding in neurons of control brain of an abundance of phosphorylated epitopes thus suggests that a neurofilament's architecture, as much as or more than its degree of phosphorylation, is the basis of Bielschowsky's silver staining in rabbit brain.

Although, in general, neurofibrillary inclusions have been linked to one or another disease process, we here have made the case that NFAs in rabbit brain are transitory and/or reversible in nature, given the right circumstances; under those circumstances, furthermore, their rise and fall can occur quite quickly. Given the far longer time-frame characteristic of Alzheimer's disease, however, it has recently been proposed that in addition to the lack of a universal occurrence of

neurofibrillary tangles (NFTs), the cells which do develop them may continue to survive in spite of their presence for long periods of time (ten to twenty years on average). Even though there exist substantial differences between NFTs and NFAs, not the least of which is their relative lifespan, it appears that the conclusions arrived at by Morsch *et al.* {Morsch, Simon, et al. 1999 1697 /id} for Alzheimer's tangles are equally applicable to aluminum-induced neurofilamentous arrays. For one, NFTs cannot be assumed to be the direct cause of death of the host neuron (and in fact the total numbers of dying neurons in Alzheimer's brain far exceed the number having NFTs) {Morsch, Simon, et al. 1999 1697 /id}. Likewise, NFAs cannot be considered de facto evidence of neurodegeneration.

What, then, is the reason for NFA occurrence? Even though there was evidence of hind-limb "motor deficits" in rabbits 7-8 days after intraventricular or intracisternal aluminum injection, Simpson et al. {Simpson, Yates, et al. 1985 2312 /id} concluded that no "gross effect on neuronal metabolism" had been wrought either by aluminum or the presence of NFAs. In the absence of overt mobilization of protein synthetic machinery, such as would be indicated by enlarged Golgi saccules and proliferated endoplasmic reticulum, and considering that a great deal of neurofilament protein is already present (even in neurons not exposed to aluminum) we have suggested that the filaments which make up NFAs are assembled in large part from proteins already on hand. It has been proposed that, in Alzheimer's disease, paired helical filaments are able to form and accumulate because their composition is so similar to "normal" cytoskeletal proteins as to escape the degradative and exocytotic mechanisms that ordinarily would be triggered by the presence of foreign materials {De Boni & McLachlan 1980 2322 /id}. The

situation for aluminum-induced NFAs might in fact be even more subtle. Aluminum's effects are multifocal; some studies have indicated that nuclear chromatin is especially sensitive to this ion {Walker, Leblanc, et al. 1989 2327 /id}, and histochemical stains specific for aluminum furthermore localize on chromatin {Boni, Otvos, et al. 1976 2164 /id}{De Boni, Scott, et al. 1974 2321 /id}, thus implying that aluminum and chromatin have in fact a certain, perhaps deadly, affinity for one another.

While aluminum may bind directly to genetic material, it appears to be at work as well out in the cytoplasm. In an early study with the Solochrome-Azurine method for aluminum localization, Klatzo et al.{Klatzo, Wisniewski, et al. 1965 931 /id} found staining of both nucleoli and NFAs. It appears that the presence of aluminum ion promotes the aggregation of phosphorylated cytoskeletal proteins {Shea, Clarke, et al. 1989 84 /id}{Diaz-Nido & Avila 1990 1160 /id}. It seems likely, in the normal course of a nerve cell's metabolic day, that there exists a balance between buildup and breakdown of various structures, among them individual neurofilaments. Goldstein et al. {Goldstein, Sternberger, et al. 1987 2316 /id} found that phosphorylated neurofilaments are resistant to proteinase action, while dephosphorylated ones are more susceptible. In their comparison of aluminum intoxication with Alzheimer's disease, Yokel et al. {Yokel, Provan, et al. 1988 51 /id} proposed that sufficient inhibition of proteinase activity would interrupt the normal cycle of filament breakdown in the neurons, thus leading to the production of large filament aggregations. One may speculate therefore that aluminum can subvert production of proteinase at the nuclear transcription/translation level, while in the cytoplast simultaneously promoting both the assembly and architectural stability of neurofilament

arrays.

We conclude, therefore, that the formation of NFAs in the aluminum-treated animal can serve our understanding of the role of NFTs in the Alzheimer's disease brain, and that both--although classical neuropathological colophons of their respective disorders-- might not in fact cause neuronal death. Rather, these fibrillar accumulations might represent a protective response by neurons, buffering the effect of neurotoxins in an attempt to minimize apoptotic (and perhaps necrotic) cell death.

ACKNOWLEDGMENTS

This work was supported by grant #DAMD 1799-1-9552 from the United States Department of the Army to Dr. John Savory. The transmission electron microscope used for this study was provided and maintained by the Central Electron Microscope Facility of the University of Virginia School of Medicine. The authors also acknowledge with thanks helpful discussions with Dr. Carlo Bruni, Professor Emeritus of the University of Virginia.

FIGURE LEGENDS

Figs. 1-6. Silver-stained (Bielschowsky's method) coronal 50-μm sections through [parietal?] cortex showing pyramidal neuron cytoskeletal components in untreated young female rabbit (Figs. 1, 3) and aluminum-treated female (50 mM aluminum maltolate, seven days exposure) (Figs. 2, 4-6).

Fig. 1. Silver staining confers a delicate, threadlike pattern that runs in the vertical axis throughout much of the cortex (diagonal in this field). Although cell nuclei stain lightly with silver (cf. Fig. 3), cell outlines are not evident in control tissue. X .

Fig. 2. An equivalent section from an animal exposed to aluminum for 7 days. A layer of cortical pyramidal neurons stand out in silhouette because of the argyrophilic staining of their contents. X .

Fig. 3. Detail of control cortex. The lightly opacified dots scattered throughout this field are cell nuclei (*Nu*). The pattern of silver staining here is limited to extensive thin profiles of cytoskeletal material, the majority associated with the axons. X .

Figs. 4-7. Cortex from aluminum-treated animal (treatment as described in Fig. 1).

Fig. 4. Aluminum-treated animal. Although some nuclei can be discerned, the picture is dominated by densely-staining cortical cells, made evident by the prominent contents of their apical (*AD*) and basal (*BD*) dendrites, the latter fanning out from the bases of the neurons. X .

Fig. 5. Aluminum-treated. The elongate silver-positive bodies within apical dendrites in some instances display a twisted or "corkscrew"-like morphology; in places along their lengths, parallel separate strands of stained material can be discerned. Equivalent masses in the basal dendrites are heavily stained, but much less extensive. X

Fig. 6. In this pyramidal cortical neuron, the silver-stained cytoskeletal material is continuous from the apical dendrite, extending as several thin strands through the cell body that pass around the nuclear zone (*Nu)* to merge with the material in each basal dendrite. X

Fig. 7. "Semi-thin" (ca. 0.25 μm) section from plastic-embedded cortex, stained with toluidine blue and viewed in an orientation similar to that seen in Fig. 6. Here the nucleus (*Nu*) is seen in section, partly surrounded by a contiguous mass of proliferated cytoskeletal material, which in this preparation appears lucent against the basophilia of the other cytoplasmic contents, and extends from the apical dendrite into the cell soma. X

Figs. 8-16. Transmission electron micrographs of cerebral cortex from aluminum-treated rabbit brain (see Fig. 1), documenting the ultrastructure of neurofilamentous arrays (NFAs) that characterize the aluminum-induced neuropathy.

Fig. 8. Survey of pyramidal neuron (approximately same orientation as previous illustrations); within the apical dendrite (*AD*) and the soma appear lucent zones that represent sections through masses of filaments. Toward the bottom of the field, similar masses are directed away from the lower portion of the cell into the cytoplasmic extensions that form basal dendrites (*BD*). Neither the nuclear profile nor any of the other cytoplasmic contents appear altered. X

Fig. 9. Cortical neuron in similar orientation to that in Fig. 8, but from Bielschowsky silver-stained section for comparison. Dominating the field is an opacified NFA that extends from the cell body up into the apical dendrite (*AD*). The fibrillar component of the neuron's nucleolus (*Nuc*) is also stained, as are the neurofilaments that fill nearby myelinated axons (*Ax*). X .

Fig. 10. In this somatic NFA, the majority of filaments are cut in transverse section. The NFA is almost entirely composed of 14-nm-diameter neurofilaments (detail shown in *inset*) with only an occasional embedded profile of a mitochondrion (*Mi)* or ER tubule. X

Fig. 11. Longitudinal section through NFA in apical dendrite. The closely-packed neurofilaments observe strict parallel arrangement. Periodic crossbridges extend between adjacent filaments, merging with an amorphous substance that coats the filament shafts. X .

Fig. 12. Transversely-cut NFA, showing distribution of neurofilaments, many of which are connected laterally by poorly-defined crossbridges that hold the adjacent filaments in register with a center-to-center spacing of ca. 33 nm. Amorphous material adheres to the profiles of the individual filaments as well. X .

Fig. 13. One of two small perinuclear concentrations of neurofilaments in a nerve cell found adjacent to other neurons that contained large NFAs. The component neurofilaments are flanked by Golgi saccules (*GA*), and as in definitive NFAs are oriented largely parallel to one another. X .

Fig. 14. An isolated skein of parallel neurofilaments is suspended in the long axis of an apical dendrite. This sort of de novo assembly, along with somatic accumulations like those seen in Fig. 13, appears to represent the beginnings of NFA formation. Although this grouping is far less extensive than NFAs in fully-involved neurons, its components have similar spacing, coatings and crossbridges (see *inset*). X .; inset X .

Figs. 15-18. Immunostaining for phosphorylated neurofilament epitope.

Fig. 15. Untreated cortex. Pyramidal neurons are clearly stained throughout the cell bodies and dendrites. X .

Figs. 16, 17. Aluminum-exposed cortex. Although casual inspection of Fig. 16 shows these neurons to be similar in size and appearance to those in Fig. 15, the regions of immunostaining are notable in the degree of concentration of their opacified contents. This is particularly visible in the apical (*AD*) and basal dendrites (*BD*), which at higher magnification (Fig. 17) appear darker and thicker than those in untreated cells. Fig. 16, X ; Fig. 17, X

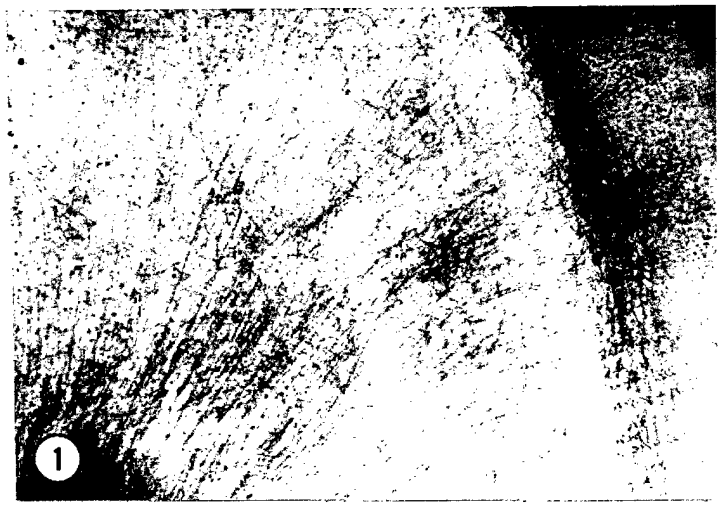

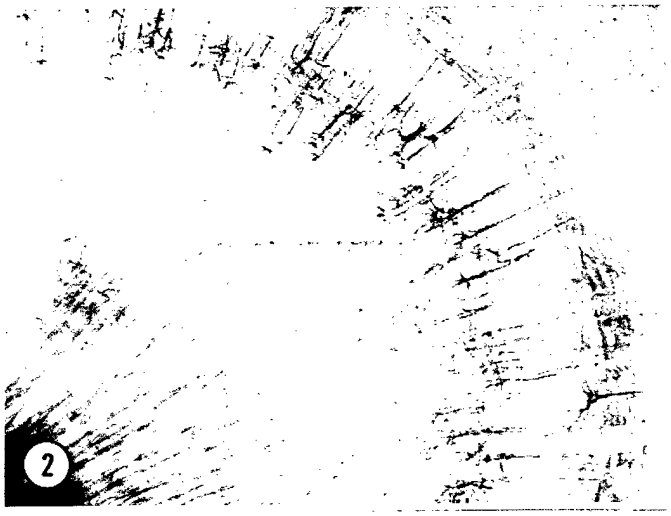

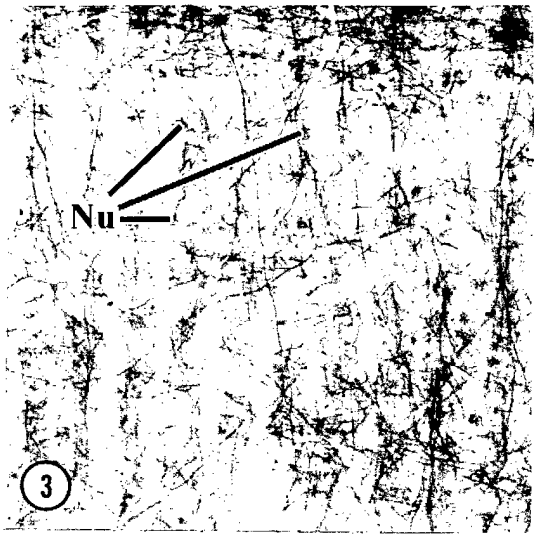
Nu

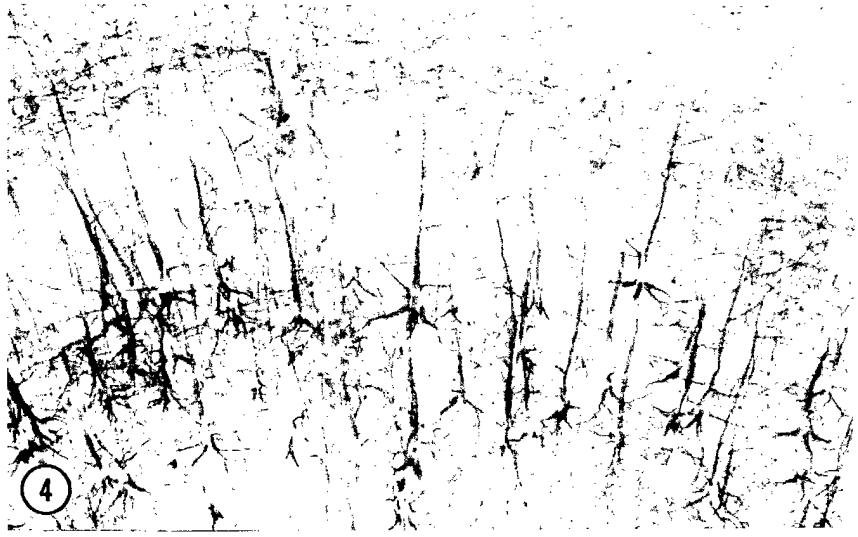


AD


Nu


Nu

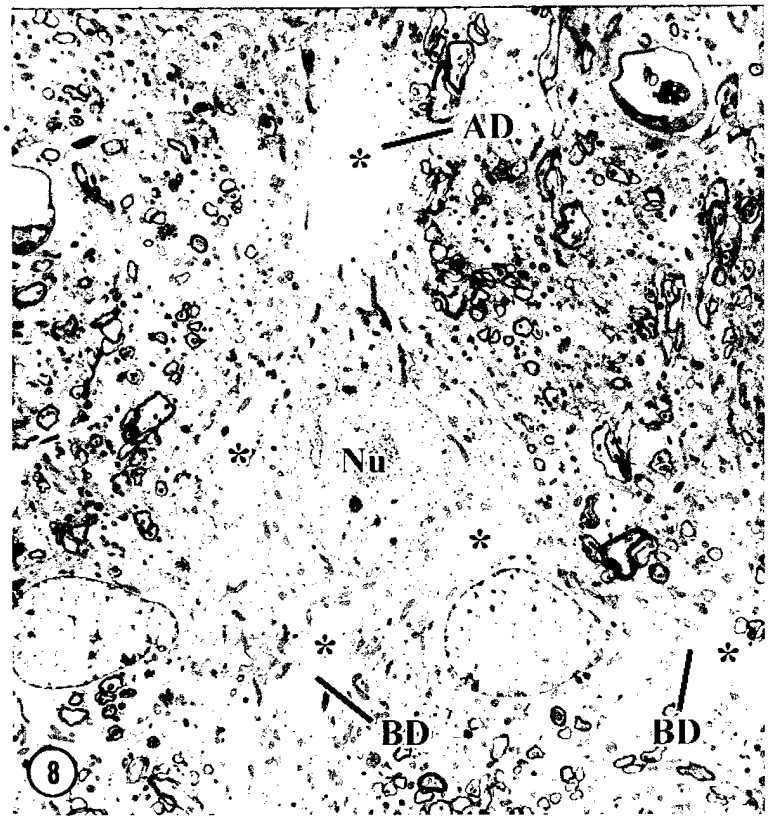

8

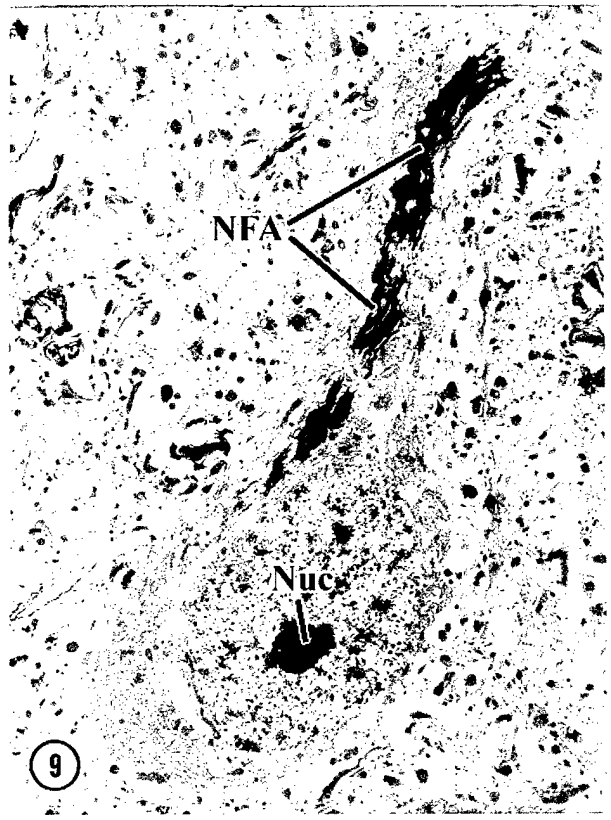

9

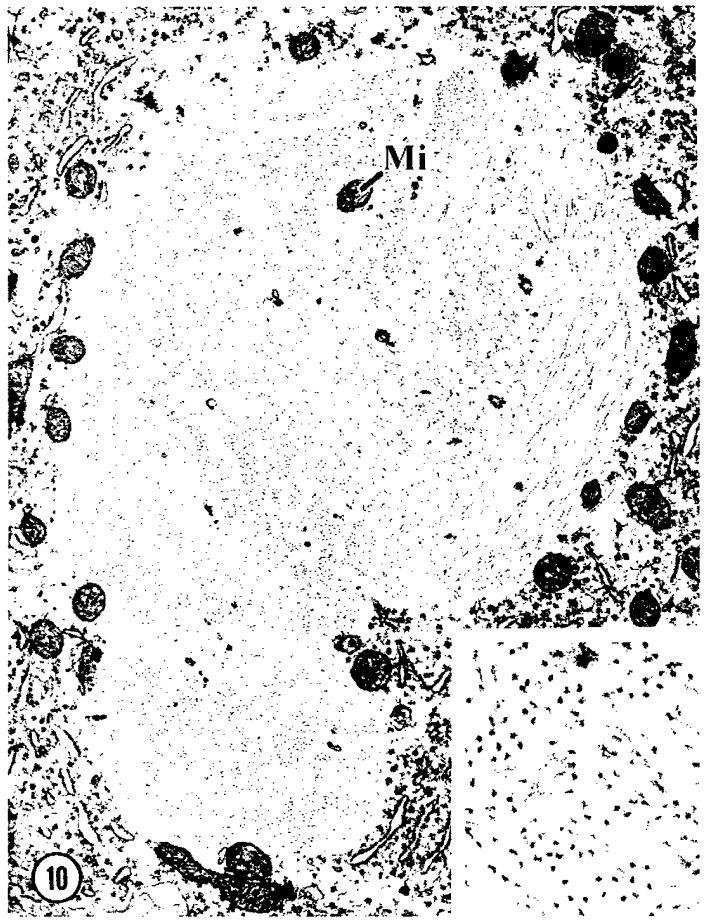

10

11

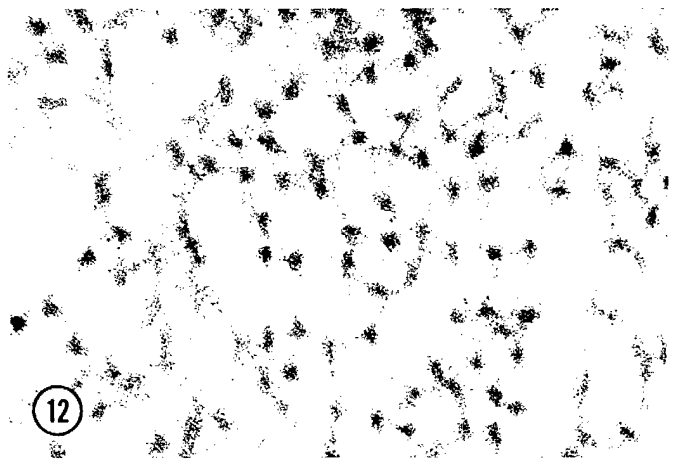

12

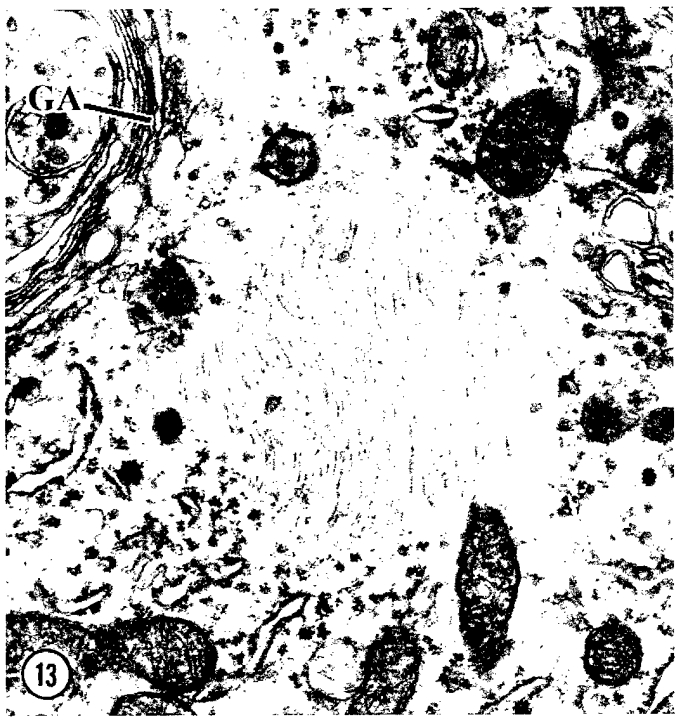

13

14


15
16
BD
17
AD
BD

APPENDIX VI

Aluminium and neuronal cell injury: inter-relationships between neurofilamentous arrays and apoptosis

$¶JOHN SAVORY, $OTHMAN GHRIBI, $MICHAEL S. FORBES and, *MARY M. HERMAN

$ Departments of Pathology, ¶Biochemistry and Molecular Genetics, University of Virginia, Charlottesville, VA; and *IRP, NIMH, NIH, Bethesda, MD 20892 U.S.A.

Correspondence to: Dr. John Savory, Department of Pathology, University of Virginia Health Sciences Center, Box 168, Charlottesville, Virginia 22908 U.S.A.
(804) 924-5682 - FAX (804) 924-5718-Email js2r@virginia.edu

The material covered in this manuscript was presented as the J.D. Birchall Memorial Lecture entitled: "Aluminium and cell suicide: Oh what a tangled web we weave". It was presented as a tribute to a creative and productive scientist.

Introduction to the Birchall lecture

It is a great honour for me to be invited to present the Derek Birchall memorial lecture at the Fourth Keele Meeting on Aluminium. Although I have made my home and formed an academic career in the United States, I shared a common heritage with Professor Birchall in that we both were native Lancastrians and were raised only a few miles from each other; thus, we shared many common interests. I met Derek at the Second International Conference on Aluminium and Health held in Tampa, Florida in February, 1992. This was the only time that our paths crossed but we became well-aquainted during the few days of that meeting. I found Derek to be highly intelligent with a wonderful sense of humour. His knowledge of bioinorganic chemistry was extensive and he was a leader in this field, particularly as it applied to aluminium and silicon. Despite his gentle personality, he was scathing in his criticism of some of the speakers at the Conference, when it was clear that their experiments were compromised due to a lack of understanding of the chemistry of aluminium. I trust that the experiments that have been carried out in our laboratory at the University of Virginia have not made the same mistake. We have been guided over the years by a colleague, Professor Bruce Martin, who along with Professor Birchall and Professor R.J.P. Williams have done much to help us to understand the chemistry of aluminium in solution and in biology. I present here results mostly from my own laboratory, where we have used aluminium maltolate *in vivo* to assess mechanisms of the formation of neurofilamentous arrays (NFAs) as a model for the neurofibrillary tangles seen in human neurodegenerative disorders, such as

Alzheimer's disease, and to unravel the complex process of programmed cell death known as apoptosis. This mechanism of cell death is considered by many neuroscientists to be a primary cause of neuronal loss in neurodegeneration.

Aluminium and human neurodegenerative diseases

The hypothesis that aluminium neurotoxicity plays a role in these disorders, either major or minor, remains highly controversial, and has been largely discarded by scientists working in the field despite considerable supporting evidence [1]. This heated debate hinges primarily on the results of complex epidemiological studies relating aluminium in drinking water with the incidence of Alzheimer's disease, and on the possible findings that neurofibrillary tangles which characterize this disease (along with neuritic plaques), contain deposits of aluminium (reviewed in [1]). Certain findings provide fuel for the "aluminium hypothesis" skeptics, i.e. that longterm exposure to antacids containing massive amounts of aluminium, occupational exposures, or the use of aluminium-containing antiperspirants fail to correlate with an increased incidence of Alzheimer's disease. It has been suggested that aluminium in drinking water is more bioavailable than other routes of exposure, a hypothesis that can be supported by an understanding of the solution chemistry of aluminium. Certainly, the presence of aluminium in water supplies precipitated the complications of hemodialysis, namely dialysis encephalopathy and dialysis osteodystrophy, although exposure in this case was in the use of the water to prepare dialysis solutions and not primarily its use for drinking purposes [2]. The possible presence of aluminium deposits in neurofibrillary tangles or neuritic plaques

remains controversial. Instrumental methods for intracellular localization that have been used include laser microprobe mass analysis, secondary ion mass spectrometry, scanning electron microscopy with energy-dispersive x-ray spectrometry, and particle-induced x-ray emission. Conflicting reports have emerged as to whether aluminium is present in increased amounts in neurofibrillary tangles or neuritic plaques, although a majority of reports, albeit a marginal majority, do in fact support such a finding, particularly as to its colocalization within tangles [1]. Other evidence supporting the possible role of aluminium in the pathogenesis of Alzheimer's and related diseases is provided by the possible efficacy of the aluminium chelater, desferrioxamine, in the treatment of Alzheimer's disease patients, although only one clinical trial has been carried out to date [3].

Aluminium-induced encephalomyelopathy in experimental animals

The first connection between aluminium-induced neuronal changes and Alzheimer's disease was drawn by Klatzo et al in 1965 [4] who found that the intracisternal administration of aluminium phosphate to New Zealand white rabbits led to the production of intraneuronal bodies which after silver staining appeared remarkably similar to the neurofibrillary tangles of Alzheimer's disease. This finding was serendipitous, since their investigations of the immune response of the central nervous system had at one point required the intracerebral introduction of an antigen prepared in Holt's adjuvant (I. Klatzo, personal communication, 1997), the latter containing aluminium phosphate. As a result, within two days the rabbits developed neurological

symptoms so severe as to require their sacrifice. Examination of the brain tissue revealed characteristic aluminium-induced neurofibrillary degeneration, consisting of argyrophilic fibrillary inclusions, located predominantly in the neuronal cell bodies and proximal neurites (dendrites and axon hillock) [4]. Light microscopic examination indicated a close resemblance between the aluminium-induced neurofibrillary aggregates and excessive numbers of neurofibrillary tangles that are a major histopathologic characteristic of Alzheimer's disease. However, other hallmarks of Alzheimer's, such as neuritic plaques, do not appear in the experimental Al-induced encephalopathy. Interestingly, the abundance of neurofibrillary tangles and relative paucity of neuritic plaques is typical of the ALS/parkinsonism-dementia complex of Guam; this implies that the widespread occurrence of neurofibrillary tangles, without plaques and/or significant Aβ deposition, is the structural correlate of neurological decline [5] and is supported by studies by Terry of neuropathological changes in Alzheimer's disease [6-8].

Some degree of scepticism is present concerning the similarity between aluminium-induced neurofibrillary degeneration in rabbits and neurodegenerative disorders in humans, since there exist certain ultrastructural differences between the two categories. Namely, the tangles of Alzheimer's disease are composed primarily of paired helical filaments [9-11], whereas the intraneuronal bodies produced by aluminium predominantly contain straight (intermediate-like) filaments both *in vivo* [12] and *in vitro* [13].

Typical findings seen in aluminium-induced neurofibrillary degeneration are depicted in the following experiment. Young New Zealand White rabbits were injected intracisternally with a single 5 μmole dose of aluminium maltolate. By seven days post-injection, these animals typically developed distinct neurological symptoms, including a variable loss of hind-limb function and the righting reflex. For microscopic evaluation of these brains, animals were perfusion-fixed with an aldehyde solution, and 50 μm coronal sections were cut with a vibrating microtome. Sections were prepared for light microscopic examination and stained with the Bielschowsky's silver method, which has an affinity for collections of neurofilaments in cells (Fig. 1A); or they were embedded in plastic for correlated light and transmission electron microscopy (Fig. 1 B-D). In certain regions of the brain, including the cerebral cortex and medulla, neurons display large silver-positive bodies that nearly fill the entire neuronal cell body (Fig. 1A). These are especially prominent in the nucleus of the facial nerve (Fig.1A-D), and examination by electron microscopy confirms that these bodies consist of vast numbers of neurofilaments, a component of the neuronal cytoskeleton which is a type of "intermediate filament." Despite the striking appearance of NFAs, no overt signs of neurodegeneration (such as pyknotic nuclei or swollen mitochondria and endoplasmic reticulum) can be detected in the affected neurons; however, profound biochemical changes in the apotosis-related regulatory proteins, Bcl-2 and Bax, are evident in these animals as discussed later.

Furthermore, aggregates in aluminium-induced neurofibrillary degeneration stain immunohistochemically with antibodies that are specific for the hyperphosphorylated

epitopes of neurofilament protein [14,15]. In contrast, the primary constituent of paired helical filaments in human neurofibrillary tangles is a microtubule-associated protein, tau, although other proteins are present, including abnormally phosphorylated neurofilament proteins, ubiquitin, α1-antichymotrypsin, amyloid precursor protein and its derived peptide, Aβ. Studies in the authors' laboratory over the past six years [16-18], which have been confirmed by others [19,20], have shown that there exist far more immunochemical similaritities between the aluminium-induced lesions and those found in Alzheimer's disease than originally thought; tau, ubiquitin, α1-antichymotrypsin, amyloid precursor protein and its derived peptide, Aβ, are all increased in the neurons of aluminium-treated rabbits, together with abnormally phosphorylated neurofilament protein.

Abnormally phosphorylated tau [18] has been found in aluminium-induced neurofilamentous aggregates with mAbs that recognize both nonphosphorylated and phosphorylated tau [16,19], among them Tau-1, Tau-2, AT8, PHF-1 and Alz-50, thus indicating the presence of both phosphorylated and nonphosphorylated tau. We also have determined the time required for the formation of these cytoskeletal protein aggregates [21], finding argyrophilic bodies within 24 hours after aluminium maltolate administration, with a predominance of neurofilament proteins. Non-phosphorylated, phosphorylation-independent epitopes appear first, as detected by mAb SMI-33 (Sternberger Monoclonals Inc. Baltimore, MD), followed at about 72 hours by phosphorylated forms, immunostained by mAb SMI 31. Tau is also detectable at the 72-hour mark, although the characteristic epitopes of Alzheimer's disease, as recognized by

mAbs AT8 and PHF-1, become most distinct at 6-7 days following aluminium injection. It has been proposed that phosphorylation of cytoskeletal proteins induces the formation of neurofilamentous aggregates, particularly in human neurodegenerative disorders. Given that these aggregates are hyperphosphorylated, phosphorylation alone would make these protein accumulations unstable because of the preponderance of negative charges on the phosphate groups. Therefore it can be postulated that a positively-charged species would represent an inherent factor for both the formation and stabilization of the neurofibrillary aggregates, in Alzheimer's disease as well as in experimental aluminium-induced neurofibrillary degeneration; Al^{3+} is the obvious candidate for this role in the latter.

Whether these protein changes themselves cause neuronal death, or whether they reflect a response to cell injury, remains to be determined.

Apoptosis in Alzheimer's and related diseases

The mechanism(s) of neuronal cell death in Alzheimer's and related diseases has not been firmly established. Apoptosis and necrosis probably are both involved and represent different but sometimes overlapping mechanisms of cell death. The topic of apoptosis in neurodegenerative disorders has been the subject of recent reviews [22,23]. Apoptosis refers to programmed cell death, and is an active process controlled by genes which can be activated by a variety of stimuli, including oxidative stress and exposure to hormones, toxins and drugs. Regulation of apoptosis in the central nervous system is

crucial during embryogenesis and fetal development, where half of the post-mitotic neurons die due to a limited amount of trophic support. Mechanisms for programming this massive cell death are thus important in the developing brain, and perhaps triggering of this same process would be detrimental and sometimes devastating during aging. Understanding apoptosis in human neurodegeneration requires access to autopsy tissue, although information obtained is of limited value due to delays in harvesting the tissue. The development of suitable animal model systems is therefore very important in achieving an understanding of these processes.

Induction and regulation of apoptosis in aluminium-induced neurotoxic injury

The key processes that are active in apoptosis involve the activation of a family of cysteine proteases, termed the caspases, which demonstrate a specificity for aspartate substrates. These proteases are produced as procaspases which possess minimal proteolytic activity; however upon activation, cell death eventually results. An understanding of the processes leading to apoptosis is still developing, but it appears that there are three pathways for caspase activation. One pathway, triggered by extracellular signals, acts through death receptors and involves adaptor molecules such as Fas-associating protein with death domain (FADD), leading to the activation of caspase 8. A second pathway results from mitochondrial injury and appears to be a primary event in the cell death occuring in Alzheimer's disease (for review see [24]. Following cytotoxic stimuli, cytochrome *c* , which is an apoptogenic factor, is released into the cytoplasm from the inner membrane space of the mitochondria [24-27].

Release of cytochrome *c* from the mitochondria has been shown to involve two distinct pathways. One implicates the opening of the mitochondrial permeability transition pore (MTP), and the second, triggered by the proapoptogenic Bax, is independent of the MTP opening [28]. While Bax has been shown to trigger cell death [29], the antiapoptotic Bcl-2 can block cytochrome *c* release and caspase activation. Cyclosporin A, an immunosuppressant agent, also inhibits the opening of the MTP [30]. Our laboratory has reported, in aged rabbit hippocampus, the induction of cytochrome *c* translocation into the cytosol as early as 3 hours after the intracisternal administration of aluminium maltolate [31]. Pretreatment with cyclosporin A, an inhibitor of the mitochondria permeability transition pore (MTP), blocks this cytochrome *c* release [31]. Therefore, it appears that the aluminium maltolate-induced cytochrome *c* release results from an opening of the MTP.

Although apoptosis under mitochondrial control has received considerable attention, mechanisms utilized within the endoplasmic reticulum in mediating apoptotic signals are not well understood. We have shown in a second study, that the intracisternal treatment of young adult rabbits with 5 μmole aluminium maltolate and sacrificed 3 days later, induces both cytochrome *c* translocation into brain cytosol and the activation of caspase-3. Caspase-3 is considered to be a key marker of apoptosis, and in the aluminium-treated rabbit it can be detected in brain tissue by its enzymatic proteolysis of a fluorogenic substrate, Ac-DEVD-AMC, with and without the caspase-3 inhibitor, Ac-DEVD-CHO. The presence of caspase-3 in these tissue specimens also can be detected by

immunohistochemical methods. Detection of DNA fragmentation, a classical marker for apoptosis, also gave positive results on tissue from these aluminium-treated rabbits using the terminal deoxynucleotidyl transferase-mediated dUTP nick end labeling (TUNEL) technique. Thus, aluminum maltolate injected directly into the central nervous system of rabbits certainly can induce apoptosis, but the amount of aluminium administered has to be high enough to also cause severe clinical symptoms. These effects are accompanied by a decrease in Bcl-2 and an increase in Bax reactivity in the endoplasmic reticulum [32]. Thus it appears that mitochondria, as well as the endoplasmic reticulum, are involved in mediating the aluminium-induced apoptosis in rabbit brain. Therefore, the rabbit-aluminium experimental system offers excellent possibilities for understanding the complex process of apoptosis, and may be particularly relevant to an understanding of this process in human neurodegenerative disorders.

The application of aluminium neurotoxicity in rabbits in developing therapeutic strategies for the treatment of neurodegenerative disorders

The "holy grail" for neuroscientists in the field of neurodegeneration is to discover effective ways of treating patients with Alzheimer's, Parkinson's and related diseases. The similarities in features of the rabbit/aluminium model system offers opportunities for assessing potential therapeutic approaches. Studies in the authors' laboratory [33] have been directed towards one therapeutic agent, namely glial cell derived neurotrophic factor (GDNF). Administration of GDNF has been shown to protect neurons after brain injury; following permanent occlusion of the middle cerebral artery in rats [34], in primate

models of Parkinson's disease [35], against ischemic/hypoxic-induced brain injury in neonatal rats [36], and against oxidative stress in cultured mesencephalic neurons and glial cells [37]. The mechanisms by which GDNF exerts its neuroprotective effect are as yet unknown, but recent evidence demonstrates that the rescue and repair of injured neurons is a consequence of the antiapoptotic properties of this agent. In the authors' laboratory young adult New Zealand white rabbits have been treated intracisternally (as described above) with 5 μmole of aluminium maltolate which induce the following: cytochrome *c* release from mitochondria, a decrease in Bcl-2 in both mitochondria and endoplasmic reticulum, Bax translocation into mitochondria, activation of caspase-3, and DNA fragmentation. When GDNF is injected intracisternally with the aluminium compound we have observed an inhibition of these Bcl-2 and Bax changes, an upregulation of Bcl-X_L, and an absence of caspase-3 activity. Furthermore, treatment with GDNF dramatically inhibits apoptosis, as assessed by the TUNEL technique for detecting DNA damage. Most interesting is the fact that the GDNF treatment delays the onset of clinical symptoms from 3 days to 9 days for half of the animals, with the other half showing no symptoms for several weeks. How effective GDNF will be in treating human diseases remains to be determined. However, it promises some success for the treatment of Parkinson's disease, as demonstrated by the delivery of GDNF via lentiviral vectors into the brain of primates, both aged and with parkinsonian symptoms [38].

Conclusions

The direct injection of aluminium compounds into rabbit central nervous system mimics many abnormalities found in human neurodegenerative diseases. The rabbit/aluminium model system provides a means of elucidating mechanisms of neurodegeneration, particularly those involving apoptosis and neurofilamentous abnormalities. This *in vivo* system also promises to provide a means for evaluating potential therapeutic approaches to the treatment of human neurodegenerative disorders. The changes induced by the neurotoxic effects of aluminium in experimental animals support, but by no means prove, that aluminium may be one of many causative agents in the pathogenesis of Alzheimer's disease.

FIGURE LEGENDS

Fig. 1. Motor nucleus of the facial nerve in the medulla of young rabbit after 7 days' exposure to aluminium maltolate injected into the cisterna magna, resulting in the appearance of massive "neurofilamentous arrays" (NFAs) within the neurons.

A. Fifty-micrometer-thick section of brain, stained by Bielschowsky's silver technique, which is selective for the neurofibrillary components of neurons. Virtually every cell in the facial nucleus displays multiple profiles of intensely argyrophilic material. X 142.

B. "Semithin" (ca. 0.25 μm) section of plastic-embedded tissue, stained with alkaline toluidine blue. In the perikaryon of this large neuron, the Nissl substance and mitochondria (nearest the nucleus) are darkly basophilic, while the slightly more peripheral NFA profiles are relatively lucent and occupy most of the cell profile. X 710.

C. Low-power transmission electron micrograph (TEM) of a facial nucleus neuron, showing a normal-appearing nucleus (at far left center of field) and small regions of cytoplasm filled with granular endoplasmic reticulum and mitochondria. The majority of the field is occupied by masses of NFAs, which are largely contiguous, and composed almost entirely of neurofilaments. X 4000.

D. Higher magnification TEM of a NFA, demonstrating that its major component consists of multitudes of individual neurofilaments that are arrayed in whorls and skeins. X 42,500.

References

1. J. Savory, C. Exley, W. F. Forbes, Y. Huang, J. G. Joshi, T. Kruck, D. R. McLachlan, I. Wakayama, J. Toxicol. Environ. Health. 48 (1996) 615-635 .

2. M. R. Wills and J. Savory, Crit. Rev. Clin. Lab. Sci. 27 (1989) 59-107 .

3. M. D. Crapper, A. J. Dalton, T. P. Kruck, M. Y. Bell, W. L. Smith, W. Kalow, D. F. Andrews, Lancet 337 (1991) 1304-1308 .

4. I. Klatzo, H. M. Wisniewski, E. Streicher, J. Neuropathol. Exp. Neurol. 24 (1965) 187-199 .

5. M. Mawal-Dewan, M. L. Schmidt, B. Balin, D. P. Perl, V. M. Lee, J. Q. Trojanowski, J. Neuropathol. Exp. Neurol. 55 (1996) 1051-1059 .

6. R. D. Terry, Prog. Brain Res. 101 (1994) 383-390 .

7. R. D. Terry, Ann. Neurol. 41 (1997) 7 .

8. W. Samuel, R. D. Terry, R. DeTeresa, N. Butters, E. Masliah, Arch. Neurol. 51 (1994) 772-778 .

10. R. D. Terry, J. Neuropathol. Exp. Neurol. 22 (1963) 629-642

9. M. Kidd, Brain 87 (1964) 307-320.

11. H. M. Wisniewski, H. K. Narang, R. D. Terry, J. Neurol. Sci. 27 (1976) 173-181 .

12. D. Dahl and A. Bignami, Exp. Neurol. 58 (1978) 74-80.

13. C. D. Hewitt, M. M. Herman, M. B. Lopes, J. Savory, M. R. Wills, Neuropathol. Appl. Neurobiol. 17 (1991) 47-60 .

14. C. D. Katsetos, J. Savory, M. M. Herman, R. M. Carpenter, A. Frankfurter, C. D. Hewitt, M. R. Wills, Neuropathol. Appl. Neurobiol. 16 (1990) 511-528.

15. I. Wakayama, V. R. Nerurkar, M. J. Strong, R. M. Garruto, Acta Neuropathologica 92 (1996) 545-554 .

16. J. Savory, Y. Huang, M. M. Herman, M. R. Reyes, M. R. Wills, Brain Res. 669 (1995) 325-329 .

17. J. Savory, Y. Huang, M. M. Herman, M. R. Reyes, J. C. Boyd, M. R. Wills, in: K. Iqbal, J. A. Mortimer, B. Winblad, H. M. Wisniewski, Eds. Research Advances in Alzheimer's Disease and Related Disorders, Wiley and Sons, West Sussex, UK, 1995, pp. 543-551.

18. Y. Huang, M. M. Herman, J. Liu, C. D. Katsetos, M. R. Wills, J. Savory, Brain Res. 771 (1997) 213-220.

19. N. A. Muma and S. M. Singer, Neurotoxicol. Teratol. 18 (1996) 679-690.

20. S. M. Singer, C. B. Chambers, G. A. Newfry, M. A. Norlund, N. A. Muma, NeuroToxicol. 18 (1997) 63-76.

21. J. Savory, Y. Huang, M. M. Herman, M. R. Wills, Brain Res. 707 (1996) 272-281.

22. C. Behl, J. Neural Transm. 107 (2000) 1325-1344.

23. L. S. Honig and R. N. Rosenberg, Am. J. Med. 108 (2000) 317-330.

24. D. S. Cassarino, J. K. Parks, W. D. Parker, J. P. Bennett, Biochim. Biophys. Acta - Molecular Basis of Disease 1453 (1999) 49-62.

25. X. Liu, C. N. Kim, J. Yang, R. Jemmerson, X. Wang, Cell 86 (1996) 147-157.

26. J. J. Lemasters, A. L. Nieminen, T. Qian, L. C. Trost, S. P. Elmore, Y. Nishimura, R. A. Crowe, W. E. Cascio, C. A. Bradham, D. A. Brenner, B. Herman, Biochim. Biophys. Acta 1366 (1998) 177-196.

27. Y. Morita-Fujimura, M. Fujimura, M. Kawase, S. F. Chen, P. H. Chan, Neurosci. Lett. 267 (1999) 201-205.

28. R. Eskes, B. Antonsson, A. Osen-Sand, S. Montessuit, C. Richter, R. Sadoul, G. Mazzei, A. Nichols, J. C. Martinou, J. Cell Biol. 143 (1998) 217-224.

29. A. Gross, J. Jockel, M. C. Wei, S. J. Korsmeyer, EMBO Journal 17 (1998) 3878-3885.

30. V. Kostic, V. Jackson-Lewis, F. de Bilbao, M. Dubois-Dauphin, S. Przedborski, Science 277 (1997) 559-562.

31. O. Ghribi, D. A. DeWitt, M. S. Forbes, A. Arad, M. M. Herman, J. Savory, J Alzheimers Disease (2001) in press.

32. O. Ghribi, D. A. DeWitt, M. S. Forbes, M. M. Herman, J. Savory, Brain Res. (2001) in press.

33. O. Ghribi, M. S. Forbes, ., D. A. DeWitt, M. M. Herman, J. Savory, Neurobiol. Dis. in press (2001).

34. H. Kitagawa, T. Hayashi, Y. Mitsumoto, N. Koga, Y. Itoyama, K. Abe, Stroke 29 (1998) 1417-1422.

35. J. H. Kordower, M. E. Emborg, J. Bloch, S. Y. Ma, Y. Chu, L. Leventhal, J. McBride, E. Y. Chen, S. Palfi, B. Z. Roitberg, W. D. Brown, J. E. Holden, R.

Pyzalski, M. D. Taylor, P. Carvey, Z. Ling, D. Trono, P. Hantraye, N. Deglon, P. Aebischer, Science 290 (2000) 767-773.

36. T. Ikeda, X. Y. Xia, Y. X. Xia, T. Ikenoue, B. Han, B. H. Choi, Acta Neuropathol. (Berl) 100 (2000) 161-167.

37. E. Iwata-Ichikawa, Y. Kondo, I. Miyazaki, M. Asanuma, N. Ogawa, J. Neurochem. 72 (1999) 2334-2344.

38. A. S. Mandir, V. L. Dawson, T. M. Dawson, Trends Pharmacol. Sci. 22 (2001) 103-105.

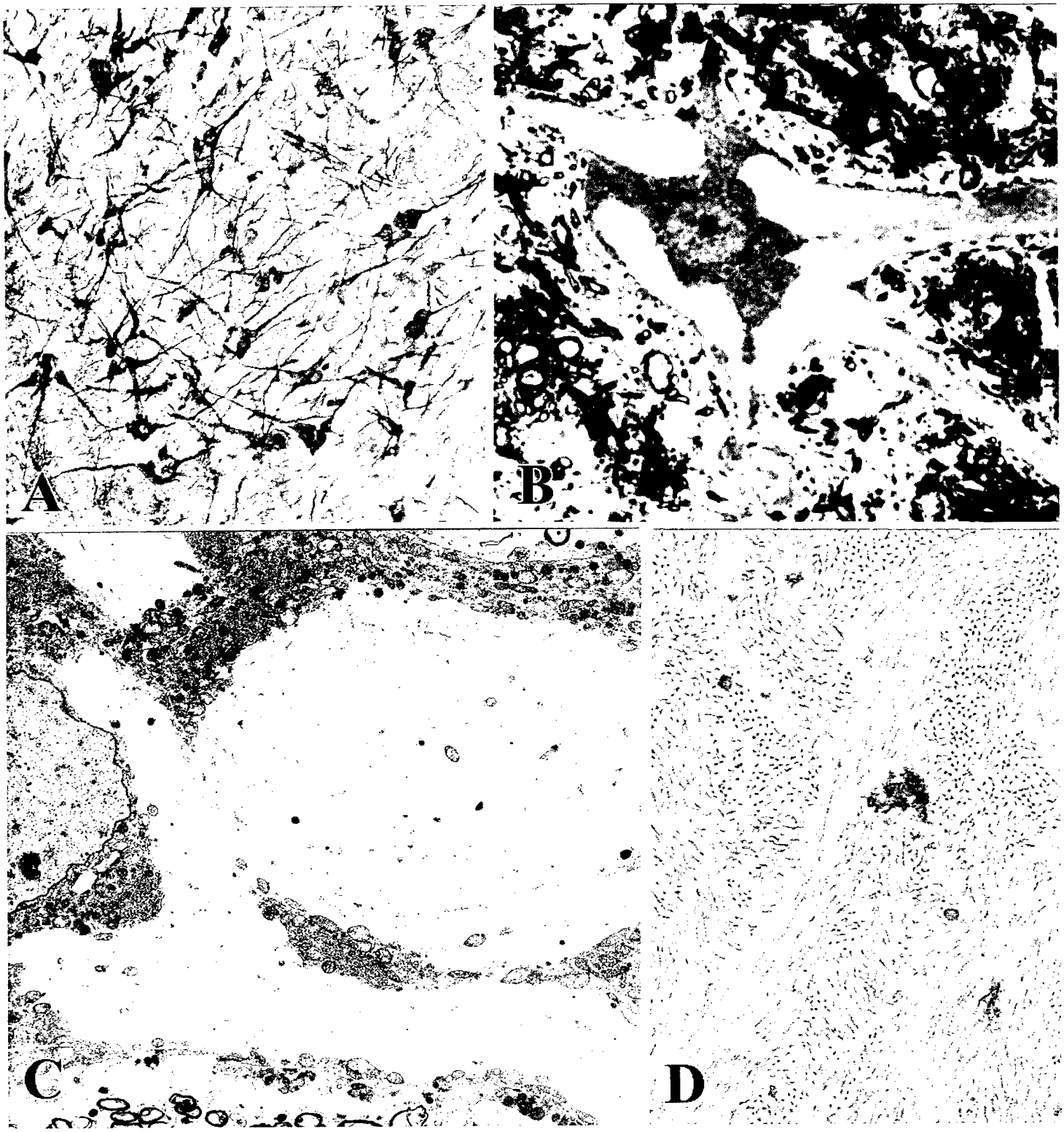
A
B
C
D

APPENDIX VII

Aluminium and Alzheimer's Disease
The Science that Describes the Link
C. Exley (Editor)

CHAPTER 10

The Rabbit Model System for Studies of Aluminum-Induced Neurofibrillary Degeneration: Relevance to Human Neurodegenerative Disorders

John Savory [1,2,*], Othman Ghribi [1], Michael S. Forbes [1] and Mary M. Herman [3]

Departments of [1]Pathology, [2]Biochemistry and Molecular Genetics, University of Virginia, Charlottesville, VA 22908, USA; [3] IRP, NIMH, NIH, Bethesda, MD 20892, USA

* Corresponding author, email: js2r@virginia.edu

Abbreviations: Al – aluminum; NFA – neurofibrillary aggregate; AD – apical dendrite

Summary

Rabbits are particularly sensitive to aluminum neurotoxicity and develop severe neurological changes, especially if the metal is administered directly into the central nervous system. Other routes of administration determine the degree of severity of such clinical symptoms, with oral administration exhibiting minimal effects. The complex chemistry of aluminum must be understood before designing these experiments in order to avoid formation of insoluble aluminum hydroxide complexes. However, by selecting appropriate aluminum compounds to be administered to the animals, neuropathological and biochemical changes bearing similarities to those seen in Alzheimer's disease are observed, thus supporting the hypothesis that aluminum is involved in the pathogenesis of this disease.

Historical Perspective

Introduction

Studies using the rabbit may be particularly relevant to the investigation of human disease since, according to the sequences of 88 proteins, this animal belongs to the mammalian order Lagomorpha, a group which has been reported to resemble primates more closely than rodents (Graur *et al.*, 1996). The first experiment suggesting that aluminum (Al)-induced neuronal changes might have relevance to Alzheimer's disease was that of Klatzo *et al.* (1965) who reported that the intracisternal administration of Al phosphate to New Zealand white rabbits produced intraneuronal protein aggregates which, with silver staining, appeared remarkably similar to the neurofibrillary tangles

of Alzheimer's disease. This was a serendipitous finding, since the experiment was designed to study the immune response of the central nervous system, and an antigen had been administered intracerebrally to rabbits in Holt's adjuvant (I. Klatzo, personal communication, 1997), the latter containing Al phosphate. For almost 70 years, makers of vaccines have used either Al sulphate, Al hydroxide or Al phosphate as adjuvants to improve the body's immune system, in order to favor an earlier response to an antigen (Malakoff, 2000). In the pioneering experiment of Klatzo, the rabbits developed severe neurological symptoms within 2 days of the injection, and had to be sacrificed. Examination of brain tissue from these animals revealed the characteristic Al-induced neurofibrillary degeneration; that is, silver-impregnated (argyrophilic) fibrillary inclusions found predominantly in the neuronal cell bodies (perikarya) and proximal neurites (dendrites and axon hillock) (Klatzo *et al.*, 1965). Al-induced neurofibrillary aggregates at the light microscopic level closely resemble neurofibrillary tangles, one of the histologic hallmarks of Alzheimer's disease.

Other histopathologic hallmarks of Alzheimer's disease, such as neuritic plaques, were not present in this Al-induced encephalopathy. Interestingly, an abundance of neurofibrillary tangles coupled with a relative paucity of neuritic plaques characterizes the amyotrophic lateral sclerosis/parkinsonism-dementia complex of Guam, indicating that widespread neurofibrillary tangles (without plaques and/or significant Aβ deposition) may be the cellular correlate of neurological decline, as reviewed in Mawal-Dewan *et al.* (1996). Often neuritic plaques show a perivascular predilection, suggesting that the dystrophic neurites and the attendant amyloidogenic accumulation may be pathogenetically linked to vascular (or microvascular)-associated factor(s). Cerebrovascular pathology may be relevant in the pathogenesis of naturally-occurring Alzheimer's disease, and may account for increased Al accumulation during central nervous system damage. Conversely, in experimental Al-induced neurofibrillary degeneration, the factor of cerebrovascular pathology is not present, at least with respect to the non-senescent laboratory rabbit. Also, in the first experiments of Klatzo *et al.* (1965) the mode of Al delivery in the central nervous system was direct (intracerebral or intracisternal), thereby effectively bypassing the blood–brain barrier. Thus, it is not surprising that the type and distribution of neurofibrillary degeneration in rabbits treated in this manner was in some respects different from the more naturally-occurring neurofibrillary tangles in Alzheimer's disease in humans. Also, the formation of neuritic plaques appears to be species-dependent, being found in few mammalian species and then only in the aged (Martin *et al.*, 1994; Satou *et al.*, 1997). As is developed below, these differences are less compelling when compared to the broad array of immunochemical similarities which exist between experimental Al-induced neurofibrillary degeneration in rabbits and the various neurofibrillary lesions of the neurodegenerative disorders in humans.

The first experiments of Klatzo *et al.* (1965) and many subsequent studies, employed the direct injection of an Al compound into the rabbit central nervous system, using the intracisternal, intraventricular or intraparenchymal routes of injection. These direct administrations simplify the experimental system since the blood–brain barrier is bypassed. However, the better control achieved in the animal system is countered in part by the acute neurotoxicity which is usually produced, while Alzheimer's disease is of course a chronic disease. Monthly intracisternal injections of Al salts have been used to induce

experimental chronic neurodegeneration in the rabbit (Strong *et al.*, 1991; Strong and Garruto, 1991a; Strong and Garruto, 1991b), as will be discussed later. Both the systemic and oral routes of Al administration to rabbits have been proposed as a means for studying changes pertaining to Alzheimer's disease *in vivo*. All routes of administration will be discussed in detail later in this review.

Aluminum Speciation Issues

A complicating factor in assessing neurotoxic effects of Al in rabbits (and other experimental animals) has been the variety of Al compounds used in the experiments. The chemistry of Al is extremely complex, as has been discussed in detail by Martin (1986; 1988; 1990; 1991; 1992; 1997a; 1997b). As we have observed in a recent review of experimental Al encephalomyelopathy (Rao *et al.*, 1998), an understanding of the chemistry of Al is of considerable importance in the experimental design of studies related to Al toxicity. An understanding of the complex hydrolysis chemistry of Al as a function of pH is important and has been reviewed (Martin, 1997a). Below pH 5.0, Al (III) exists as an octahedral hexahydrate ($Al(H_2O)_6^{3+}$), usually abbreviated as Al^{3+} . As the solution becomes acidic, $Al(H_2O)_6^{3+}$ undergoes deprotonation to yield $Al(OH)^{2+}$ and $Al(OH)_2^{+}$. In neutral and alkaline solutions, $Al(OH)_3$ precipitates and soluble $Al(OH)_4^{-}$ is formed. Aluminum speciation in the stock solutions must be evaluated, since it hydrolyzes readily; at pH 7.0 there is a strong tendency for precipitation of $Al(OH)_3$ which makes the preparation of Al stock solutions difficult. Calculation of the molarity of Al solutions cannot be made by just adding a known quantity of an Al compound to water, without taking hydrolysis reactions into account. Martin (1991) has provided an example of how such properties of Al affect the design and interpretation of biological experiments. When an Al chloride solution of 0.01 M is added to tissue at pH 7.0 the permissible free Al^{3+} is only $10^{-10.3}$ M and that of all soluble forms is 2 μM. Unless the remainder of the added Al(III) has been complexed by other ligands then insoluble $Al(OH)_3$ will be formed. Al maltolate is particularly suitable for toxicological studies because of its defined molecular structure in solution and its neutral charge, high solubility and hydrolytic stability at pH 7.0 (Finnegan *et al.*, 1986), and for this reason it serves to reduce the formation of insoluble Al salts maintaining a much higher proportion of Al in solution in a bioavailable form.

Several studies have been carried out in the authors' laboratory using this compound for both in vitro (Hewitt *et al.*, 1991) and in vivo (Bertholf *et al.*, 1989; Wills *et al.*, 1993a; Katsetos *et al.*, 1990; Savory *et al.*, 1993; 1994; 1995a; 1995b; 1996) experiments via the oral, intravenous, and intracerebral routes of administration. With direct administration of as little as 2 μmole of Al injected directly into the central nervous system of rabbits, the effect of Al maltolate is dramatic, even at regions distant to the injection site.

Direct Injection of Al into the Central Nervous System of Rabbits

Direct injection of Al compounds into adult rabbit brain has constituted the most common route of administration for studies of the neurochemical characteristics of Al-induced

neurodegeneration. Intracranial Al administration has been carried out by several routes: either directly into the brain parenchyma, intraventricularly using a stereotaxic frame, or intracisternally. Klatzo *et al.* (1965) injected Al phosphate into the anterior portion of the left cerebrum, and reported for the first time epileptogenic effects and neurofibrillary degeneration. Pendlebury *et al.* (1988), using an intraventricular route of administration of Al chloride, found similarities between the distribution of neurofibrillary aggregates in rabbit brain and the formation of neurofibrillary tangles in Alzheimer's disease. In the same study, phosphorylated neurofilaments were shown to accumulate in neuronal perikarya containing the neurofibrillary aggregates, and double-labeling techniques suggested that the projection type neurons were primarily affected. With this route of Al chloride administration, the Al-induced neurofibrillary aggregates differed antigenically from the neurofibrillary tangles seen in Alzheimer's disease (Kowall *et al.*, 1989), although studies from our laboratory would suggest that these differences are less than thought originally (Huang *et al.*, 1997). Perhaps the development of improved reagents over the past decade could explain the differences. Nevertheless, using the intraventricular route of administration, Kowall *et al.* (1989) observed that many neuronal subsets that are particularly susceptible to Alzheimer's disease are also affected by Al-induced neurofibrillary degeneration. Indeed, in this mode of administration, widespread perikaryal neurofibrillary degeneration, characterized by positive Bielschowsky's silver impregnation and by immunostaining with the monoclonal antibody SMI-31 to detect phosphylated neurofilament proteins, was noted in the cerebral cortex, ventral hippocampus, basal forebrain, raphe nucleus, and brainstem nuclei, including the locus ceruleus (Kowall *et al.*, 1989). The thalamus and striatum were not involved, and only occasional Purkinje cells of the cerebellum showed these characteristic neurofibrillary changes. Studies from the same laboratory (Beal *et al.*, 1989), again using the intraventricular mode for treatment with Al chloride, demonstrated neurochemical changes that paralleled those seen in Alzheimer's disease, particularly a significant reduction of choline acetyltransferase activity in the entorhinal cortex and hippocampus. In contrast, there was no decrease in somatostatin and neuropeptide Y in the Al-treated rabbits, which differs markedly from observations in Alzheimer's disease patients (Beal *et al.*, 1989).

Forrester and Yokel (1985) compared the intraventricular administration of Al lactate to the subcutaneous route. Details of the systemic treatment experiments are given below. Rabbits treated via the intraventricular route were given either 5 or 10 μmole in 50 μL of solution. Typical clinical symptoms of hindlimb weakness, arching of the neck and seizures were observed. Surprisingly, no abnormalities in the righting reflex, which is the ability to quickly resume a normal stance after being forcibly turned onto one side, were seen. The symptoms appeared suddenly, following a symptom-free period. Clinical abnormalities were always associated with neurofibrillary changes in the hippocampus and frontal cortex, as detected by histological methods using the Bielschowsky's silver method and hematoxylin-eosin and cresyl violet staining. As discussed below, the effects in animals treated via the intraventricular route were remarkably similar to those treated subcutaneously (Beal *et al.*, 1989; Solomon *et al.*, 1990).

Intracisternal administration represents another route for drug delivery and is widely applied for the direct injection of Al compounds into the rabbit brain. Unfortunately, this mode of injection of Al compounds, besides producing neurofibrillary degeneration,

induces neurological signs involving the motor neuron system, and all of the rabbits develop seizures and die within 2 to 4 weeks. As has been demonstrated with other studies using this or similar modes of administration (Beal *et al.*, 1989), a severe encephalomyelopathy was observed in about 7 days, characterized by quadriparesis and weight loss (Beal *et al.*, 1989; Kowall *et al.*, 1989). Wisniewski *et al.* (1984), recognizing the limitations of the intracisternal route of administration in adult rabbits, suggested that Al-chloride should be injected into infants rather than adults, using the same technique. In an investigation applying this protocol, both young and old rabbits developed neurofibrillary degeneration consisting of intraneuronal neurofilamentous aggregates, but in the case of the infant animals, about 50% of them survived for many months and many did not develop neurological signs or seizures (Rabe *et al.*, 1982). The chronic intracisternal injection of Al chloride in rabbits has been shown to induce neurofibrillary tangle formation in cortical neurons (Wisniewski *et al.*, 1984) as well as profound neurofibrillary changes in neurons of the spinal cord and cerebrum (Wisniewski *et al.*, 1980). Troncoso *et al.* have demonstrated that intracisternal administration of Al chloride produces the accumulation of neurofilaments in axons and perikarya of motor neurons, associated with impaired axonal transport of neurofilament proteins (Troncoso *et al.*, 1986) and with axonal swellings (Troncoso *et al.*, 1982). Extensive dendritic degeneration, together with perikaryal neurofilamentous accumulation in motor neurons, has also been reported following the intracisternal injection of Al sulphate in rabbits (Wakayama *et al.*, 1993). Chronic administration of low doses of Al chloride, also by the intracisternal route, has been demonstrated to induce neurofilament inclusions in motor neurons (Strong *et al.*, 1991). In the young rabbits, co-administration of Al chloride and N-butyl benzenesulfonamide, a neurotoxin known to induce myelopathy, has resulted in a fulminant myelopathy, as well as striking behavioral changes (Strong and Garruto, 1991b). More recently, studies in the authors' laboratory with young adult New Zealand white rabbits have shown that the intracisternal administration of Al maltolate produces neurofilamentous aggregates possessing a number of similarities to the biochemical changes observed in Alzheimer's disease (Huang *et al.*, 1997). Examples of such features obtained in Al maltolate-treated rabbits are shown in Figs. 1–5. The photomicrographs shown in these figures are from an untreated New Zealand white rabbit and an animal subjected to the intracisternal injection of 100 μL of 25 mM Al maltolate and sacrificed after 7 days, by which time severe neurological symptoms were evident. Details of the clinical symptoms and methods of perfusion and tissue procurement have been reported by us previously (Savory et al, 1996). The photomicrographs shown in Figs. 1–5 depict pyramidal neurons in the parietal cortex of rabbit brain prepared by staining 50-μm sections cut on a vibrating microtome. Staining was with either Bielschowsky's silver impregnation or immunohistochemistry using the monoclonal antibody, SMI-31 (Sternberger Monoclonals Inc., Baltimore, MD) which recognizes phosphorylated epitopes on the high and medium molecular weight isoforms of neurofilament protein. Immunohistochemical detection was carried out with the ABC Elite kit (Vector Laboratories Inc., Burlingame, CA). Silver staining techniques are in common use for neuropathological diagnosis of Alzheimer's disease. In addition, one of the most significant findings from the authors' laboratory was the observation that microtubule-associated tau (tau) is a component of the Al-induced neurofilamentous

lesions (Savory *et al.*, 1995a,b); tau has been demonstrated to be a major constituent of the neurofibrillary tangles found in Alzheimer's disease (Iqbal *et al.*, 1994). Confirmation that tau is indeed a component of Al-induced neurofibrillary degeneration in rabbits has been provided by other workers (Singer *et al.*, 1997). Furthermore, the present authors also have reported Al maltolate-induced increased apoptosis in aged animals, as compared

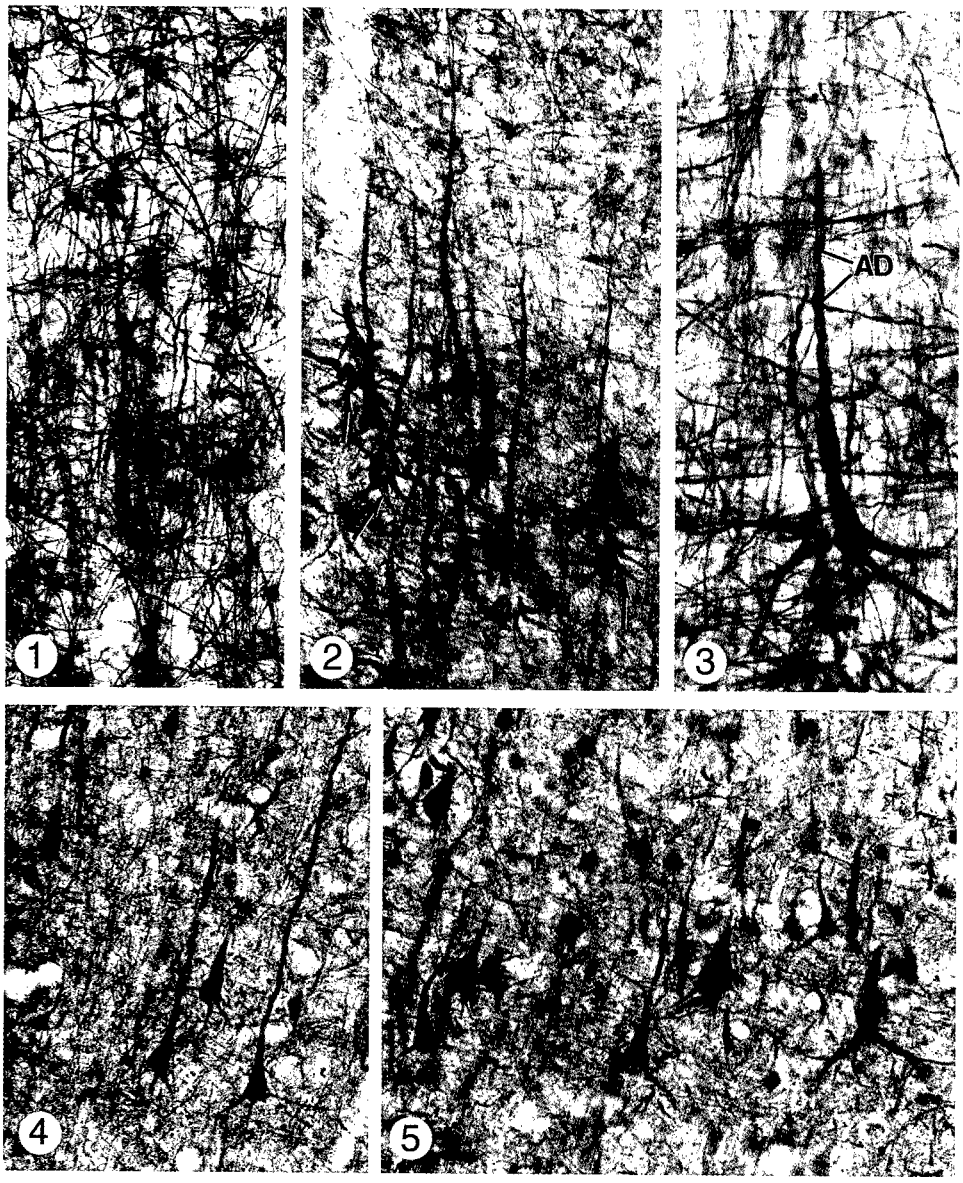

to young adult rabbits and untreated controls of both ages (Savory *et al.*, 1999). These findings strongly support a key role of oxidative stress in the process of neurodegeneration in aging.

Systemic Administration of Al in Rabbits

One of the first studies using the systemic administration of Al into adult rabbit brain (exact age not stated) was that of De Boni *et al.*(1976) who injected Al lactate or Al tartrate subcutaneously daily for up to 30 days. An assessment of Al toxicity in rabbits with a variety of Al compounds, both inorganic and organometallic, was also carried out by the intravenous administration of Al maltolate into adult rabbits 3–5 times per week for 40–443 days (Favarato and Zatta, 1993; Fontana *et al.*, 1991). These authors pointed out the necessity of using a neutral, water-compatible Al complex as a tool for studying Al toxicity, and suggested that an aqueous solution of Al maltolate showed considerable promise for such studies (Favarato and Zatta, 1993; Fontana *et al.*, 1991). With the same compound, studies in the authors' laboratory have examined neuronal cytoskeletal changes in adult New Zealand white rabbits treated 3 times per week intravenously with Al maltolate for 8–30 weeks (Bertholf *et al.*, 1989; Katsetos *et al.*, 1990). Although no consistent neurological symptoms were observed in Al-treated animals, weight loss was noted. Neurofibrillary changes were found in the oculomotor nucleus in about one-third of the treated rabbits, as demonstrated by a monoclonal

---

All photomicrographs depict pyramidal neurons in the parietal cortex of rabbit brain, prepared by staining 50-μm sections cut on a vibrating microtome.

Fig. 1. Untreated New Zealand white rabbit; Bielschowsky's silver impregnation. The intraneuronal cytoskeletal material is strongly argyrophilic and appears in the form of delicate, threadlike densities that mark the locations and orientations of the neuronal cell processes. × 210 .

Fig. 2. Section from an Al maltolate-treated rabbit sacrificed after 7 days, by which time severe neurological symptoms were evident. Orientation of section is comparable to Fig. 1. In contrast to the untreated control animal, the profiles of the Bielschowsky-stained neurons are evident and contain thickened opaque cords of cytoskeletal material ('neurofibrillary aggregates' or NFAs) that fill much of the cell body and both apical and basal dendrites (basal dendrites shown by *arrows*), the latter of which are especially prominent and darkly stained. × 210 .

Fig. 3. Higher magnification of a silver-stained pyramidal neuron in Al-treated rabbit cortex. The apical dendrite (*AD*) has a twisted profile. The NFAs in both apical and basal dendrites extend into the cell body and therefore obscure the nuclear profile. × 240.

Fig. 4. Normal cortex immunostained with a monoclonal antibody (SMI-31) directed against a phosphorylated epitope of neurofilament protein. Though neurofilaments are not present in great numbers in unchallenged neurons, the epitope is evidently present in substantial quantities (cf. Fig. 5) in a distribution similar to the NFAs seen in Al-treated brain. × 210.

Fig. 5. SMI-31 immunoreactivity in brain of an Al-treated rabbit. Distribution of the antigen in the pyramidal cortical neurons is similar to that shown in Fig. 4, despite the finding that in cells exposed to Al there is a massive increase in neurofilaments. × 210.

antibody to the 200 kDa subunit of neurofilament protein (Bertholf *et al.*, 1989). In a later study of tissue from these same animals, using the monoclonal antibodies SMI-31, -32 and -33, discrete focal perikaryal and proximal neuritic positivity in the form of spheroids and neuritic threads in a small number of pyramidal neurons were observed in the occipital striate cortex (Katsetos *et al.*, 1990). The monoclonal antibodies SMI-31, -32 and -33 recognize phosphorylated, non-phosphorylated/phosphate-dependent and non-phosphorylated/phosphate-independent epitopes of the high and medium isoforms of neurofilament proteins respectively.

More distinct evidence of neurofibrillary changes has been detected by Forrester and Yokel (1985) in a comparative study of subcutaneous and intraventricular administration of Al lactate to adult New Zealand white rabbits. For the subcutaneous study, rabbits received daily subcutaneous injections of 400 μmole/kg Al lactate, over a period of 28 days. Although no consistent clinical pattern of neurotoxicity was apparent, two of the animals displayed some evidence of motor abnormalities, as assessed by foot spread on landing, gait analysis and the righting reflex. Neurofibrillary changes, detected by Bielschowsky's silver method, hematoxylin-eosin, and cresyl violet stains, were evident in the hippocampus and frontal cortex of the affected animals. The neuronal perikarya and/or processes demonstrated positivity for neurofibrillary aggregates, and correlated with associated behavioral changes, such as seizures, postural changes, aggressiveness and excitability. An unexpected observation to us was the marked similarity in clinical and neuropathological abnormalities of animals treated subcutaneously with Al compared with those treated intraventricularly. In a later report aimed specifically at relating Al neurotoxicity to age, Yokel (1989) used the same mode of injection to older (2–3.4 years) New Zealand white rabbits; unexpectedly in the older animals, administration of 400 μmole/kg dose of Al lactate was lethal, so a lower dose of 200 μmole/kg was used. Tissue Al concentrations in the frontal gray cortex and hippocampus were significantly elevated. No histologic examination of tissue was performed.

Oral Administration of Al in Rabbits

Aluminum toxicity has been examined following the oral administration of Al citrate to young Japanese white rabbits fed a calcium and magnesium-deficient diet. This treatment induced neurofibrillary degeneration in the anterior horn of the spinal cord (Kihira *et al.*, 1994). Studies in the authors' laboratory following the oral administration of Al citrate to New Zealand white rabbits over a 3–12 month period has demonstrated no accumulation of Al in the brain and no evidence of neurofibrillary changes (Wills *et al.*, 1993a).

Neurobehavioral Effects Following Al Administration in Rabbits

To our knowledge, no behavioral studies on rabbits treated orally with Al have been performed. We have evaluated the long-term oral administration of Al maltolate to young adult rabbits (Hewitt *et al.*, 1992; Wills *et al.*, 1993a;b). Although decreased weight gain was noted, we performed no specific behavioral studies. Behavioral evaluation in

rabbits has been carried out following either the direct injection of Al compounds into the brain or systemic administration. Intracisternal administration of Al to New Zealand white rabbits of either sex has been reported to produce deficits in water maze acquisition (Rabe *et al.*, 1982). This water maze had three chambers with an escape ramp in the third chamber. Rabbits were trained by 3-spaced trials daily for 5 consecutive days. In this model, adult New Zealand white rabbits were injected intracisternally with 50 μL of 1% $AlCl_3$ (3.75 μmole) in physiological saline. Interestingly, administration of this amount resulted in neurological symptoms affecting the motor system within 1–3 weeks, and all animals died from seizures within 2–4 weeks. However, when $AlCl_3$ was injected intracisternally into infant rabbits on the 15th day of life, neurofibrillary changes were found in the cerebrum, brainstem and spinal cord, but there were no apparent clinical symptoms. Importantly however, this treatment of infant animals caused a significant learning deficit, as evaluated by the water maze test described above. Whether this deficit was due to the neurofibrillary changes or to some other effect of Al was unclear to the authors (Rabe *et al.*, 1982). It is indeed surprising that there has been little follow-up of this significant brief report.

The rabbit is not typically used for behavioral studies, but the classically conditioned-defensive eyeblink reflex is a useful tool and has been examined. This test appears to reflect the effects of Al on neural pathways and structures subserving simple forms of learning and memory; the hippocampus and cerebellum are structures that may be involved in these processes (Yokel, 1994). Using the intracisternal route of Al administration, Pendelbury *et al.* (1988) and Solomon *et al.* (1988) have demonstrated learning and memory deficits in 4–6 month old New Zealand white rabbits (sex not stated) by studying the acquisition or retention of the eyeblink reflex. In a series of experiments, Yokel applied the subcutaneous route of injection of Al lactate, and was able to demonstrate learning and memory deficits, but only in adult and aged (2–3.4 years) female New Zealand white rabbits (Yokel, 1983; 1984; 1985; 1987; 1989). This suggested, as we have also proposed (Savory *et al.*, 1999), that aging increases the susceptibility of the brain to Al toxicity, at least in rabbits. Yokel at al. (1994) related the Al-induced learning deficits in rabbits to patients with Alzheimer's disease by demonstrating that 4-aminopyridine, a compound reported to improve learning in Alzheimer's disease subjects, also reduced the severity of the Al-induced learning deficit in rabbits.

Informed Opinion

Does Al-Induced Neurodegeneration in Experimental Animals Support the Hypothesis that Al Might Play a Role in the Pathogenesis of Alzheimer's Disease?

There have been several animal models proposed as an aid in understanding Alzheimer's disease neuropathology, including transgenic mice (Sugaya *et al.*, 1997), rat, monkey, and dog (Brining *et al.*, 1996; Games *et al.*, 1995; Uno *et al.*, 1996). Transgenic mice have been used mainly to examine the process of Aβ deposition (Sugaya *et al.*, 1997), while individual events such as apoptosis, Aβ deposition, and neurofibrillary degeneration have been explored in other animals (Brining *et al.*, 1996; Games *et al.*, 1995;

Uno *et al.*, 1996). Yokel (1989) demonstrated over a decade ago that 2–3.4 years old aged female rabbits were more susceptible to Al following the subcutaneous route of administration than were young adults, and moreover also exhibited marked changes in behavior. Studies in the authors' laboratory have demonstrated that Al maltolate-treated rabbits (especially aged female animals, 3–4 year old), exhibit widespread formation of intraneuronal neurofilamentous aggregates which share significant immunochemical/antigenic characteristics with the neurofibrillary tangles found in the central nervous system of patients with Alzheimer's disease and in amyotrophic lateral sclerosis (ALS), a motoneuron disease. Typically these neurofilamentous aggregates contain hyperphosphorylated tau, amyloid precursor protein, Aβ, α-1-antichymotrypsin and ubiquitin (Savory *et al.*, 1996; Huang *et al.*, 1997). Interestingly, similarities have been reported in eyeblink classical conditioning between aged New Zealand White rabbits (up to 7 years of age) and patients with Alzheimer's disease (Woodruff-Pak and Trojanowski, 1996).

The relationship of Al-induced neurofibrillary degeneration in rabbits to human neurodegenerative disorders has been viewed with skepticism, because of apparent ultrastructural differences between the experimental lesions in rabbits and human neurofibrillary tangles. Compared to the tangles of Alzheimer's disease, which mostly contain paired helical filaments (Kidd, 1964; Terry, 1963; Wisniewski *et al.*, 1976), those produced by Al are predominantly straight, intermediate-like filaments (Dahl and Bignami, 1978; Wisniewski and Sturman, 1989). This difference in the ultrastructural properties of the intraneuronal neurofilamentous aggregates could be due to the different time course of their formation. In Alzheimer's disease, this time could be months or years, whereas in the acute animal experiments the time course is only a few days (Savory *et al.*, 1996). Supporting the argument that these protein aggregates might arise from a similar mechanism has been the observation that tau can form Alzheimer's-like filaments *in vitro* (Crowther *et al.*, 1994; Murayama *et al.*, 1999).

Aluminum-induced neurofibrillary degeneration is characterized predominantly by immunohistochemical staining with antibodies specific for the hyperphosphorylated epitopes of neurofilament protein (Katsetos *et al.*, 1990; Savory *et al.*, 1996; Wakayama *et al.*, 1996). The primary constituent of paired helical filaments in human neurofibrillary tangles is tau, although other proteins are present, including abnormally phosphorylated neurofilament proteins, ubiquitin, α1-antichymotrypsin, amyloid precursor protein and its derived peptide, Aβ. Studies in the authors' laboratory over the past five years, which now have been confirmed by others (Muma and Singer, 1996; Singer *et al.*, 1997), have shown that immunochemical similarities between the composition of Al-induced lesions and those found in Alzheimer's disease are far closer than was originally surmised. Rao *et al.* (2000) also have confirmed these observations.

Abnormally phosphorylated tau has been detected in these neurofilamentous aggregates (Huang *et al.*, 1997), using a variety of mAbs that recognize both nonphosphorylated and phosphorylated tau (Muma and Singer, 1996; Savory *et al.*, 1995b). Among the monoclonal antibodies applied for this immunostaining have been Tau-1, Tau-2, AT8, PHF-1 and Alz-50, indicating that both phosphorylated and nonphosphorylated tau are present. The time course of aggregation of these cytoskeletal proteins has been evaluated in the authors' laboratory (Savory *et al.*, 1996). The results indicate that the aggregates become detectable by silver staining within 24 hours following Al maltolate administration, and

that neurofilament proteins predominate; non-phosphorylated phosphorylation-independent epitopes as detected by mAb SMI-33 (Sternberger Monoclonals Inc. Baltimore, MD) are found first, followed by phosphorylated forms, immunostained by mAb SMI 31 (same vendor), at approximately 72 hours. Tau is also detectable by around 72 hours, although the characteristic epitopes of Alzheimer's disease as recognized by mAbs AT8 and PHF-1 are most distinct at 6–7 days following Al injection. It has been proposed that phosphorylation of cytoskeletal proteins drives the formation of the neurofilamentous aggregates, particularly in human neurodegenerative disorders. Since the aggregates are hyperphosphorylated, phosphorylation alone would render these protein accumulations unstable, because of the preponderance of negative charges on the phosphate groups. Thus, it is reasonable to propose that some positively-charged species constitute an inherent factor in the formation and stabilization of the neurofibrillary degeneration, both in Alzheimer's disease and in experimental Al-induced neurofibrillary degeneration; in the latter, Al^{3+} is an obvious candidate for this role.

We have proposed that aging in rabbits is an important factor regarding the susceptibility of neurons to oxidative stress and to subsequent apoptosis (Savory *et al.*, 1999); both processes have been observed in the Alzheimer's disease brain (Smith *et al.*, 1996; Su *et al.*, 1994). Protein changes controlling apoptosis, such as those of the *Bcl-2* family and caspases, also are altered in the Alzheimer's brain (Kitamura *et al.*, 1998). We have shown similar responses in aged rabbits treated intracisternally with Al maltolate (Savory *et al.*, 1999). Brain tissue from these aged animals exhibited intense intraneuronal silver positivity, indicative of the formation of neurofilamentous aggregates, together with oxidative stress. The changes occurred in the CA1 region of the hippocampus as well as in cerebral cortical areas. Apoptosis, assessed by the TUNEL *in situ* technique, colocalized with oxidative stress. Young animals treated with Al showed few of these alterations, while age-matched controls were essentially negative. Further studies on the time course of these and related changes have demonstrated that oxidative stress and redox-active iron accumulation in hippocampal neurons occurred very rapidly, within a period of 3 hours, and increased in intensity at 72 hours. Changes suggestive of apoptosis were apparent by 24 hours and were pronounced at 72 hours. In aged animals there was an initially intense immunopositivity at 3 hours for Bcl-2, with negative staining for Bax. By 72 hours, when apoptosis was strongly evident, Bcl-2 was negative and Bax strongly positive. In contrast to the aged rabbits, young animals treated similarly with Al exhibited much less oxidative stress with no apoptosis, and maintained Bcl-2 immunopositivity and negative Bax staining. Our findings strongly support the key role that oxidative damage plays in the process of neurodegeneration and in the increased vulnerability to Al-induced injury in the aged animal. These findings have demonstrated that Al can produce relevant neuropathological and biochemical changes in experimental animals, albeit in an animal system quite different from that in Alzheimer's disease.

Another relevant finding in Al-induced neurodegeneration has been the observation of amyloid precursor protein and Aβ immunopositivity in neurons following Al treatment in rabbits (Huang *et al.*, 1997) and in rats (Shigematsu and McGeer, 1992). Neurofibrillary tangles in Alzheimer's disease also exhibit this Aβ staining, but the most prevalent pattern is the presence of Aβ in the neuritic plaques. It is logical to hypothesize that in Alzheimer's disease, increased Aβ first appears intracellularly, followed by extracellular

deposition. Plassman and Breitner (1996) have described an Al-induced secondary structural transition in the non-Aβ component of Alzheimer's disease amyloid (NACP), also known as α-synuclein, which generated an approximately 33% α-helix, thus rendering the α-synuclein resistant to proteases. Based on this finding it was suggested that Al may influence α-synuclein turnover and induce aggregation via structural modifications, thus leading to Aβ deposition. Paik *et al.* (1999) have investigated the self-oligomerization of α-synuclein by various metal ions including Al. Copper and zinc induced oligomerization with copper being most effective. Aluminum was also studied but had less of an effect. However, this work totally ignored the fact that all metals studied were prepared at a concentration of 0.5 mM in 20 mM MES, pH 6.5 which would allow for a 0.5 mM concentration of both Cu^{2+} and Zn^{2+} but, as was discussed earlier, the concentration of Al^{3+} would be many times lower due to the formation of insoluble Al salts.

Deregulation of Al and iron homeostasis may play a role in Alzheimer's disease and in Al neurotoxicity. A study by Bouras *et al.* (1997) described the presence of high concentrations of Al and iron in the hippocampus and inferior temporal cortex in both Alzheimer's disease and in dementia pugilistica. The predominant findings were those of the coaccumulation of Al and iron, both in neurofibrillary tangles and in the nuclei of tangle-bearing neurons. Also, concentrations of Al and iron in nuclei of tangle-free neurons and neuropil were similar in Alzheimer's disease and in dementia pugilistica. These studies suggest the existence of an association between the deposition of Al and iron with neurofibrillary tangle formation, and support the possibility of a global dysregulation of Al and iron transport in Alzheimer's disease and dementia pugilistica. It has been hypothesized that the deregulation of Al and iron homeostasis permits the existence of colocalization of these two metals, and contributes to the accumulation of metabolic errors, leading to neuronal disorders, including the formation of neurofibrillary tangles and Aβ deposition (Berthon, 1996). Cells in the rat brain possess a specific high-affinity receptor for transferrin that is independent of the metal being transported. This system is postulated to be the route whereby iron in the general circulation reaches the brain (Roskams and Connor, 1990). Transferrin is thought to be mainly an iron transporter protein, based on the relatively high abundance of iron in the circulation and the high affinity of transferrin for iron (Martin *et al.*, 1987). However, as mentioned earlier, transferrin also has a high affinity for Al, although not to the same extent as iron (Martin *et al.*, 1987), and this property should provide an avenue for the transportation and intracellular deposition of Al. Evidence for this pathway is provided in a report that aluminum accumulation was accompanied by an increase in iron uptake in primary cultures of the rat cerebral cortex (Oshiro *et al.*, 1998).

Shin *et al.* (1995) have shown that Al selectively binds to the paired helical filament-tau, induces aggregation, and retards the in vivo proteolysis of this protein aggregate. Their data suggest that Al may serve as a cofactor in the formation of neurofibrillary tangles by its interaction with tau. Madhav *et al.* (1996) using circular dichroism revealed a five-fold increase in the observed ellipticity of the tau-Al assembly which they attributed to Al-induced aggregation of the protein. More recently Tarbox and Goux (1999) have studied Al interactions with tau protein using circular dichroism spectroscopy, and have shown that Al induces marked conformational changes independent of tau phosphorylation.

All of the above studies indicate that Al contributes to the formation of neurofibrillary lesions in neurons, and thus may play a role in the pathology of Alzheimer's disease and other human neurodegenerative disorders. The biochemical similarities of the Al animal model to the intraneuronal lesions of Alzheimer's disease make this system valuable for studying perturbations of the neuronal cytoskeleton, particularly in view of the lack of optimal animal models. In the context of the present review, the animal studies cited do not prove that Al is a risk factor, but convincingly demonstrate that this metal can produce significant neurofibrillary pathology and biochemical changes that are important features of neurodegenerative disorders.

Acknowledgments

We gratefully acknowledge support from the United States Department of the Army, Grant # DAMD 17-99-1-9552 to John Savory Ph.D., in the preparation of this review.

References

Beal M.F., Mazurek M.F., Ellison D.W., Kowall N.W., Solomon P.R., & Pendlebury W.W. (1989) Neurochemical characteristics of aluminum-induced neurofibrillary degeneration in rabbits. *Neuroscience* **29**, 339–346.

Bertholf R.L., Herman M.M., Savory J., Carpenter R.M., Sturgill B.C., Katsetos C.D., VandenBerg S.R., & Wills M.R. (1989) A long-term intravenous model of aluminum maltol toxicity in rabbits: tissue distribution, hepatic, renal, and neuronal cytoskeletal changes associated with systemic exposure. *Toxicology & Applied Pharmacology* **98**, 58–74.

Berthon G. (1996) Chemical speciation studies in relation to aluminium metabolism and toxicity. *Coordination Chemistry Reviews* **149**, 241–280.

Boni U.D., Otvos A., Scott J.W., & Crapper D.R. (1976) Neurofibrillary degeneration induced by systemic aluminum. *Acta Neuropathologica (Berl)* **35**, 285–294.

Bouras C., Giannakopoulos P., Good P.F., Hsu A., Hof P.R., & Perl D.P. (1997) A laser microprobe mass analysis of brain aluminum and iron in dementia pugilistica — comparison with Alzheimers-disease. *European Neurology* **38**, 53–58.

Brining S.K., Jones C.R., & Chang M.C. (1996) Effects of chronic beta-amyloid treatment on fatty acid incorporation into rat brain. *Neurobiology of Aging* **17**, 301–309.

Crowther R.A., Olesen O.F., Smith M.J., Jakes R., & Goedert M. (1994) Assembly of Alzheimer-like filaments from full-length tau protein. *FEBS Letters* **337**, 135–138.

Dahl D. & Bignami A. (1978) Immunochemical cross-reactivity of normal neurofibrils and aluminum-induced neurofibrillary tangles. Immunofluorescence study with antineurofilament serum. *Experimental Neurology* **58**, 74–80.

Favarato M. & Zatta P.F. (1993) Differential aluminium lactate toxicity in rabbits using either aqueous solutions or liposomal suspensions. *Toxicology Letters* **66**, 133–146.

Fontana L., Perazzolo M., Stella M.P., Tapparo A., Corain B., Favarato M., & Zatta P. (1991) A long-term toxicological investigation on the effect of tris(maltolate)aluminum(III) in rabbits. *Biological Trace Element Research* **31**, 183–191.

Finnegan M.M., Rettig S.J., & Orvig C. (1986) A neutral water-soluble aluminum complex of neurological interest. *Journal of the American Chemical Society* **108**, 5033–5035.

Forrester T.M. & Yokel R.A. (1985) Comparative toxicity of intracerebroventricular and subcutaneous aluminum in the rabbit. *NeuroToxicology* **6**, 71–80.

Games D., Adams D., Alessandrini R., Barbour R., Berthelette P., Blackwell C., Carr T., Clemens J.,

Donaldson T., & Gillespie F. (1995) Alzheimer-type neuropathology in transgenic mice overexpressing V717F beta-amyloid precursor protein. *Nature* **373**, 523–527.

Graur D., Duret L., & Gouy M. (1996) Phylogenetic position of the order Lagomorpha (rabbits, hares and allies). *Nature* **379**, 333–335.

Hewitt C.D., Herman M.M., Lopes M.B., Savory J., & Wills M.R. (1991) Aluminium maltol-induced neurocytoskeletal changes in fetal rabbit midbrain in matrix culture. *Neuropathology & Applied Neurobiology* **17**, 47–60.

Hewitt C.D., Innes D.J., Herman M.M., Savory J., & Wills M.R. (1992) Hematological changes after long-term aluminum administration to normal adult rabbits. *Annals of Clinical & Laboratory Science* **22**, 85–94.

Huang Y., Herman M.M., Liu J., Katsetos C.D., Wills M.R., & Savory J. (1997) Neurofibrillary lesions in experimental aluminum-induced encephalopathy and Alzheimer's disease share immunoreactivity for amyloid precursor protein, Aβ, α_1-antichymotrypsin and ubiquitin–protein conjugates. *Brain Research* **771**, 213–220.

Iqbal K., Alonso A.C., Gong C.X., Khatoon S., Singh T.J., & Grundke-Iqbal I. (1994) Mechanism of neurofibrillary degeneration in Alzheimer's disease. *Molecular Neurobiology* **9**, 119–123.

Katsetos C.D., Savory J., Herman M.M., Carpenter R.M., Frankfurter A., Hewitt C.D., & Wills M.R. (1990) Neuronal cytoskeletal lesions induced in the CNS by intraventricular and intravenous aluminium maltol in rabbits. *Neuropathology & Applied Neurobiology* **16**, 511–528.

Kidd M. (1964) Alzheimer's disease: an electron microscopic study. *Brain* **87**, 307–320.

Kihira T., Yoshida S., Uebayashi Y., Wakayama I., & Yase Y. (1994) Experimental model of motor neuron disease: oral aluminum neurotoxicity. *Biomedical Research-Tokyo* **15**, 27–36.

Kitamura Y., Shimohama S., Kamoshima W., Ota T., Matsuoka Y., Nomura Y., Smith M.A., Perry G., Whitehouse P.J., & Taniguchi T. (1998) Alteration of proteins regulating apoptosis, Bcl-2, Bcl-x, Bax, Bak, Bad, ICH-1 and CPP32, in Alzheimer's-disease. *Brain Research* **780**, 260–269.

Klatzo I., Wisniewski H.M., & Streicher E. (1965) Experimental production of neurofibrillary degeneration. 1. Light microscopic observations. *Journal of Neuropathology & Experimental Neurology* **24**, 187–199.

Kowall N.W., Pendlebury W.W., Kessler J.B., Perl D.P., & Beal M.F. (1989) Aluminum-induced neurofibrillary degeneration affects a subset of neurons in rabbit cerebral cortex, basal forebrain and upper brainstem. *Neuroscience* **29**, 329–337.

Madhav TR., Vatsala S., Ramakrishna T., Ramesh J., & Easwaran KR. (1996) Preservation of native conformation during aluminum-induced aggregation of tau protein. *NeuroReport* **7**, 1072–1076.

Malakoff D. (2000) Public health. Aluminum is put on trial as a vaccine booster. *Science* **288**, 1323–1324.

Martin L.J., Pardo C.A., Cork L.C., & Price D.L. (1994) Synaptic pathology and glial responses to neuronal injury precede the formation of senile plaques and amyloid deposits in the aging cerebral cortex. *American Journal of Pathology* **145**, 1358–1381.

Martin R.B. (1986) The chemistry of aluminum as related to biology and medicine. *Clinical Chemistry* **32**, 1797-1806.

Martin R.B. (1988) Bioinorganic chemistry of aluminum. *Metal Ions in Biological Systems* **24**, 1–57.

Martin R.B. (1990) Bioinorganic chemistry of magnesium. *Metal Ions in Biological Systems* **26**, 1–13.

Martin R.B. (1991) Aluminum in biological systems. In *Aluminum in chemistry, biology and medicine* (Eds. P. Nicolini, P.F. Zatta, & B. Corain,) Raven Press, New York, pp 3–20.

Martin R.B. (1992) Aluminium speciation in biology. *Ciba Foundation Symposium* **169**, 5–18.

Martin R.B. (1997a) Chemistry of aluminum in the central nervous system. (Eds. M. Yasui, M.J. Strong, K. Ota, & M.A. Verity,) Mineral and Metal Neurotoxicology edn. CRC Press, New York, pp 75–80.

Martin R.B. (1997b) Importance of aluminium chemistry in biological systems. In *Aluminium toxicity in infant's health and disease* (Eds. P.F. Zatta, & A.C. Alfrey,) World Scientific, Singapore, pp 3–15.

Martin R.B., Savory J., Brown S., Bertholf R.L., & Wills M.R. (1987) Transferrin binding of Al3+ and Fe3+. *Clinical Chemistry* **33**, 405–407.

Mawal-Dewan M., Schmidt M.L., Balin B., Perl D.P., Lee V.M., & Trojanowski J.Q. (1996) Identification of phosphorylation sites in PHF-TAU from patients with Guam amyotrophic lateral sclerosis/parkinsonism-dementia complex. *Journal of Neuropathology & Experimental Neurology* **55**, 1051–1059.

Muma N.A. & Singer S.M. (1996) Aluminum-induced neuropathology: transient changes in microtubule-associated proteins. *Neurotoxicology & Teratology* **18**, 679–690.

Murayama H., Shin R.W., Higuchi J., Shibuya S., Muramoto T., & Kitamoto T. (1999) Interaction of aluminum with PHFtau in Alzheimer's disease neurofibrillary degeneration evidenced by desferrioxamine-assisted chelating autoclave method. *American Journal of Pathology* **155**, 877–885.

Oshiro S., Kawahara M., Mika S., Muramoto K., Kobayashi K., Ishige R., Nozawa K., Hori M., Yung C., Kitajima S., & Kuroda Y. (1998) Aluminum taken up by transferrin-independent iron uptake affects the iron metabolism in rat cortical cells. *Journal of Biochemistry* **123**, 42–46.

Paik SR., Shin H-J., Lee J-H., Chang C-S., & Kim J. (1999) Copper(II)-induced self-oligomerization of α-synuclein. *Biochemical Journal* **340**, 821–828

Pendlebury W.W., Perl D.P., Schwentker A., Pingree T.M., & Solomon P.R. (1988) Aluminum-induced neurofibrillary degeneration disrupts acquisition of the rabbit's classically conditioned nictitating membrane response. *Behavioral Neuroscience* **102**, 615–620.

Plassman B.L. & Breitner J.S. (1996) Recent advances in the genetics of Alzheimers disease and vascular dementia with an emphasis on gene-environment interactions. *Journal of the American Geriatrics Society* **44**, 1242–1250.

Rabe A., Lee M.H., Shek J., & Wisniewski H.M. (1982) Learning deficit in immature rabbits with aluminum-induced neurofibrillary changes. *Experimental Neurology* **76**, 441–446.

Rao J.S., Katsetos C.D., Herman M.M., & Savory J. (1998) Experimental aluminium encephalomyelopathy; relationship to human neurodegenerative disease. *Clinics in Laboratory Medicine* **18**, 687–698.

Rao JKS., Anitha S., & Latha KS. (2000) Aluminum-induced neurodegeneration in the hippocampus of aged rabbits mimics Alzheimer's disease. *Alzheimer's Reports* **3**, 83–88.

Roskams A.J. & Connor J.R. (1990) Aluminum access to the brain: a role for transferrin and its receptor. *Proceedings of the National Academy of Sciences of the United States of America* **87**, 9024–9027.

Satou T., Cummings B.J., Head E., Nielson K.A., Hahn F.F., Milgram N.W., Velazquez P., Cribbs D.H., Tenner A.J., & Cotman C.W. (1997) The progression of beta-amyloid deposition in the frontal cortex of the aged canine. *Brain Research* **774**, 35–43.

Savory J., Herman M.M., Erasmus R.T., Boyd J.C., & Wills M.R. (1994) Partial reversal of aluminium-induced neurofibrillary degeneration by desferrioxamine in adult male rabbits. *Neuropathology & Applied Neurobiology* **20**, 31–37.

Savory J., Herman M.M., Hundley J., Seward R.L., Griggs C.M., Katsetos C.D., & Wills M.R. (1993) Quantitative studies on aluminum deposition and its effects on neurofilament protein expression and phosphorylation, following the intraventricular administration of aluminum maltolate to adult rabbits. *NeuroToxicology* **14**, 9–13.

Savory J., Huang Y., Herman M.M., Reyes M.R., Boyd J.C., & Wills M.R. (1995a) Chapter 59. Abnormal tau accumulation and partial reversal by desferrioxamine, in Al-induced neurofibrillary degeneration in rabbits. In *Research Advances in Alzheimer's Disease and Related Disorders* (Eds. K. Iqbal, J.A. Mortimer, B. Winblad, & H.M. Wisniewski,) John Wiley and Sons Ltd., pp 543–551.

Savory J., Huang Y., Herman M.M., Reyes M.R., & Wills M.R. (1995b) Tau immunoreactivity associated with aluminum maltolate-induced neurofibrillary degeneration in rabbits. *Brain Research* **669**, 325–329.

Savory J., Huang Y., Herman M.M., & Wills M.R. (1996) Quantitative image analysis of temporal changes in tau and neurofilament proteins during the course of acute experimental neurofibrillary degeneration; non-phosphorylated epitopes precede phosphorylation. *Brain Research* **707**, 272–281.

Savory J., Rao J.K.S., HuangY., Letada P., & Herman M.M. (1999) Age-related hippocampal changes in Bcl-2:Bax ratio, oxidative stress, redox-active iron and apoptosis associated with aluminum-induced neurodegeneration: increased susceptibility with aging. *NeuroToxicology* **20**, 805–818.

Shigematsu K. & McGeer P.L. (1992) Accumulation of amyloid precursor protein in damaged neuronal processes and microglia following intracerebral administration of aluminum salts. *Brain Research* **593**, 117–123.

Shin R.W., Lee V.M., & Trojanowski J.Q. (1995) Neurofibrillary pathology and aluminum in Alzheimer's disease. *Histology & Histopathology* **10**, 969–978.

Singer S.M., Chambers C.B., Newfry G.A., Norlund M.A., & Muma N.A. (1997) Tau in aluminum-induced neurofibrillary tangles. *NeuroToxicology* **18**, 63–76.

Smith M.A., Perry G., Richey P.L., Sayre L.M., Anderson V.E., Beal M.F., & Kowall N. (1996) Oxidative damage in Alzheimer's. *Nature* **382**, 120–121.

Solomon P.R., Koota D., & Pendlebury W.W. (1990) Disrupted retention of the classically conditioned nictitating membrane response in the aluminum-intoxicated rabbit using electrical stimulation of the brain as a conditioned stimulus. *Neurobiology of Aging* **11**, 523–528.

Solomon P.R., Pingree T.M., Baldwin D., Koota D., Perl D.P., & Pendlebury W.W. (1988) Disrupted retention of the classically conditioned nictitating membrane response in rabbits with aluminum-induced neurofibrillary degeneration. *NeuroToxicology* **9**, 209–221.

Strong M.J. & Garruto R.M. (1991a) Chronic aluminum-induced motor neuron degeneration: clinical, neuropathological and molecular biological aspects. *Canadian Journal of Neurological Sciences* **18**, Suppl-31.

Strong M.J. & Garruto R.M. (1991b) Potentiation in the neurotoxic induction of experimental chronic neurodegenerative disorders: N-butyl benzenesulfonamide and aluminum chloride. *NeuroToxicology* **12**, 415–425.

Strong M.J., Wolff A.V., Wakayama I., & Garruto R.M. (1991) Aluminum-induced chronic myelopathy in rabbits. *NeuroToxicology* **12**, 9–21.

Su J.H., Anderson A.J., Cummings B.J., & Cotman C.W. (1994) Immunohistochemical evidence for apoptosis in Alzheimer's disease. *Neuroreport* **5**, 2529–2533.

Sugaya K., Reeves M., & Mckinney M. (1997) Topographic associations between DNA fragmentation and Alzheimers-disease neuropathology in the hippocampus. *Neurochemistry International* **31**, 275–281.

Tarbox, T, Goux, W.J. (1999) Conformations of phosphorylated and non-phosphorylated tau peptides in the presence of calcium and aluminum. *Abstracts of the Society for Neuroscience, 29th Annual Meeting, Miami Beach, FL, October 23–28, 1999* **25**, 1098.

Terry R.D. (1963) The fine structure of neurofibrillary tangles in Alzheimer's disease. *Journal of Neuropathology & Experimental Neurology* **22**, 629–642.

Troncoso J.C., Price D.L., Griffin J.W., & Parhad I.M. (1982) Neurofibrillary axonal pathology in aluminum intoxication. *Annals of Neurology* **12**, 278–283.

Troncoso J.C., Sternberger N.H., Sternberger L.A., Hoffman P.N., & Price D.L. (1986) Immunocytochemical studies of neurofilament antigens in the neurofibrillary pathology induced by aluminum. *Brain Research* **364**, 295–300.

Uno H., Alsum P.B., Dong S., Richardson R., Zimbric M.L., Thieme C.S., & Houser W.D. (1996) Cerebral amyloid angiopathy and plaques, and visceral amyloidosis in aged macaques. *Neurobiology of Aging* **17**, 275–281.

Wakayama I., Nerurkar V.R., & Garruto R.M. (1993) Immunocytochemical and ultrastructural evidence of dendritic degeneration in motor neurons of aluminum-intoxicated rabbits. *Acta Neuropathologica (Berl)* **85**, 122–128.

Wakayama I., Nerurkar V.R., Strong M.J., & Garruto R.M. (1996) Comparative study of chronic aluminum-induced neurofilamentous aggregates with intracytoplasmic inclusions of amyotrophic lateral sclerosis. *Acta Neuropathologica* **92**, 545–554.

Wills M.R., Hewitt C.D., Savory J., & Herman M.M. (1993a) Long-term oral aluminum administration in rabbits. II. Brain and other organs. *Annals of Clinical & Laboratory Science* **23**, 17–23.

Wills M.R., Hewitt C.D., Sturgill B.C., Savory J., & Herman M.M. (1993b) Long-term oral or intravenous aluminum administration in rabbits. I. Renal and hepatic changes. *Annals of Clinical & Laboratory Science* **23**, 1–16.

Wisniewski H.M., Narang H.K., & Terry R.D. (1976) Neurofibrillary tangles of paired helical filaments. *Journal of the Neurological Sciences* **27**, 173–181.

Wisniewski H.M., Shek J.W., Gruca S., & Sturman J.A. (1984) Aluminum-induced neurofibrillary changes in axons and dendrites. *Acta Neuropathologica (Berl)* **63**, 190–197.

Wisniewski H.M. & Sturman J.A. (1989) Neurotoxicity of aluminum. In *Aluminum and Health, a Critical Review* (Ed. H.J. Gitelman H.J.,) Marcel Dekker, Inc., New York, pp 125–165.

Wisniewski H.M., Sturman J.A., & Shek J.W. (1980) Aluminum chloride induced neurofibrillary changes in the developing rabbit: A chronic animal model. *Annals of Neurology* **8**, 479–490.

Woodruff-Pak D.S. & Trojanowski J.Q. (1996) The older rabbit as an animal model: implications for Alzheimer's disease. *Neurobiology of Aging* **17**, 283–290.

Yokel R.A. (1983) Repeated systemic aluminum exposure effects on classical conditioning of the rabbit. *Neurobehavioral Toxicology &.Teratology* **5**, 41–46.

Yokel R.A. (1984) Toxicity of aluminum exposure during lactation to the maternal and suckling rabbit. *Toxicology & Applied Pharmacology* **75**, 35–43.

Yokel R.A. (1985) Toxicity of gestational aluminum exposure to the maternal rabbit and offspring. *Toxicology & Applied Pharmacology* **79**, 121–133.

Yokel R.A. (1987) Toxicity of aluminum exposure to the neonatal and immature rabbit. *Fundamentals of.Applied Toxicology* **9**, 795–806.

Yokel R.A. (1989) Aluminum produces age-related behavioral toxicity in the rabbit. *Neurotoxicology & Teratology* **11**, 237–242.

Yokel R.A. (1994) Aluminum exposure produces learning and memory deficits: a model of Alzheimer's disease. In *Toxin-Induced Models of Neurological Disorders* (Eds. M.L. Woodruff, & A.J. Nonneman,) Plenum Press, New York, pp 301–318.

Yokel R.A., Allen D.D., & Meyer J.J. (1994) Studies of aluminum neurobehavioral toxicity in the intact mammal. *Cell & Molecular Neurobiology* **14**, 791–808.

APPENDIX VIII

A

MASS SPECTRUM
10/18/00 13:30:00 + 5:18
SAMPLE: 8-HYDROXYGUANINE
CONDS.: EM1200
TEMP: 226 DEG. C

DATA: 8HG #318
CALI: CAL1018 #3

BASE M/Z: 440
RIC: 9388030.

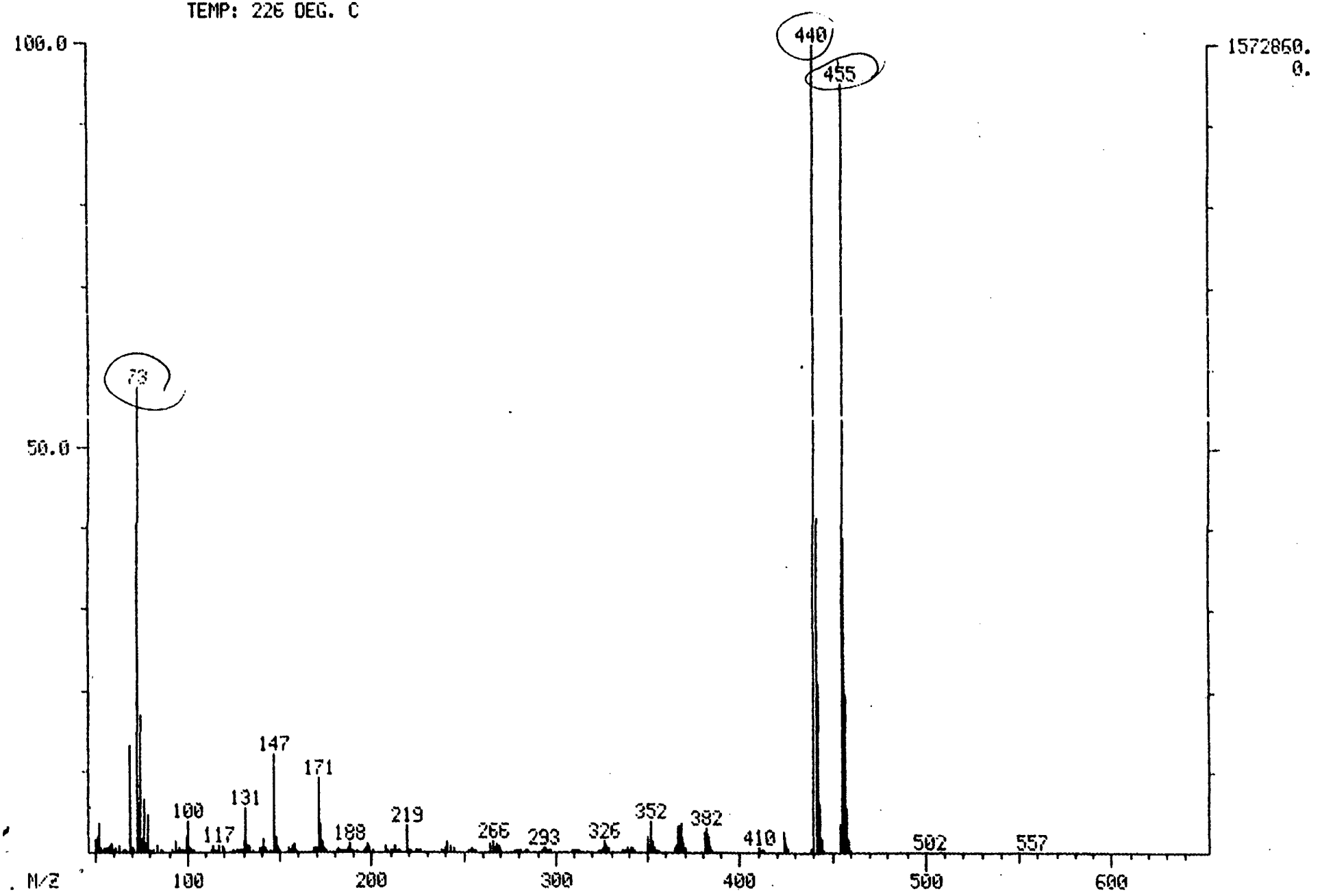

B

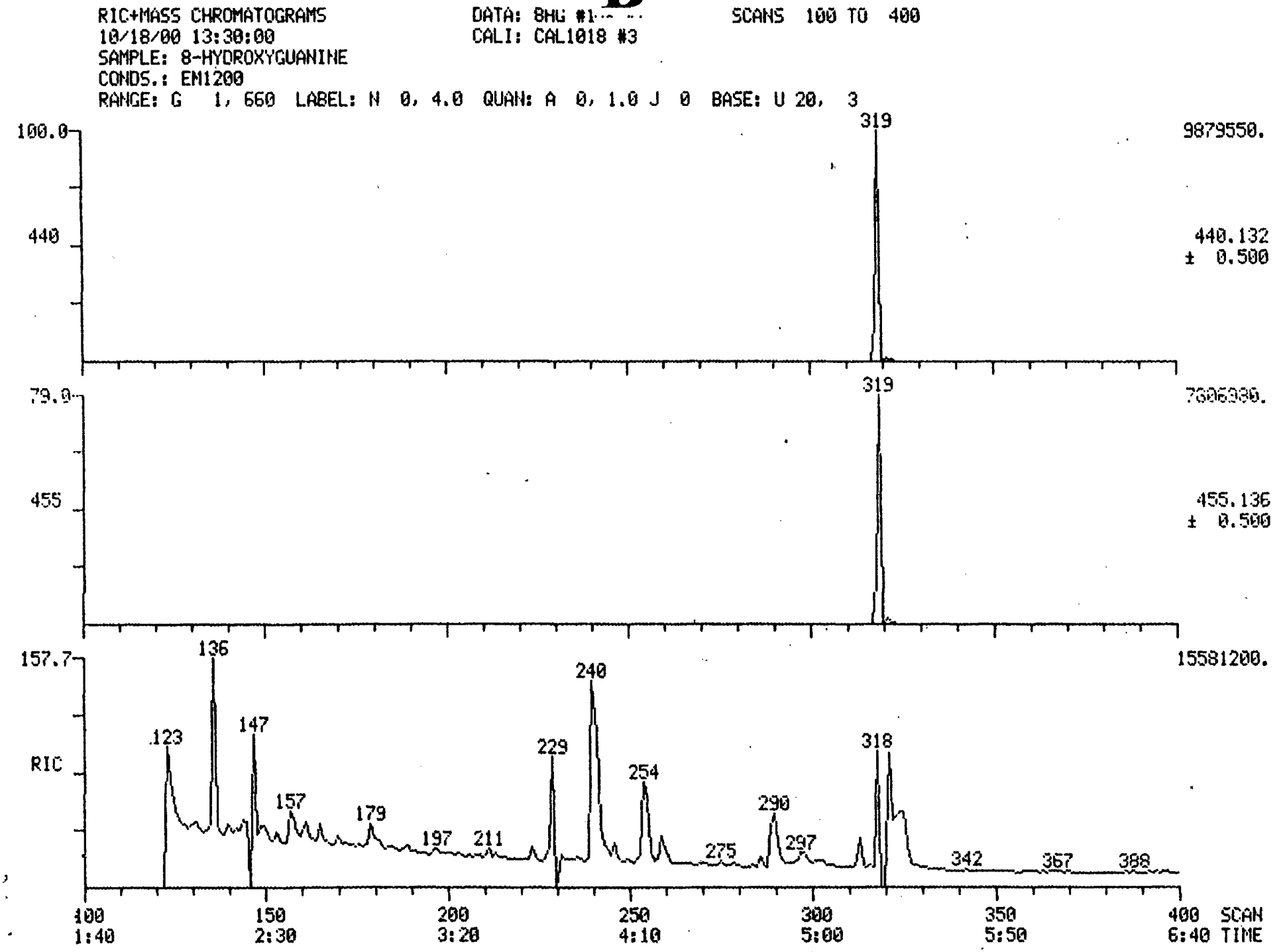
RIC+MASS CHROMATOGRAMS
DATA: 8HG #1
SCANS 100 TO 400
10/18/00 13:30:00
CALI: CAL1018 #3
SAMPLE: 8-HYDROXYGUANINE
CONDS.: EM1200
RANGE: G 1, 660 LABEL: N 0, 4.0 QUAN: A 0, 1.0 J 0 BASE: U 20, 3
100.0
319
9879550.
440
440.132
± 0.500
79.0
319
7606380.
455
455.136
± 0.500
157.7
15581200.
RIC
136
240
147
123
229
254
318
157
290
179
197
211
275
297
342
367
388
100
150
200
250
300
350
400 SCAN
1:40
2:30
3:20
4:10
5:00
5:50
6:40 TIME

C

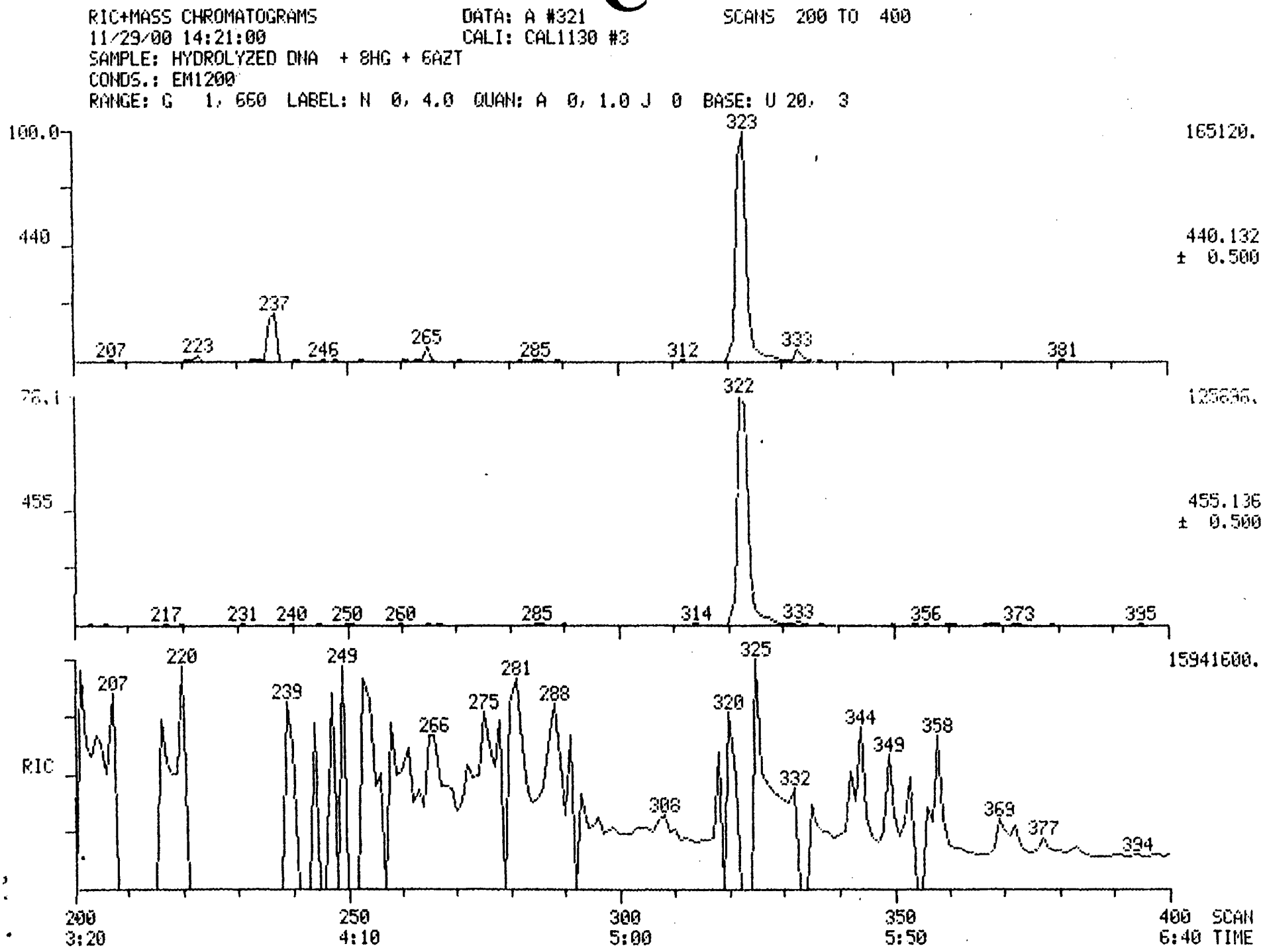
RIC+MASS CHROMATOGRAMS
DATA: A #321
SCANS 200 TO 400
11/29/00 14:21:00
CALI: CAL1130 #3
SAMPLE: HYDROLYZED DNA + 8HG + 6AZT
CONDS.: EM1200
RANGE: G 1, 660 LABEL: N 0, 4.0 QUAN: A 0, 1.0 J 0 BASE: U 20, 3
100.0
165120.
440
440.132
± 0.500
323
237
207
223
246
265
285
312
333
381
455
455.136
± 0.500
322
217
231
240
250
260
285
314
333
356
373
395
RIC
15941600.
220
207
239
249
266
275
281
288
308
320
325
332
344
349
358
369
377
394
200
3:20
250
4:10
300
5:00
350
5:50
400 SCAN
6:40 TIME